EVALUATION OF CEMENT-STABILIZED FULL-DEPTH-RECYCLED BASE MATERIALS FOR FROST AND EARLY TRAFFIC CONDITIONS

By

Heather J. Miller, Ph.D., P.E.
Associate Professor
Department of Civil and Environmental Engineering
University of Massachusetts Dartmouth
North Dartmouth, MA 02747
(508) 999-8481 Voice
(508) 999-8964 Fax
hmiller@umassd.edu

W. Spencer Guthrie, Ph.D.
Assistant Professor
Department of Civil and Environmental Engineering
Brigham Young University
Provo, UT 84602
(801) 422-3864 Voice
(801) 422-0159 Fax
guthrie@byu.edu

Rebecca A. Crane
Research Assistant
Department of Civil and Environmental Engineering
Brigham Young University
Provo, UT 84602
rcrane11@gmail.com

Brad Smith
Graduate Research Assistant
Department of Civil and Environmental Engineering
Brigham Young University
Provo, UT 84602
brad@earthtectesting.com

Disclaimer

This material is based on work supported by the Federal Highway Administration under Cooperative Agreement No. DTFH61-98-00095 through the Recycled Materials Resource Center at the University of New Hampshire, Durham, New Hampshire. The findings, opinions, and recommendations expressed within this document are those of the authors and not necessarily those of the University or the Federal Awarding Agency.

TABLE OF CONTENTS

APPENDICES

LIST OF TABLES

LIST OF FIGURES

1. INTRODUCTION

Highway agencies throughout the United States are faced with problems associated with disposal and/or recycling of millions of cubic yards of deteriorated asphalt pavement every year. If an existing pavement with a base failure is reconstructed by conventional methods, then the existing pavement material must be excavated and hauled from the site. This produces additional hauling costs, consumes fuel for transportation, provides additional wear on nearby roads, and consumes valuable landfill space. In addition, the construction of the replacement pavement uses virgin aggregate, hauled over the same roads, using additional fuel for transportation and construction.

Full-depth recycling (FDR) has the potential to provide agencies with tremendous cost and environmental advantages by facilitating the reuse of existing asphalt materials in pavement base layer reconstruction. Specifically, FDR is the process whereby a failed asphalt pavement is pulverized, blended with the underlying base material, and often stabilized with an additive such as cement to create a new pavement base layer. This stabilized base is then surfaced with asphalt or concrete to complete the process. A comprehensive description of each step of the FDR process, from project analysis to inspection, is provided by the Asphalt Recycling and Reclamation Association (AARA) in its manual (2001).

The use of FDR is most appropriate for roads with less than 7 inches of asphalt, because some base material is necessary to blend with the reclaimed asphalt pavement (RAP). In the U.S., considering local, state, and federal roads, there are approximately 2.5 million center-line miles of this type of pavement, termed “Low Flexible Pavement” by the Federal Highway Administration (FHWA, 2000). Therefore, it is relatively easy to see the potential cost savings and environmental benefits that arise from rehabilitating a road using the FDR process.

The main emphasis in FDR technology today is on developing appropriate engineering standards of practice. New mix design procedures have been investigated, considering different options for stabilizers (Carbó and Luco, 2001; Mallick, et al., 2002). To address the problem of reflective cracking in cement-stabilized pavements, the concept of micro-cracking was developed (Litzka and Haslehner, 1995; Scullion, 2002; PCA, 2003). The durability of FDR mixtures have been studied (Sommer, 2001) and new test procedures, like the tube suction test (TST), have been used to evaluate durability and moisture sensitivity (Syed et al., 1999). These research projects, among others, reflect the growing interest in recycled pavement materials.

Portland cement is one of the stabilizers commonly used in conjunction with FDR. FDR with Portland cement offers many advantages that have been well described in the past (PCA 1992; Prusinski, 2000; Chakrabarti et al., 2001). The addition of cement to the RAP and aggregate base material increases the strength and durability of the base layer (Guthrie et al., 2002). In cold regions, cement treatment is especially useful for improving the durability of frost-susceptible base materials. Since moisture is a major factor influencing the long-term performance of base materials, the goal in cement stabilization is to add enough cement to effectively reduce moisture ingress into the base, but not so much cement that the base becomes too rigid and thus prone to cracking. Cement treatment may also benefit the overall pavement system by improving the capacity of base layers to bridge over frost-susceptible subgrade soils that become weakened during the spring thaw period. Based upon research conducted at the Texas Transportation Institute (TTI), the Portland Cement Association recommends adding sufficient cement to achieve target 7-day unconfined compressive strength (UCS) values between 300 and 400 psi and a "good" moisture susceptibility rating in the TST (Scullion et al. 2000).

In light of these criteria, a primary goal of this research was to characterize the properties of cement-treated base (CTB) materials constructed from RAP and aggregates obtained from several locations in New England. Extensive laboratory testing was performed to evaluate the strength and durability of the materials in the untreated condition and after treatment with various levels of cement. Testing included determinations of particle-size distributions, moisture-density relationships, UCS values, and moisture susceptibility classifications for the materials.

The results of the laboratory testing were used to establish design parameters for field test sections constructed in the summer of 2005. Field testing was conducted to characterize the structural properties of both cement-treated and untreated FDR base materials subjected to early trafficking. One of the field test sites was also monitored during the 2005-2006 winter and spring to examine variations in performance-related properties that result from seasonal changes in temperature and moisture content.

In addition to conducting the laboratory and field testing, the scope of this project included evaluation of six mechanistic-empirical models for predicting fatigue of CTB layers. Knowledge of the fatigue life of CTB layers is useful to pavement engineers during the design process, especially in situations in which the base layer will be expected to bridge over weak subgrades. For example, during spring in cold regions, frost-susceptible subgrade soils may exhibit severe thaw weakening and markedly reduced bearing capacities. In this situation, the decreased support beneath the CTB layers permits the occurrence of greater horizontal tensile stress in the CTB layer at its interface with the subgrade. Depending on the magnitude of the induced tensile stress relative to the tensile strength of the CTB material, bottom-up cracking may occur, deteriorating the pavement integrity. Based upon the available numerical models, charts were developed to predict expected pavement life associated with varying asphalt concrete and CTB thicknesses and varying CTB and subgrade modulus values.

This report describes the laboratory and field testing that was conducted, as well as the numerical modeling regarding the fatigue life of CTB layers. The research findings and design recommendations are summarized in the conclusion, and suggested specifications for construction of cement-treated FDR base layers are included in Appendix B.

2. OBJECTIVES

Two of the most prominent issues with regard to cement-stabilized recycled bases are the effects of (1) frost and (2) early traffic. Therefore, the major goal in this project was to conduct field and laboratory testing to evaluate cement-stabilized FDR bases with regard to performance in frost areas and under early traffic conditions. Additionally, the scope of this project included evaluation of mechanistic-empirical models for predicting fatigue of CTB layers, and development of design charts to predict expected pavement life and mode of failure associated with cement-treated recycled base layers. The ultimate objective of this research is to provide generalized engineering guidelines that can be utilized by local and state transportation agencies so that they can potentially benefit from the significant cost and environmental advantages of FDR with cement-treated base materials.

3. SCOPE OF WORK

A unique multi-disciplinary research team worked together to accomplish the project goals. The principal investigators were Dr. Heather Miller at UMass Dartmouth (UMD) and Dr. Spencer Guthrie at Brigham Young University (BYU). Research assistants from both universities actively participated in the experimental program and the numerical modeling. In addition, three representatives from the cement industry actively participated in the project by contributing in-kind engineering services. Mr. Wayne Adaska, P.E., and Dr. David Luhr, P.E., provided technical support from the Portland Cement Association (PCA), and Ms. Carolina Carbó provided specific expertise on FDR procedures. She is the Pavement Recycling Specialist for the New England Region of the Road Recycling Council. Other collaborators on this project included personnel from the USDA Forest Service, the Federal Highway Administration (FHWA), and Worcester Polytechnic Institute (WPI).

To accomplish the project goals, a series of specific tasks was conducted as outlined below:

Task 1: *Review State-of-the-Art in Pavement Design for Frost-Affected Areas and Develop Experimental Plan*

Literature was reviewed to assess the state-of-the-art in pavement design for frost-affected areas, and a survey of state departments of transportation was conducted to investigate material and construction specifications and to define current pavement design practices. A general description of the survey is presented in Section 4 of this report, and a detailed analysis of the survey is included in Appendix A.

Task 2: *Laboratory Testing*

Laboratory testing was performed to characterize the strength and durability of recycled asphalt base materials prepared with various levels of cement. Details are provided in Section 5 of this report.

Task 3: *Field Testing*

Field testing was conducted at two sites during the summer of 2005 to characterize the structural properties of both cement-treated and untreated FDR base materials subjected to early trafficking. One of the field test sites was also monitored during the 2005-2006 winter and spring to examine variations in performance-related properties that result from seasonal changes in temperature and moisture content. Details are described in Section 5 of this report.

Task 4: *Analysis*

Analysis of the data obtained from the laboratory and field test programs is included in Section 6 of this report. Additionally, the scope of this project included evaluation of mechanistic-empirical models for predicting fatigue of CTB layers, and development of design charts to predict expected pavement life and mode of failure associated with cement-treated, recycled base layers. Details of that work are described in Section 7 of this report.

Task 5: *Development of Design and Construction Recommendations*

General conclusions and design recommendations formulated from the results of this research are included in Section 8 of this report. Suggested specifications for construction of cement-treated recycled base layers are included in Appendix B.

4. DESIGN AND CONSTRUCTION OF PAVEMENTS IN COLD REGIONS: SURVEY REGARDING STATE OF THE PRACTICE

GENERAL

The effects of frost action introduce many challenges in the design and construction of roadways in cold regions throughout the United States. The penetration of frost into pavement structures can lead to differential frost heave during winter and thaw weakening during spring (NCHRP, 1974; Freitag and McFadden, 1997). Both of these damage mechanisms lead to premature pavement distress, structural deterioration, and poor ride quality (Janoo, 2002; Huang, 1993). For example, a pavement designed to last for 12 to 15 years under non-frost-susceptible conditions may require major maintenance in just 5 years in an area with frost-susceptible subgrades (Mackay et al., 1992). Because the availability of naturally occurring non-frost-susceptible pavement base materials is rapidly diminishing in many areas while project budgets remain largely inadequate, pavement engineers are utilizing alternative materials and techniques to minimize such damage.

Therefore, the purpose of this research task was to investigate and document the state of the practice concerning the design and construction of pavements in cold regions. In particular, the various methods and standards employed for characterizing materials, improving soils and aggregates, and determining pavement layer thicknesses were explored. To this end, a questionnaire survey was conducted to investigate the state of the practice concerning identification of frost-susceptible materials and the use of soil and aggregate stabilization in cold regions within the United States. The survey was directed primarily at identifying practices utilized by state DOTs in climates with freezing temperatures, although a response from Sweden was also solicited and received. Individuals most capable of describing the state of the practice concerning the identification and treatment of frost-susceptible materials were identified through telephone calls to each state DOT office.

In addition to the survey sent to Sweden, surveys were e-mailed to 42 DOTs (all except Alabama, Delaware, Florida, Georgia, Hawaii, Louisiana, Mississippi, and New Jersey), and responses were received from the following 23 DOTs: Alaska, Arizona, Colorado, Connecticut, Idaho, Indiana, Kansas, Maine, Maryland, Minnesota, Montana, Nevada, New Hampshire, New Jersey, New York, North Carolina, Ohio, Pennsylvania, South Dakota, Texas, Utah, Vermont, and West Virginia. The response rate associated with the survey was 56 percent.

The survey included 20 questions related to the identification of frost-susceptible soils and the use of stabilization methods for improving frost-susceptible soils in cold regions. Most of these questions had multiple-choice answers, but others required short-answer responses. The 20 survey questions were organized into in three different sections: climate, design and construction, and policies. The survey questions and a detailed description and analysis of the results obtained for each question are included in Appendix A. A brief summary and conclusions from the survey responses are presented in the following section.

SURVEY RESULTS

The results of the two questions addressing the climate in the regions of the different respondents indicated that frost penetration ranged from about 1 ft to greater than 10 ft. Air freezing indices in the various geographic areas represented by the survey participants varied up to 3000ºF-days.

In terms of design and construction, the AASHTO pavement design method is most commonly used, although many agencies use their own in-house methods for pavement design. A majority of the respondents indicated the use of HMA for surface layers of flexible pavements together with the use of dense-graded aggregate base material and granular subbase material. A few respondents utilize stabilized base or subbase materials. Among the responses indicating the use of rigid pavement sections, granular, stabilized, lean concrete, and asphalt bases were all reported.

The most common methods employed to identify frost-susceptible soils include field experience, laboratory testing, and particle-size distribution. Excavation and replacement of frost-susceptible soils was the most frequently cited method of constructing pavements on frost-susceptible subgrades. Other commonly used methods include the use of edge drains, open-graded drainage layers, and stabilization. The most commonly specified stabilizers are Portland cement and lime, but agencies are also using fly ash, asphalt emulsion, foamed asphalt, slag, and calcium chloride. Field experience and UCS testing are the methods most often used for determining the optimum amount of stabilizer to add to a given base or subgrade material. When geosynthetics are incorporated into the pavement structure, several of the survey respondents indicated that they permit construction of thinner pavement sections.

The majority of the survey participants do not use FDR. However, when FDR is used, the typical RAP content is 50 percent, which corresponds to a 50:50 ratio of RAP to base. Common materials and processing specifications utilized for FDR projects include gradations and the use of specific stabilizers. The majority of the survey respondents reported good, very good, or satisfactory performance of pavements constructed using the FDR process, but a few indicated poor performance.

The survey results suggest that the most commonly used method for minimizing shrinkage cracking of cement-treated layers is placement of a curing seal. Maintaining moisture levels and using minimum amounts of Portland cement were also common responses. In addition, using geogrids, requiring lower UCS values, microcracking, and only stabilizing subbase layers are methods employed to minimize cracking.

Curing times typically ranging from 3 to 7 days are most frequently required before a cement-treated pavement layer can be opened to traffic. The majority of the respondents reported very good, good, or satisfactory performance of pavements constructed using chemically or mechanically stabilized layers. At the time the survey was conducted, only a few agencies indicated plans to utilize FDR in conjunction with cement stabilization during the next construction season.

With regard to the final two questions about policies, spring load restrictions are used by approximately half of the respondents to prevent accelerated damage to pavements during thawing, but only a couple of agencies permit winter load premiums. Among the agencies that do require spring load restrictions, past experience was the most common method used to determine the timing and duration of the restrictions. Other responses included computer modeling, use of a predetermined period of time, and evaluation of snow melt, soil temperature, and air temperature.

Although the results of the questionnaire survey reveal a variety of practices, the data suggest that many DOTs utilize similar methods for the design and construction of pavements in cold regions. The information obtained in this survey represents a unique compilation of standards of practice that have been developed by DOTs based on years of experience and research in their respective jurisdictions.

5. EXPERIMENTAL METHODOLOGY

GENERAL

This research project included laboratory and field testing programs, as well as numerical modeling. For the laboratory work, aggregate base materials and RAP were collected from six locations throughout Rhode Island (material A), Massachusetts (materials B and C), Maine (materials M1 and M2) and New Hampshire (material NH). For field research, testing was conducted on two different highways that underwent rehabilitation during the 2005 construction season because they had deteriorated after many years of freeze-thaw damage. One test site was established along a section of the Kancamagus Highway (Route 112) in New Hampshire, and the other test site was located along Route 2A in Bancroft, Maine. Samples of RAP and base material were obtained from the test sites and subjected to laboratory testing. Field testing was conducted at both sites during construction activities in the summer of 2005. Monitoring of the Kancamagus Highway test site continued through the 2005-2006 winter and spring to examine variations in performance-related properties that resulted from seasonal changes in temperature and moisture content. Features of the laboratory and field testing are presented in the following sub-sections of this report, and discussion of the results of the laboratory and field tests are presented in Section 6 of this report. The numerical modeling is presented in Section 7 of this report.

LABORATORY TESTING PROGRAM

For the laboratory research conducted in this project, the aggregate base materials and RAP were blended in approximately equal proportions by weight. In some cases, the aggregate and RAP were obtained separately and blended in the laboratory, and in other cases the aggregate and RAP were blended in the field with a reclaimer and then transported to the laboratory. All samples were subjected to sieve analyses. Since the materials were all non-plastic, accurate determination of Atterberg limits was not possible. In all but two cases, the materials were dried and then separated over several sieve sizes to facilitate construction of replicate specimens having the same gradations as the original samples. For the two materials obtained from sites in Maine, the air-dry materials were scalped on the 0.75-in. sieve and then separated into appropriately sized fractions using a splitter to ensure that the gradations of the specimens were as similar as possible. Compaction tests following American Association of State Highway and Transportation Officials (AASHTO) T-180-01 Method C were performed to determine the optimum moisture content (OMC) of each untreated material.

During the initial laboratory testing phase, trial cement contents were selected based upon recommendations provided by PCA (PCA 1992). One specimen of each material type was compacted at each of three trial cement contents, extruded from the Proctor mold, and cured in a fog room at 100 percent relative humidity for 7 days. After curing, the specimens were capped with high-strength gypsum, soaked under water for 4 hours, and tested in unconfined compression at a stress-controlled rate of approximately 20 psi per second using a mechanical press with a floating head. For each material, the collected data were used to determine the cement contents corresponding to the following target 7-day UCS values:

- 200 psi (low end)
- 400 psi (mid-range)
- 600 psi (high end)

For each of the selected cement contents, a compaction test was performed to more definitively determine the OMC for each of the cement-treated materials. The new OMC values were used as the molding water contents for preparing specimens for the experimental program, which consisted of performing a more extensive series of UCS tests, as well as TST evaluations.

For each series of UCS tests, specimens were compacted, cured at 100 percent relative humidity, and tested as described previously, except that nine replicate specimens were prepared for each material at each cement content. Preparation of nine replicate specimens allowed testing of three specimens at each of three curing periods, including 3 days, 7 days, and 28 days.

The TST is a relatively new test designed to evaluate the durability and moisture susceptibility of aggregates used as base materials in pavements (Scullion and Saarenketo 1997). The test consists of measuring the surface dielectric value of compacted specimens during 10 days of capillary soaking in the laboratory. The interpretation of test results is based on an empirical relationship between measured dielectric values and expected performance of aggregate base materials in the field. Research performed at TTI (Syed et al. 1999) indicates that this new methodology may represent a much quicker and more cost-effective means of assessing base durability than the traditional American Society for Testing and Materials D 559 and D 560 protocols, which require more than a month to perform.

For evaluation in the TST, three replicate specimens of each material were compacted at each cement content following AASHTO T-180-01 Method C, except that specimens were formed within 4-in.-diameter plastic molds placed inside a standard Proctor compaction mold that was slightly modified to accommodate the inner plastic molds. The plastic molds were standard 4-in.

by 8-in. concrete molds that were trimmed to about 5.5 inches in height and had 1/16-inch-diameter holes drilled around the circumference of the mold at a horizontal spacing of 1/2 in. along a line approximately 1/4 in. above the bottom. Four holes were also drilled in the bottom of the molds (one in each quadrant) about 1 in. from the center.

After compaction, specimens were removed from the Proctor mold (but left in the plastic molds) and placed in a fog room to cure for 7 days. The specimens were then dried back for 72 hours in an oven maintained at 140°F. Six initial dielectric readings were taken on each specimen surface using a surface dielectric probe, and then the specimens were placed inside an ice chest filled with distilled water to a depth of 1/2 in. The testing continued for 10 days, with dielectric readings and moist weights obtained once each day. The highest and lowest values measured each day were discarded, and the average of the remaining four values was used for analysis.

The final average dielectric values were used to rate the moisture susceptibility of the specimens. Aggregates with final dielectric values less than 10 are expected to provide good performance, while those with dielectric values above 16 are expected to provide poor performance as base materials. Aggregates having final dielectric values between 10 and 16 are expected to be marginally moisture susceptible (Scullion and Saarenketo 1997).

FIELD TESTING PROGRAM

In Situ Evaluation of Pavement Materials

Several destructive and non-destructive devices are available for assessing the strength or stiffness of pavement materials in situ. These include the soil stiffness gauge (SSG), heavy Clegg impact soil tester (CIST), dynamic cone penetrometer (DCP), and falling-weight deflectometer (FWD). The use of these devices for evaluating strength and stiffness of CTB materials was evaluated by Guthrie et al. (2005) in conjunction with a pavement reconstruction project along Interstate 84 (I-84) in Morgan, Utah. A brief description of each device follows.

The SSG (also known as the “Geogauge”) is a portable instrument weighing 25 lb and having a height and diameter of 12 in. and 11 in., respectively. The device measures stiffness at the soil surface by imparting very small displacements, on the order of 0.00005 in., to the soil on a ring-shaped foot with a 3.5-in. inside diameter and 4.5-in. outside diameter (Humboldt Mfg. Co., 2000). According to the manufacturer, a thin layer of moist sand should be placed on the ground as bedding for the SSG foot, and the device should be removed and replaced between readings. At least 60 percent of the foot should be in contact with the ground to facilitate a valid measurement. Testing is conducted via a harmonic oscillator operating at 25 steady-state frequencies between 100 Hz and 196 Hz. Collection of data across this frequency spectrum requires about 1 minute and permits digital filtering of noise. The stiffness is determined at each frequency as the ratio of the force to the displacement and then averaged over all the frequencies. The SSG is reportedly sensitive to depths of between 9 in. and 12 in.

The heavy CIST is comprised of a 44-lb steel drop weight confined inside a 6-in.-diameter metal guide tube mounted on wheels. The weight has a hardened steel strike face and is instrumented with an accelerometer connected to a digital display unit. A 12-in. drop height is used for the heavy CIST, and the peak deceleration of the hammer upon impact is reported as the Clegg

Impact Value (CIV), where 1 CIV is equivalent to 10 times the gravitational acceleration rate (Lafayette Instrument, 2004). Four successive blows of the hammer at the same location constitute one test, which can be completed in less than 10 seconds by a single operator. The depth of interrogation may be estimated to be about two times the diameter of the drop weight, or about 12 in. for this hammer (Kestler and Berg, 2004).

The DCP is comprised of a 17.6-lb dual-mass slide hammer assembly used to manually drive a standard cone tip to a maximum depth of 39 in. into the ground. The penetration in inches/blow is reported as a function of depth. For greatest ease of operation, a manual DCP test is performed by two persons. One person lifts and drops the weight, while the other person measures and records penetration. Depending on the resistance of the ground, tests may require 5 minutes to 10 minutes each. Disposable cone tips are available to facilitate easier DCP removal in very stiff soils that may otherwise require significant extraction effort. In soils with large aggregate particles, the DCP may begin to penetrate the soil at an angle as the cone tip is driven around a stone in its path. When the DCP handle deviates laterally more than 6 in. from its original vertical position, the test should be stopped, and a second test should be attempted at a different location (Salem Tool, 2003).

The FWD is a truck- or trailer-mounted pavement evaluation apparatus that measures deflections of the pavement surface in response to impulse loads of magnitudes similar to truck traffic. Deflection sensors are placed at several radial distances from the loading plate, commonly 0, 8, 12, 18, 24, 36, and 60 in. (Von Quintus and Simpson, 2002). If the thicknesses of the pavement layers are known, the deflections may be used in computer software to backcalculate the modulus values of the pavement materials. Because of the heavy loads employed in FWD testing, the full depth of the pavement structure is usually within the zone of test influence. A single test can be conducted in less than 1 minute by a single driver, although a second person often participates in the testing to ensure that the loading plate is positioned at the desired location. Portable FWDs are also available, but they typically have only one to three deflection sensors (Kestler and Berg, 2004). Because of their lighter weight, however, they can be manually transported by a single operator and are much less expensive than a full-size FWD.

Among these four types of equipment, the DCP is the only destructive apparatus and the most tedious and time-consuming to use. Especially in crushed stone materials, the interference of large aggregates often requires many DCP tests to be repeated. Furthermore, in stiff soil and aggregate layers where numerous hammer drops are necessary to achieve desirable penetration depths, operator fatigue can become a veritable problem. In the study conducted by Guthrie et al. (2005), after less than 2 days of curing, DCP penetration values on the CTB approached 0.05 in./blow, and the drop hammer bounced upon impact, indicating refusal. Therefore, for the current project, the DCP was not selected as a tool for assessing the stiffness of the cement-treated base materials in situ.

On the other hand, the CIST, SSG, and FWD are non-destructive and relatively rapid to use. However, due to the much greater expense of the FWD, the CIST and SSG have received more attention in the pavement construction industry for routine quality control and quality assurance programs (Fiedler et al., 2004; Humboldt Mfg. Co., 2002; Al-Amoudi et al., 2002; Sebesta, 2005). Because of the shallower interrogation depth of the smaller devices, the measurements are more sensitive to individual compaction lifts and pavement surface layers, and their ease of mobility readily permits their use on a wide variety of geotechnical and pavement engineering projects. Furthermore, in cement-treated or other chemically-stabilized materials where nuclear density gauges typically give incorrect readings, the use of these portable, non-nuclear devices is especially appealing.

For this research project, the research team utilized the "Geogauge" at the field test site in New Hampshire and a heavy CIST at the field test site in Maine. FWD testing was also conducted at the New Hampshire test site on an in-kind basis by personnel from Eastern Federal Lands Division of FHWA and Worcester Polytechnic Institute (WPI). A description of the work conducted at each of the field test sites follows.

Kancamagus Highway (Route 112), NH

General

Several miles of the Kancamagus Highway in New Hampshire that had deteriorated due to frost action were rehabilitated during the 2005 construction season. Three field test sections were established within an approximately 1500-ft section of that roadway, about midway between its intersection with Route 16 on the east and Interstate Route 93 on the west. The test sections were located in the eastbound lane along a relatively straight stretch of roadway. From west to east, the test sections consisted of the following:

- Conventional reconstruction (station 46+27 to station 46+97)
- FDR with cement stabilization (station 50+50 to station 59+50)
- FDR without cement stabilization (station 60+50 to station 61+20)

The sections of roadway that underwent conventional reconstruction and FDR without cement stabilization extended for considerable distances to the west and east, respectively; however, testing for this research was confined to the 70-ft sections as indicated above.

The "conventional reconstruction" consisted of excavating about 3 ft of existing pavement, base, and subgrade soil, and then replacing that material with virgin aggregate from a local borrow pit (26 in. of crusher run gravel followed by 10 in. of crushed gravel base). The conventional reconstruction between the stations noted above was conducted during early July 2005.

Initial work on the FDR test sections began in May 2005. The existing asphalt pavement, which was about 4 in. thick, was pulverized and blended with about 4 in. of the underlying base material. In June 2005, the reclaimer was mobilized again, and the 8 in. of reclaimed material was reworked and mixed with water to increase its moisture content slightly. For the cement-stabilized section, 4 percent cement by weight of dry aggregate was then mixed into the 8-in.-thick reclaimed base material. Because the roadway had not been scraped to final grade prior to the second round of reclaiming operations, final grading resulted in a reclaimed base layer thickness of only about 5 to 6 in. for both the cement-treated and untreated sections. All three test sections were paved with hot mix asphalt, consisting of a 2-in. binder layer placed in late July 2005 and a 1.5-in. wearing course placed in October 2005.

Initial strength gain and effects of early traffic

The primary objective of the field research was to compare the structural properties of the two FDR test sections and to evaluate the effects of traffic on the initial strength gain in the CTB section. Therefore, a test program was implemented to obtain stiffness measurements beginning on the day that the cement was added to the FDR base material (June 21, 2005) and continuing for three days afterwards.

In the cement-treated section, testing locations were established as follows:

- Six stations, 20 ft apart, between station 50+50 and station 51+50
- Six stations, 20 ft apart, between station 55+37 and station 56+37
- Eight stations, 10 ft apart, between station 58+80 and station 59+50

In the untreated FDR section, testing locations were established at eight stations, 10 ft apart, between station 60+50 and station 61+20. At every station, one series of test points was established at 9 ft from the highway centerline in approximately the right wheel path, and another series of test points was established at 6 ft from the centerline, between the right and left wheel paths. All test points were located in the eastbound lane of Rt. 112.

The rationale for performing one series of tests in the wheel path and another series between wheel paths was to quantify the effects of early traffic on the CTB material. PCA recommends limiting traffic on CTB materials to only low-speed local traffic and construction equipment during the first 7 days if moist curing is used in lieu of a curing compound, which was the case on this project. Since the Kancamagus Highway has only one travel lane in each direction, the 1,000-ft CTB section could not be closed to traffic for 7 days. Instead, the CTB test section was closed to traffic one lane at a time during the initial construction operations and for 2 to 3 hours during each of the 3 days following construction to allow for Geogauge and FWD testing. Otherwise, the CTB was subjected to a substantial amount of tourist traffic, as well as to heavily-loaded construction equipment that used that section of roadway to access other portions of the highway that were under construction.

Stiffness measurements were obtained with the Geogauge and with a FWD. The FWD deflection sensors were spaced at distances of 0, 8, 12, 18, 24, 36, and 48 in. from the center of the load plate, which was 5.9 in. in radius. Four tests were performed at each of four target loads, including 6000, 9000, 12,000, and 16,000 lb. Computer software ("EverCalc") was used to backcalculate the layer modulus values (WSDOT, 1995).

Although it was planned to take stiffness measurements at every test point location on each of the four days (June 21-24, 2005), access to some of those locations was prohibited on certain days due to traffic control issues and other construction activity. A description of the number of tests conducted and the results of the Geogauge and FWD tests are presented in Section 6 of this report.

Instrumentation and long-term monitoring of test sections

Because there was significant interest in this research project from FHWA and the USDA Forest Service, instrumentation for long-term monitoring was installed at this site, and additional FWD testing was provided on an in-kind basis. The instrumentation included observation wells (OWs) and soil moisture sensors to monitor subsurface moisture regimes and thermistor assemblies to monitor subsurface temperatures.

Three observation wells were installed on June 21, 2005. OW-1 was located off the eastbound lane at approximately station 49+00, OW-2 was located off the westbound lane at about station 57+70, and OW-3 was located off the eastbound lane at about station 59+40. A forth observation well (OW-4) was installed near the intersection of Rt. 112 and Bear Notch Road in July 2005; however, that well was buried by the general contractor during unanticipated re-grading operations in mid-October 2005.

The observation wells were constructed of 10-foot lengths of schedule 40, 2-inch diameter PVC pipe. A number of ¼-inch-diameter holes were drilled in the lower 2 to 3 feet of the pipe, and the perforated section was then wrapped with a geotextile to act as a filter. The wells were installed by the New Hampshire Department of Transportation (NH DOT) using a truck-mounted drill rig. Holes were advanced with a rollerbit to a depth of about 8 feet below the existing ground surface, the well casing was installed, and the portion of the hole around the perforated casing was then backfilled with a uniformly-graded medium grained sand. A bentonite seal was installed, and then the remainder of the hole was backfilled. After installation, the elevations of the top of the well casings were determined by an optical survey. Water table elevations were subsequently established during the monitoring period by measuring the depth to the water table from the top of the casings using a hand-held electronic water level meter.

A total of six soil moisture sensors ("Hydra Probes") manufactured by Stevens Water Monitoring Systems, Inc. were installed at this site. The Hydra Probe is a relatively inexpensive sensor that measures both the real and imaginary components of the complex dielectric constant (also referred to as relative permittivity) of a soil at 50 MHz. The traditional method used to quantify soil moisture is gravimetric sampling, in which a sample of soil is physically removed from the ground, weighed in the moist condition, and then weighed again after oven drying. Because gravimetric methods are destructive, alternative methods such as the Hydra Probe have been developed to monitor soil moisture in situ. With these dielectric probes, changes in soil moisture content are related to changes in measured soil dielectric properties.

The dielectric constant of pure water at 20^{o}C is about 80, and the dielectric constant of air is close to 1. For dry soils, dielectric constant values in the range of 2.7 to 3.2 have been reported by Seyfried and Murdock (2004), and values ranging from 4.5 to 10 were suggested by Robinson et al. (2003). Since the dielectric constant increases as water fills the voids in the soil matrix, increases in soil moisture content can be empirically related to increases in measured values of dielectric constant.

Two soil moisture sensors were installed in each of the three test sections (conventional reconstruction, FDR with CTB and FDR without cement). The soil moisture sensors in the two FDR test sections were installed concurrently with installation of the thermistor assemblies, as described in the following paragraphs. In the conventional reconstruction section, moisture sensors were installed during placement and compaction of the crusher run gravel and crushed gravel base. The locations (station, elevation, and depth below top of pavement) of the soil moisture sensors are tabulated in Appendix C.

A total of six roadway thermal probes ("thermistors"), fabricated in-house by USDA Forest Service personnel, were installed at this site. Thermistors are thermally sensitive resistors which exhibit a steep drop in resistance as the temperature increases. The thermistors in each probe were spaced 4 inches apart within a clear plastic tube approximately 1 inch in diameter. The tubes were filled with an electronics grade potting epoxy. All thermistor probes were installed between wheel paths in the eastbound lane of Route 112. The approximate locations (station numbers) and the depths of the individual temperature gauges relative to the top of the pavement are tabulated in Appendix D.

The thermistors probes (and the moisture sensors in the FDR test sections) were installed in holes constructed using a truck-mounted drill rig provided and operated by the NH DOT. In the cement-treated section, the holes were advanced with a rollerbit, and in the other two test sections the holes were advanced by driving a 4-inch-diameter split spoon sampler to the desired depth. Samples of the soil removed from the holes using the split-spoon sampler were transported back to the UMD laboratory for sieve analyses in order to characterize the native subgrade beneath the FDR base materials. After the thermistors were placed in the holes, the annulus between the thermistor and the borehole wall was backfilled (approximately up to the bottom of the base material) with the sand provided by NH DOT for observation well construction. At stations where moisture sensors were also installed, the four tynes on the moisture probes were pushed into the side of the borehole wall at the desired depths. The remainder of the hole was then filled with the FDR base material that had been removed from the hole and run through a No. 4 sieve in the field to remove large particles.

The thermistors in each probe were all connected to a multistrand, 22-gauge, PVC-jacketed cable that was routed through a shallow trench out to the edge of the highway, down the side slope, and into the woods (about 35 feet off the highway shoulder). Amphenol connectors at the end of each cable (for connection to readout instrumentation) were mounted on poles that were then driven into the ground or attached to trees. The cables from moisture sensors were also routed through the same trenches, but their outlet plugs were housed within short sections of 4-inch-diameter PVC casing placed at the ground surface. Removable caps were installed on the PVC casings to protect the outlet plugs from rain and snow.

Data from the moisture sensors was obtained using a Vitel hand-held reader that had been modified by Stevens Water Monitoring Systems, Inc. to accept the output connector from the Hydra Probes. The output provided by the Hydra Probes consisted of dimensionless values of real and imaginary dielectric constants. Data from the thermistors were obtained using an Omega hand-held switchbox and digital thermometer unit that provided temperature readings in degrees Fahrenheit (° F).

Thermistor readings were obtained by USDA Forest Service personnel at three of the thermistors (one in each test section) approximately every one to two weeks during the 2005-2006 winter/spring monitoring period. Baseline data were obtained from the moisture sensors, but data were not obtained from them on a regular basis during the monitoring period. Data obtained from the thermistors and moisture sensors are tabulated in Appendices C and D, respectively, and analyses of those data are discussed in Section 6 of this report.

In addition to monitoring subsurface temperatures and water levels, optical survey measurements were obtained by the UMD research team at various times during the 2005-2006 winter and spring to evaluate frost heave and potential rutting in the three test sections. PK nails were installed just after the final paving operations in October 2005 to establish test points at the following locations:

- Conventional reconstruction: eight stations, 10 ft apart, between stations 46+27 and 46+97
- FDR with CTB: eight stations, 10 ft apart, between stations 58+80 and 59+50
- FDR without cement: eight stations, 10 ft apart, between stations 60+50 and 61+20

At every station, one series of test points was established at 9 ft from the highway centerline in approximately the right wheel path, and another series of test points was established at 6 ft from the centerline, between the right and left wheel paths. All test points were located in the eastbound lane of Route. 112.

Finally, FWD testing was conducted at this site as part of an ongoing collaborative research effort by USDA Forest Service personnel to quantify the effects of spring thaw in order to more rationally apply and remove spring load restrictions. FWD testing was conducted in October 2005 and in March, April, and May 2006. FWD tests were performed at the same stations noted above that were established for monitoring heave, except that FWD tests were performed at the wheel path locations only. Forest Service personnel are currently working on backcalculating layer modulus values from that data, which will be published in the future. A number of complexities are inherent in that analysis, because backcalculation techniques do not yield unique solutions and because it is often difficult to obtain reasonable modulus values when one is dealing with multiple layers of frozen/partially frozen/thawed materials.

Therefore, the research team at UMD concentrated on a parallel effort that included analyzing several other deflection-related pavement parameters that can be computed from FWD test data. These parameters included adjusted center deflection, area parameter, surface curvature index (SCI), shape factor, and subgrade modulus. The significance of these parameters and the methods used to compute them are briefly described below.

When loads are placed on the surface of a pavement (either by traffic or during FWD testing), the pavement will deflect downward to form a bowl-shaped depression known as a deflection basin. The shape of the deflection basin is a function of numerous variables, including the thickness and stiffness of the pavement layers and the subgrade. The outer FWD deflection sensors respond primarily to the subgrade characteristics, while the deflections at the inner sensors respond to the combined characteristics of the subgrade and upper pavement layers (FHWA, 1994). The deflections measured at the outer sensors are considered to correlate quite well with the modulus of the subgrade, while the slope of the deflection basin close to the FWD load plate is largely a function of the stiffness of the upper pavement layers (FHWA, 1994).

When conducting FWD testing at a given location, multiple tests are typically performed at different load levels, and then the deflections are normalized to a 9,000-lb load by interpolation. The deflection measured by the FWD sensor directly at the center of the load, D_o, is also usually adjusted to account for changes in asphalt stiffness that result from changes in temperature. The FWD-AREA computer program, developed by the Washington State Department of Transportation (WSDOT, 1999), was used to compute normalized deflections and temperature adjusted center deflections from the FWD data obtained on this project. The raw center deflection readings were adjusted to a standard temperature of 77 ^{o}F using Equation 1.

$$\textit{Adjusted Center Deflection} = D_o\left(1.598837 - 0.009211683 * T^{0.96}\right) \qquad (1)$$

where T = temperature of the asphalt pavement surface (^{o}F)

The area parameter can be used in conjunction with the center deflection to characterize the pavement structure condition without conducting pavement coring or extensive pavement analysis. The area parameter represents the normalized area of a slice taken through the deflection basin from 0 to 3 feet. The area is computed using the basic Trapezoidal Rule, and is then normalized by dividing it by the deflection measured at the center of the test load, as shown in Equation 2.

$$\textit{Area Parameter} = \frac{6\left(D_0 + 2D_{12} + 2D_{24} + D_{36}\right)}{D_0} \qquad (2)$$

where D_0, D_{12}, D_{24}, D_{36} are the deflection readings (in inches) from sensors located 0, 12, 24, and 36 in. from the center of the FWD loading plate, respectively.

The maximum possible normalized area parameter is 36 in., which would occur only in the unlikely event that all four deflection measurements were equal. The minimum area parameter should not be less than 11.1 in. (WSDOT, 1999). For this project, area parameter values were computed from raw FWD data using the "FWD-AREA" program, which included a temperature correction factor for the area parameter as shown in Equation 3 (WSDOT, 1999):

$$\textit{Correction Factor} = 0.7865 + \left(1.4578 * 10^{-4} * T^{1.68}\right) \qquad (3)$$

where T = temperature of the asphalt pavement surface (^{o}F)

The SCI and shape factor are both related to the slope of the deflection basin close to the FWD load plate and are therefore considered to give an indication of the relative stiffness of the upper pavement layers (FHWA, 1994). These parameters are defined in Equations 4 and 5:

$$SCI = D_0 - D_2 \qquad (4)$$

$$Shape\ Factor = \frac{(D_0 - D_2)}{D_1} \qquad (5)$$

where D_0 is the center deflection and D_1 and D_2 are the deflections at the first and second sensors, respectively (located at 8 and 12 in. from the load).

Numerous researchers have developed empirical equations to estimate subgrade modulus values directly from FWD deflection data (as opposed to using backcalculation techniques). For this project, Equation 6 (developed by Newcomb, 1986), was used to compute subgrade modulus values:

$$Subgrade\ Modulus = -466 + \left(9000 \times \frac{0.00762}{\left(\frac{D_{36}}{1000} \right)} \right) \qquad (6)$$

where subgrade modulus is given in psi, and D_{36} is the deflection reading (in inches) from the sensor located 36 in. from the center of the FWD loading plate.

Rt. 2A, Reed Plantation-Bancroft Maine

General

Route 2A runs between Macwahoc and Houlton in Aroostook County, ME. Many miles of this roadway were in need of reconstruction or rehabilitation after years of frost action and heavy truck traffic. This route accommodates truck traffic that exceeds the 30-ton weight limitation that exists for Interstate 95 in Maine. Commercial truck traffic from local logging industries and potato farms as well as commercial traffic from Canada regularly use this route. The AADT is 700 vehicles/day, and 38 percent are heavy trucks.

The Maine Department of Transportation (ME DOT) considered various options to improve this route. To minimize costs, several alternatives to total reconstruction were evaluated, including FDR with cement stabilization. A project approximately five miles in length was sent to bid in March 2005 for construction during July-September 2005. Contractors had the option of formulating bids based upon two different stabilization alternatives. Based upon cost, cement stabilization was selected for the project.

A total of 90,800 yd^2 of asphalt pavement were reclaimed and mixed with the existing base material using cement as stabilizer. The new base is a mix of 4 percent cement, the existing asphalt pavement (originally about 4 in. thick), and 4 in. of the underlying base material. Water was added to the base materials during construction to reach the optimal moisture content for compaction. The depth of the treated base is now about 8 in., and the surface consists of hot mix asphalt pavement (1-3/4 in. of ½-in base and 1-1/4 in. of 3/8-in. surface). On the northern portion of this project, a short section of the road was left as a control section (no cement treatment to the FDR base) to evaluate the benefits of the cement stabilization over time.

This is the first project in New England that has used the technique of "microcracking" on the CTB. Microcracking is the process of inducing micro-cracks into a CTB layer within 1 to 2 days following compaction. Introduction of small, closely spaced cracks minimizes the probability that the cracks will reflect into the surface layer over time (Sebesta, 2005). On this project, the CTB was subjected to three passes of a steel-drum vibratory roller operating at low speed and high vibration. Microcracking was conducted approximately two days after the cement stabilization was completed.

Initial strength gain and effects of early traffic

In August 2005, during the construction of the CTB, a Clegg Hammer was used to measure the stiffness of the CTB at three test sections. The primary objective was to evaluate the increase in stiffness of the base during the first two days of the cement hydration and to see whether early trafficking reduced the stiffness under the wheel-path locations. Additionally, CIST data were collected at one of the test sections during the third day of curing (after microcracking was conducted). In all three test sections, Clegg Hammer measurements were taken approximately between the wheel paths as well as under the outside wheel path.

As was the case at the Kancamagus Highway site, Route 2A has only one travel lane in each direction, which could not be closed to traffic during construction without affecting the local economy and other industries. ME DOT prohibited traffic from traveling on small stretches of roadway (one lane at a time) during construction operations (pulverization, cement stabilization, and paving). Both lanes were completely opened to traffic at the end of each day. Therefore, the newly stabilized base was essentially subjected to normal traffic, which includes heavily-loaded trucks as described in the previous section of this report.

The three CTB test sections were selected at random, based on the construction schedule for the first week of August 2005. Test sections 1A and 1B were on the same section of road but located in the southbound and northbound lanes, respectively. Reclamation and cement stabilization was conducted at these sections on the morning of August 1, 2005. Test section 2 was located in the northbound lane, several hundred feet away from sections 1A and 1B. Reclamation and cement stabilization was conducted on the morning of August 3, 2005 at that section. The untreated (control) section was not evaluated with the Clegg Hammer due to scheduling incompatibility. The results of Clegg Hammer tests conducted at this site are presented in Section 6 of this report.

6. TEST DATA AND ANALYSIS

LABORATORY TESTING PROGRAM

Laboratory testing included determination of grain-size distributions, moisture-density relationships, UCS values, and moisture susceptibility classifications. The grain-size distribution curves of the test materials (aggregates only and aggregate and RAP mixtures) are shown in Figure 1. Compaction tests following American Association of State Highway and Transportation Officials (AASHTO) T-180-01 Method C were performed to determine the optimum moisture content (OMC) and maximum dry unit weight ($\gamma_{d,max}$) of each material at various cement contents.

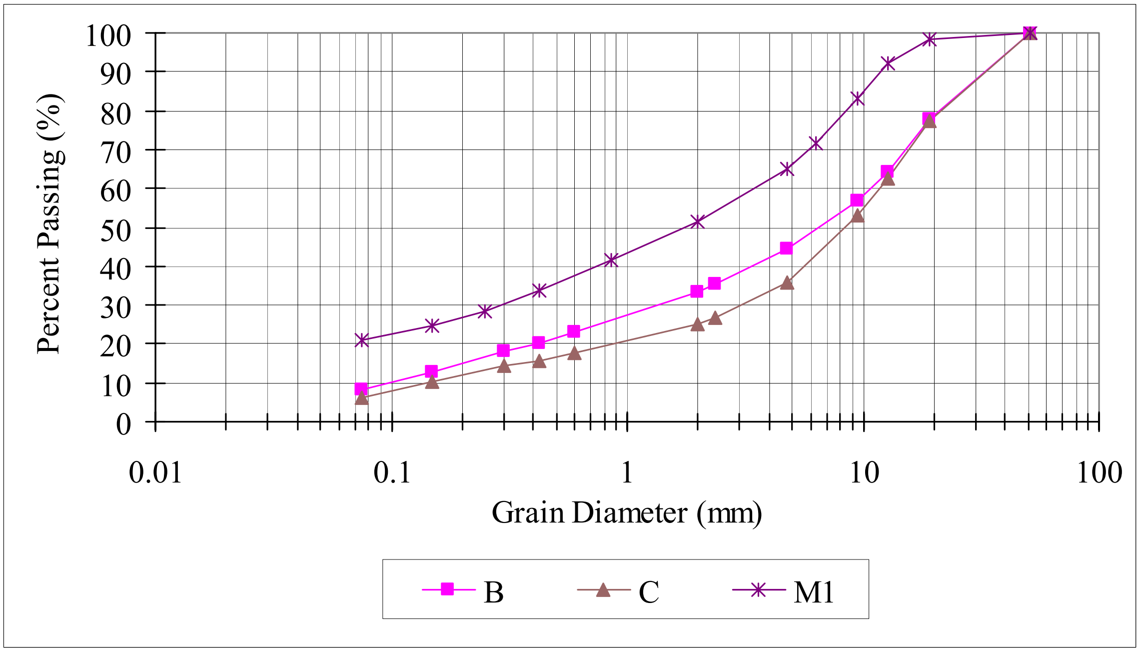

(a) Aggregate only

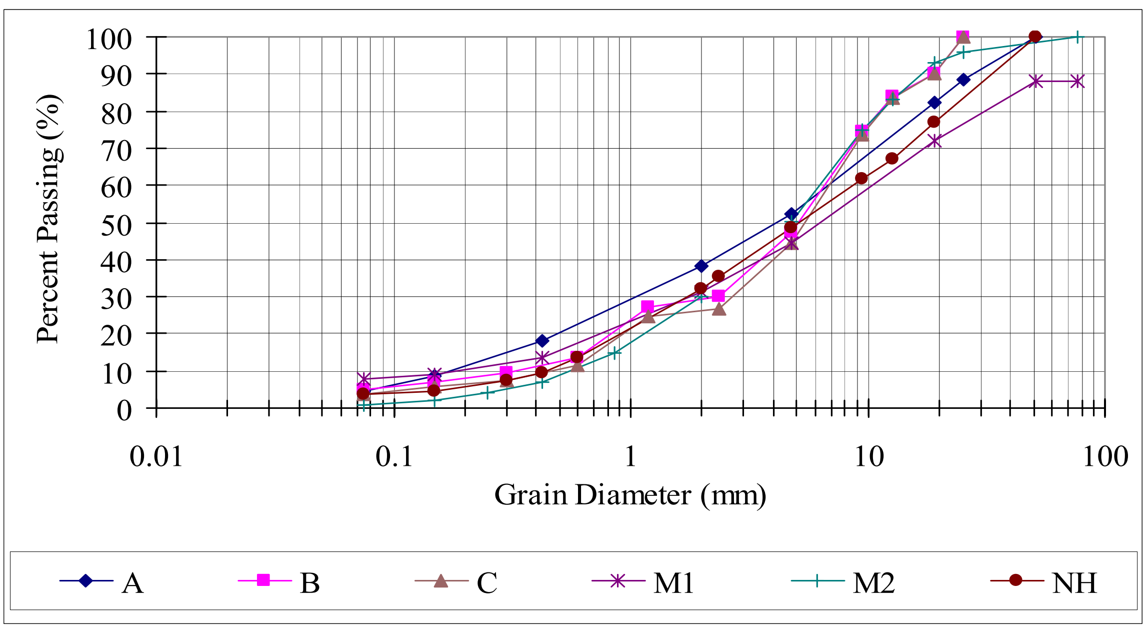

(b) Aggregate and RAP

Figure 1. Grain-size distributions of test materials.

Results of the UCS and TST evaluations are summarized in Figures 2, 3, and 4. For each material (except for material M2), the values plotted in Figures 2, 3, and 4 represent the averages obtained from tests on three replicate specimens (only one UCS test was performed at each cement content for material M2).

Figure 2 shows increasing values of UCS with increasing cement content. At a cement content of 4 percent, the UCS of four of the materials was in the recommended range of 300 to 400 psi (Scullion et al., 2000), while the UCS values of the other two materials (A and M1) approached the target range at cement contents between 2 and 3 percent.

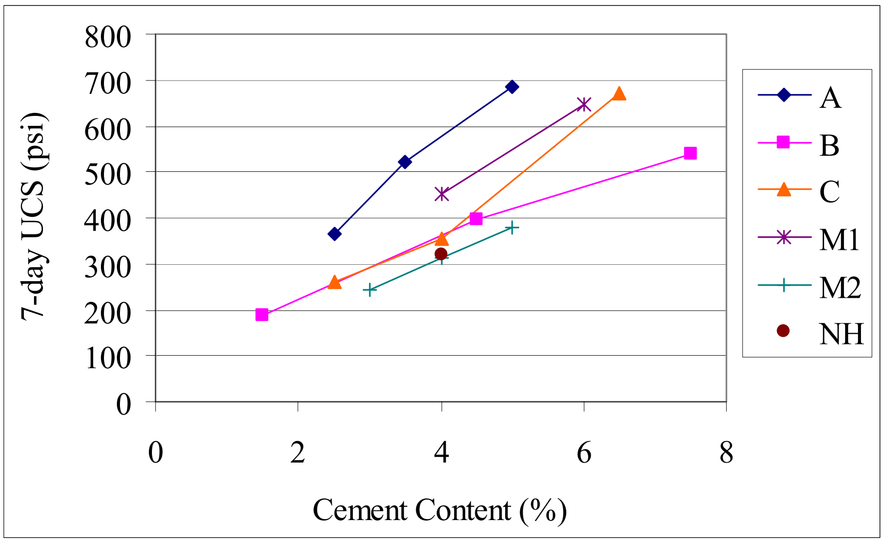

Figure 2. Results of unconfined compression tests.

The TST results in Figures 3 and 4 show some interesting trends in terms of the effect of cement content on moisture ingress for the different materials. Four of the materials show expected decreases in final dielectric value with increasing cement content. However, with the other two materials (B and C), which are both gap-graded as indicated in Figure 1, addition of cement in the range of 1 to 4 percent actually caused the dielectric values to be higher than those exhibited by the untreated specimens. The final moisture contents shown in Figure 4 follow the same trends as the final dielectric values shown in Figure 3. A similar trend (increasing dielectric values at relatively low cement contents) has also been observed in previously published research (Lay, 2005). Although further testing is underway at Brigham Young University (BYU) to investigate these observations, the data suggest that comparatively small doses of cement may effectively increase matric suction potential but inadequately reduce permeability, thereby facilitating elevated levels of moisture ingress. Therefore, for materials B and C, cement contents on the order of 6 to 8 percent may be required to achieve satisfactory durability in terms of capillary rise potential. However, such comparatively high amounts of cement can lead to the occurrence of CTB shrinkage cracking. Thus, for cement stabilization of these materials, microcracking should be considered for construction (Guthrie et al., 2002; Scullion, 2002).

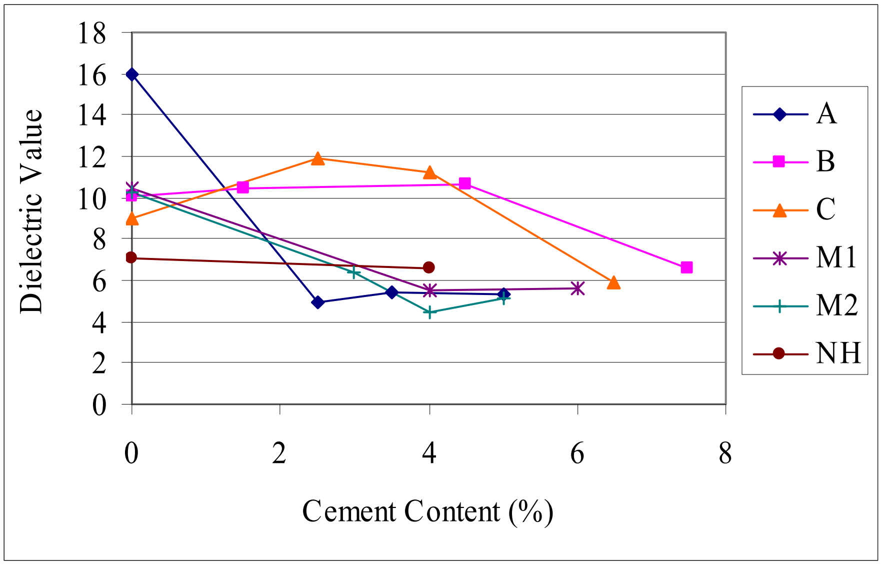

Figure 3. Final dielectric values in tube suction tests.

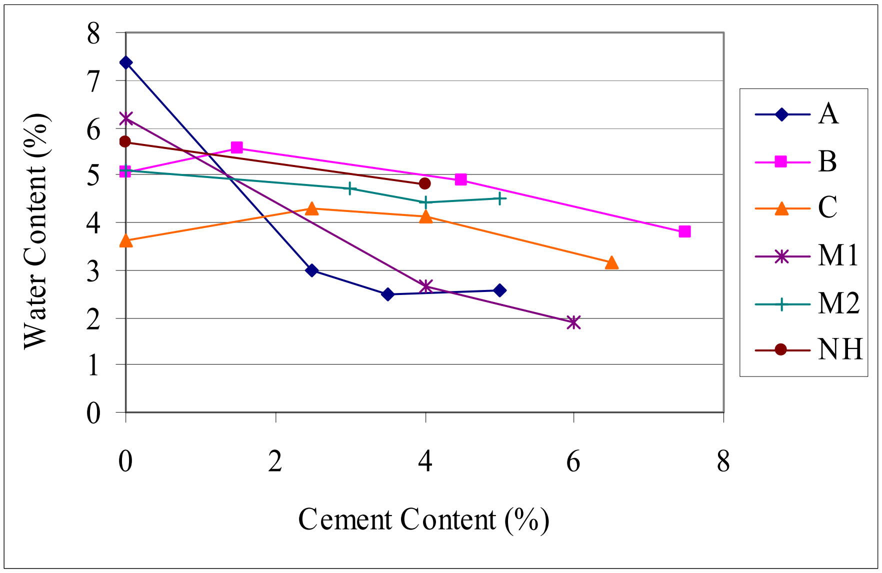

Figure 4. Final water contents in tube suction tests.

FIELD TESTING PROGRAM

Initial strength gain and effects of early traffic

The results of the FWD testing performed in June 2005 on the treated and untreated recycled base materials at the Kancamagus Highway site in NH are presented in Figure 5. Tests in wheel-path (WP) and non-wheel-path (NWP) locations are included. In that figure, each data point represents the average base modulus value computed from the six test point locations between stations 55+37 and 56+37 in the cement-treated section and from six test point locations between stations 60+70 and 61+20 in the untreated FDR section.

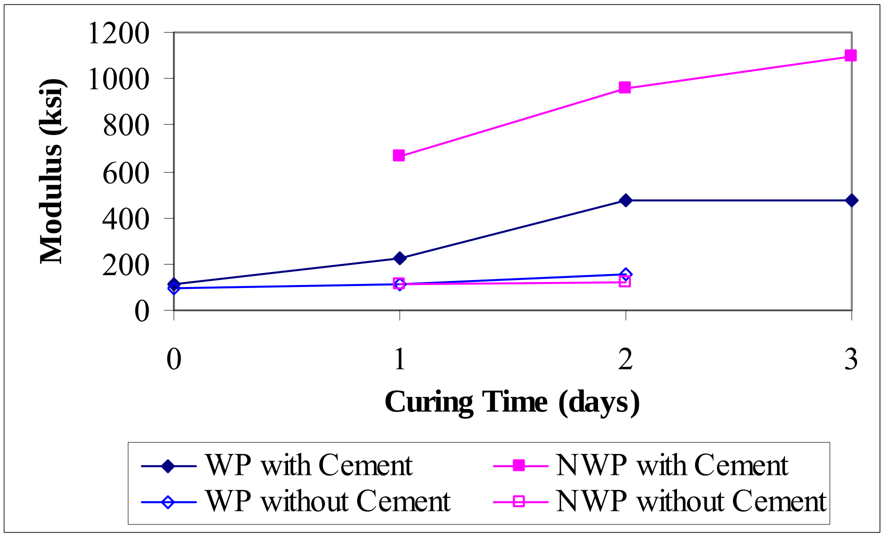

Figure 5. Results of June 2005 FWD testing at Kancamagus Highway site.

The data clearly show an increase in stiffness of the cement-treated material over time. After 2 days of curing, the modulus values in the WP and NWP test areas with cement were 200 and 700 percent greater, respectively, than the corresponding values in test areas without cement. Although the test areas without cement were apparently not sensitive to the trafficking that was permitted on the roadway, the cement-treated areas exhibited approximately 50 percent reductions in FWD base modulus values as a result of the early trafficking.

A similar plot showing the results of the Geogauge testing performed in June 2005 at the Kancamagus Highway site in NH is presented in Figure 6. In that figure, each data point on the first two days of curing represents the average value of stiffness computed from all 20 test point locations established in the cement-treated section (as described in Section 5 of this report). On the third day of curing, Geogauge stiffness measurements were only taken at 14 stations in the cement-treated section (all 8 test point locations between stations 58+80 and 59+50, and half of the test point locations between stations 55+37 and 56+37 and between stations 50+50 and 51+50). For the untreated section, the data points in Figure 6 represent the average value of stiffness computed from all 8 test point locations between stations 60+50 and 61+20.

The Geogauge data also show an increase in stiffness of the cement-treated material over time. After two days of curing, the WP and NWP test areas with cement were 85 and 106 percent stiffer, respectively, than the corresponding test areas without cement. The stiffness values measured by the Geogauge were apparently not as sensitive to the early trafficking as the modulus values determined from FWD testing. The cement-treated areas did, however, exhibit reductions in average Geogauge stiffness of about 26 percent under trafficking during the first day of curing and about 11 percent during the following two days.

Results from the Clegg Hammer tests performed at the Route 2A test site in Maine are presented in Figure 7. In that figure, each data point for Test Sections 1A and 1B represents the average CIST value computed from 5 different locations established about 10 feet apart within those test strips. Data points from Test Section 2 represent average CIST values computed from 7 different locations established about 10 feet apart within that section.

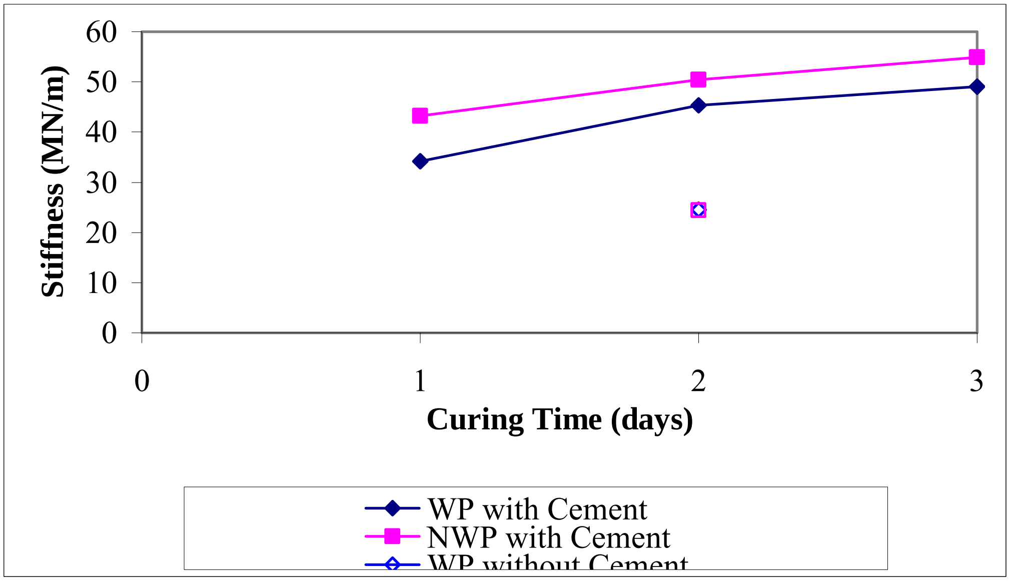

Figure 6. Results of June 2005 Geogauge testing at Kancamagus Highway, NH site.

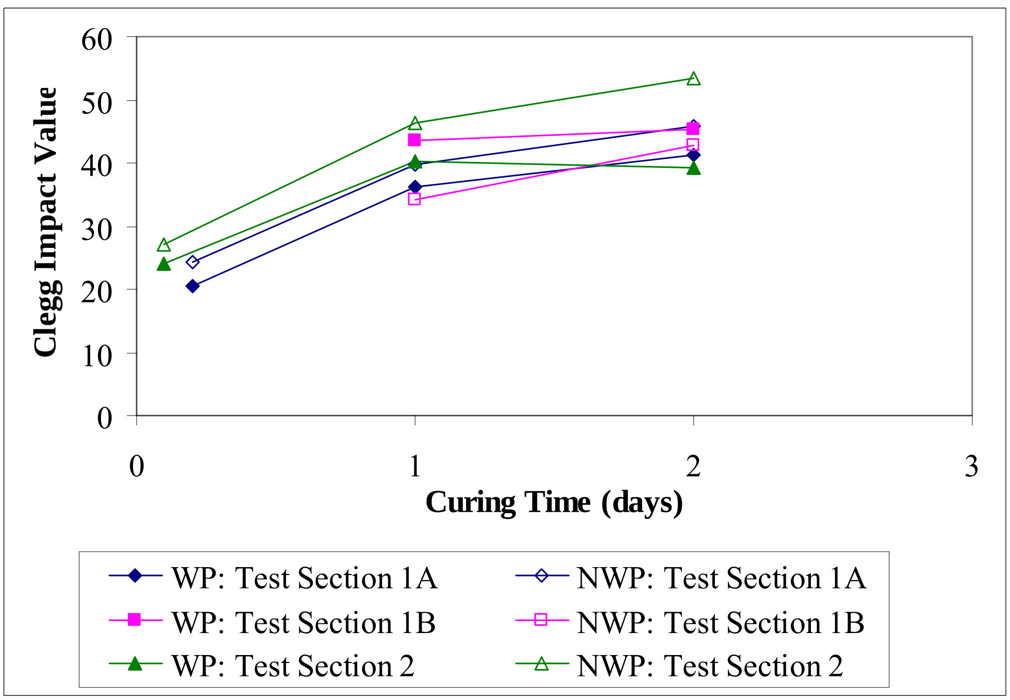

Figure 7. Results of August 2005 CIST testing at Reed Plantation, ME site.

Like the FWD and Geogauge data obtained at the Kancamagus Highway, NH, site, the CIST data from Maine also show significant increases in the stiffness of the CTB during the first two days of curing. At that site, average CIST values in the NWP locations in Test Section 1A and Test Section 2 were always larger than average values in corresponding WP locations. On the other hand, at Test Section 1B, average CIST values measured in the NWP locations were lower than the average values in corresponding WP locations. As noted previously, at the Maine test site, CIST data were collected in cement-treated sections only. The untreated (control) section was not evaluated with the Clegg Hammer due to scheduling incompatibility.

Statistical analyses were performed on the data sets from both the New Hampshire and Maine test sites to evaluate the effects of early traffic on the CTB materials. Paired *t*-tests were performed on each data set to investigate the significance of the differences between measurements taken under the wheel paths (WP) and those taken between wheel paths (NWP). The paired *t*-test is one type of hypothesis test that is commonly used as a method of statistical inference. To conduct a hypothesis test, two opposing hypothetical statements are set up to describe the data (the null hypothesis, H_o, and the alternative hypothesis, H_A). Usually, the alternative hypothesis describes what one is attempting to prove true. There are three kinds of hypothesis tests: left-tail, right-tail and two-tail. If one is trying to show that a sample mean is less than a given value, then a left-tail test is appropriate. Conversely, if one is trying to show that a sample mean is greater than a given value, then a right-tail test is appropriate. If one is attempting to detect a significant change in either direction, then a two-tail test is appropriate. Because it is easier to achieve "significant" results in a one-tailed test, they should be used cautiously and only if clearly warranted by the situation. Therefore, for this project, two-tailed tests were conducted. In these analyses, the null hypothesis was that the mean percent difference between WP and NWP measurements was equal to zero; the alternative hypothesis was that the mean percent difference was not equal to zero.

Statisticians typically set a limit, referred to as the significance level or standard error rate, which is quantified by "*p*-values." A generally accepted value for the significance level is 0.05, which means that if the *p*-value is higher than 0.05, the null hypothesis will not be rejected. Results of the paired *t*-tests performed on the field data from this project are tabulated in Appendix E.

At the standard error rate of 0.05, the FWD and Geogauge data from the NH site clearly show a statistically significant difference between WP and NWP measurements in the cement-treated test section, while the differences between WP and NWP measurements in the untreated test section are not significant.

At the Maine test site, although average CIST values in the NWP locations in Test Section 1A were always larger than average values in corresponding WP locations, the difference was statistically significant only on the day of construction (August 1, 2005). At Test Section 2, the difference was significant on the day of construction (August 3, 2005), as well as after approximately two days of curing (August 5, 2005). The 18.6 percent average increase in stiffness measured at that test section after one day of curing was not statistically significant, however. As noted previously, at Test Section 1B, average CIST values measured in the NWP locations were lower than average values in corresponding WP locations. At that test section, the difference was significant after one day of curing, but not after two days.

As discussed in Section 5 of this report, microcracking was conducted at the test site in Maine. Microcracking (three passes of a steel-drum vibratory roller operating at low speed and high vibration) was performed at Test Section 1A on 8/3/05 after about two days of curing. Average CIST values measured on 8/4/05 were 31.1 and 36.4 in the WP and NWP locations, respectively. Those values represent reductions in stiffness of 24 percent and 21 percent compared to the values measured in WP and NWP locations, respectively, just prior to microcracking. Those reductions in stiffness are somewhat less than reductions in FWD modulus values reported by Sebesta (2005) on a project in Texas where microcracking was utilized after one day of curing on a project with a reclaimed base stabilized with 4 percent cement. On that project, reductions in the average base modulus of 25 percent and 60 percent were observed after two and three passes of microcracking, respectively. FWD tests conducted after microcracking indicated that modulus values rebounded to levels comparable with those measured before cracking within two days, and that additional curing resulted in additional increases in modulus (Sebesta, 2005).

Comparison of Figures 6 and 7 yields another interesting observation. Despite the fundamental difference in units between the Geogauge and the CIST measurements, the values are remarkably similar when the Geogauge stiffness is presented in metric units, which is the default mode of operation for that device. After two days of curing, average values of stiffness measured with the Geogauge on CTB test sections in NH were 45 and 50 MN/m for the WP and NWP locations, respectively. On the third day of curing, corresponding average values of 49 and 55 MN/m were observed. At the test site in Maine, average CIST values ranged from 41 to 46 after two days of curing at Test Sections 1A and 1B; after two days of curing at Test Section 2, there was a more substantial difference between WP and NWP values (39 and 53, respectively). Similar trends were reported by Guthrie (2005), who used both a soil stiffness gauge (SSG) and a heavy Clegg impact soil tester (CIST) for evaluating strength and stiffness of cement-treated base materials at three test strips on a pavement reconstruction project in Morgan, Utah. After approximately two days of curing on that project, SSG average values of 35, 39 and 43 MN/m were observed at test strips 1, 2 and 3, respectively. Corresponding average CIST values were 28, 35 and 38, respectively, at the three test strips (Guthrie, 2005). It should be noted that 2 percent cement was added to the FDR base at the Utah test site, whereas 4 percent cement was added in both the New Hampshire and Maine test sites. Although further research is needed to fully define appropriate thresholds for these testing methods, these data suggest that both the SSG and the CIST show much promise as tools for certifying that a CTB material has sufficient strength and stiffness to withstand traffic loading.

Long-term monitoring of test sections

As discussed in Section 5 of this report, instrumentation was installed to monitor subsurface moisture and temperature regimes, and an optical survey and FWD testing was performed to measure heave and deflection-related pavement parameters, respectively, during the 2005-2006 winter and spring at the New Hampshire test site. Groundwater elevations measured in OWs from July 2005 through June 2006 are presented in Figure 8. It should be noted that the top of pavement is at approximately elevation 1228 in the western portion of the site (in the conventional reconstruction section). The top of pavement slopes down to about elevation 1225 at the eastern end of this site (in the FDR test sections).

Groundwater elevations measured from July through early September, 2005, ranged from about elevation 1216 to 1217 in OW-2, OW-3, and OW-4, which was relatively close to the bottom of those wells. The bottom of OW-1 is at elevation 1218.6, and groundwater was not encountered in that well during that period. In mid to late October, 2005, the water table rose substantially as a result of heavy rains that occurred during hurricanes that month. On October 28, groundwater was encountered at elevation 1222.6 in OW-1 and at about elevation 1220.7 at OW-2 and OW-3.

It is interesting to note that in the October 2005 readings, as well as in the mid-January 2006 readings (which were also obtained after a substantial rainfall event), the water table at OW-1 was 2 to 3 feet higher than at OW-2 and OW-3. Thus, there may be some spatial variability in subsurface groundwater flow patterns that causes localized spikes in the water table in the western portion of this site after heavy rainfall events.

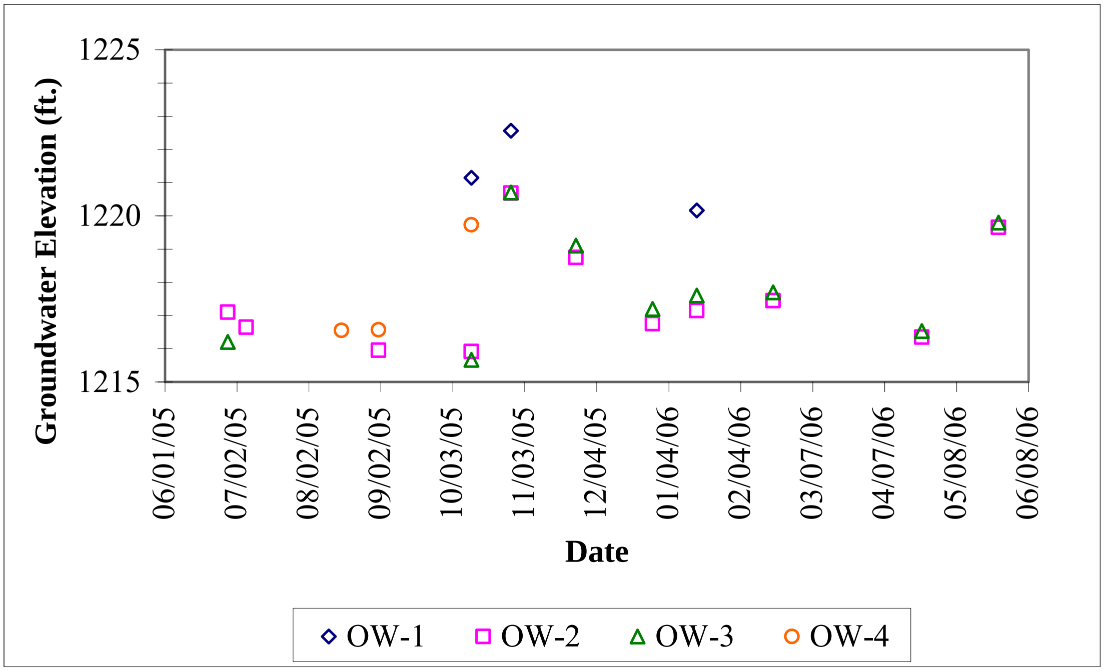

Figure 8. Groundwater Elevations at Kancamagus Highway, NH site.

Optical survey measurements obtained during the 2005-2006 winter and spring to evaluate frost heave in the three test sections are presented in Figure 9. Baseline (i.e., "zero heave") data were collected just after the final paving operations in October 2005. While heave in the conventional reconstruction section appears to be negligible, a substantial amount of heave occurred in both of the FDR test sections. Although there is no obvious explanation for why the cement-treated section appeared to heave more than the untreated FDR section, it is likely that the differences between the conventional reconstruction section and the two FDR sections may be due to differences in subgrade soils, as discussed in the following paragraphs.

Sieve analyses were performed on samples of the native subgrade soils obtained during drilling operations at this site, as described in Section 5 of this report. The results of those analyses are presented in Figures 10 and 11 for the FDR and the conventional reconstruction test sections, respectively. Figure 11 also includes grain-size distribution curves for the fill materials (crusher run gravel and crushed gravel) that were used to replace existing subgrade soils above a depth of about three feet in the conventional reconstruction test section.

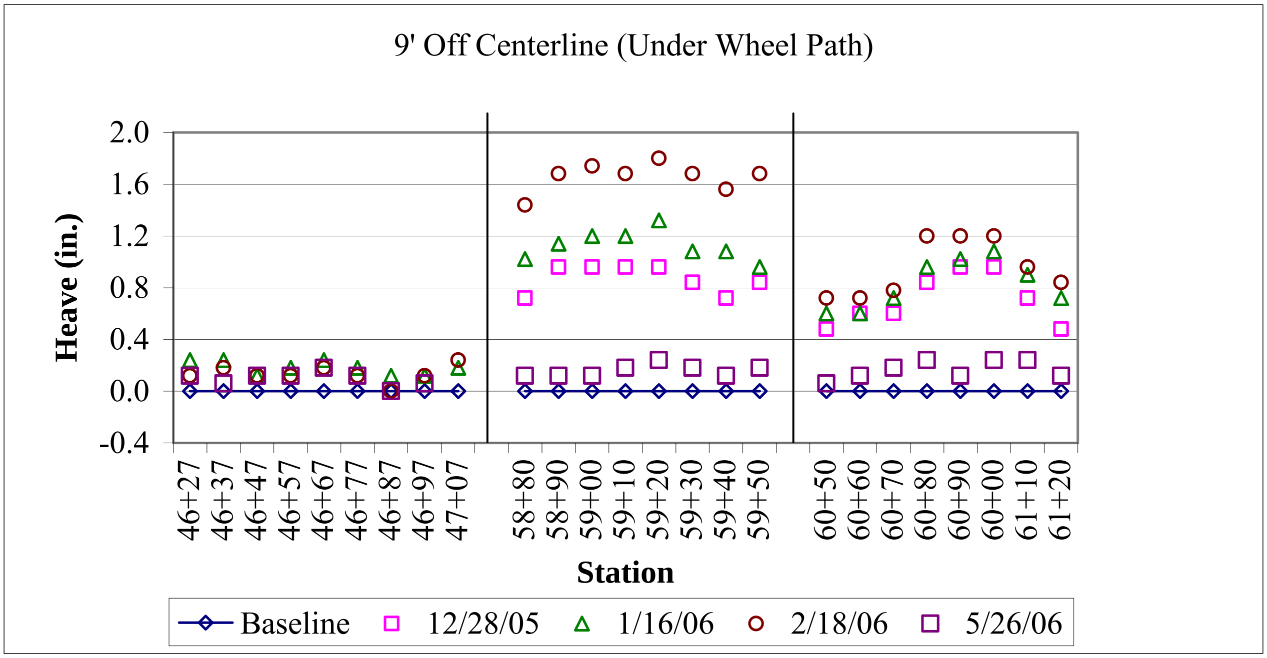

(a) Measurements under wheel paths

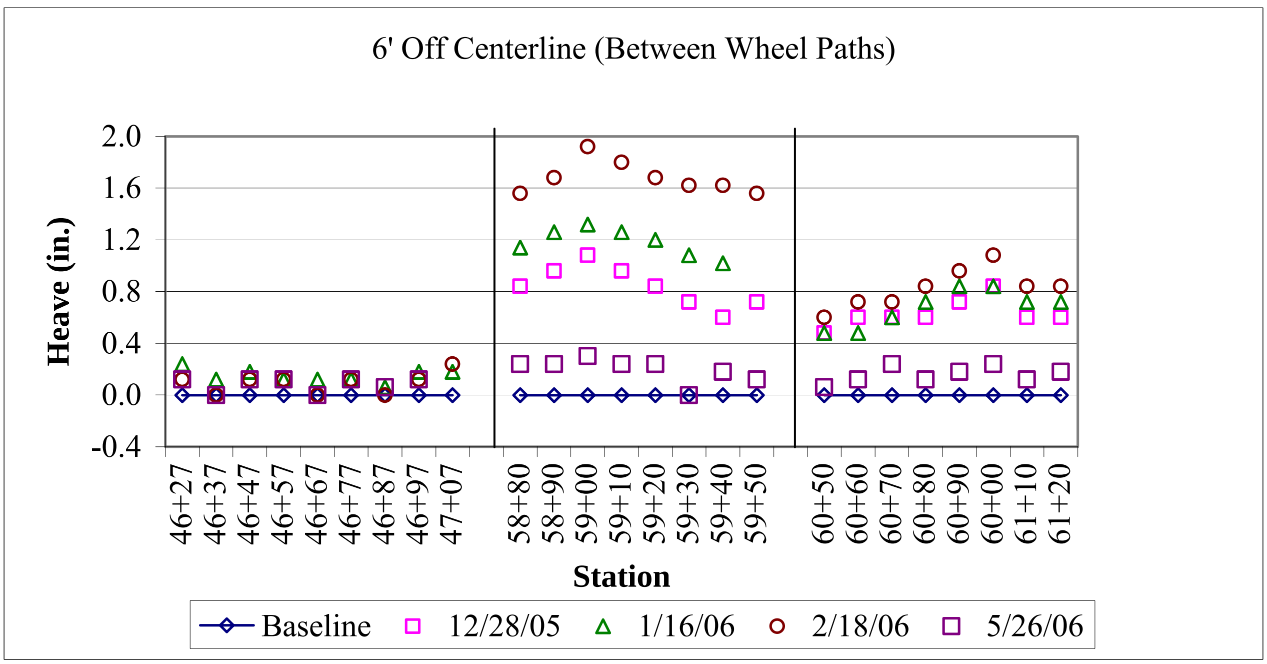

(b) Measurements between wheel paths

Figure 9. Optical survey data from Kancamagus Highway, NH site.

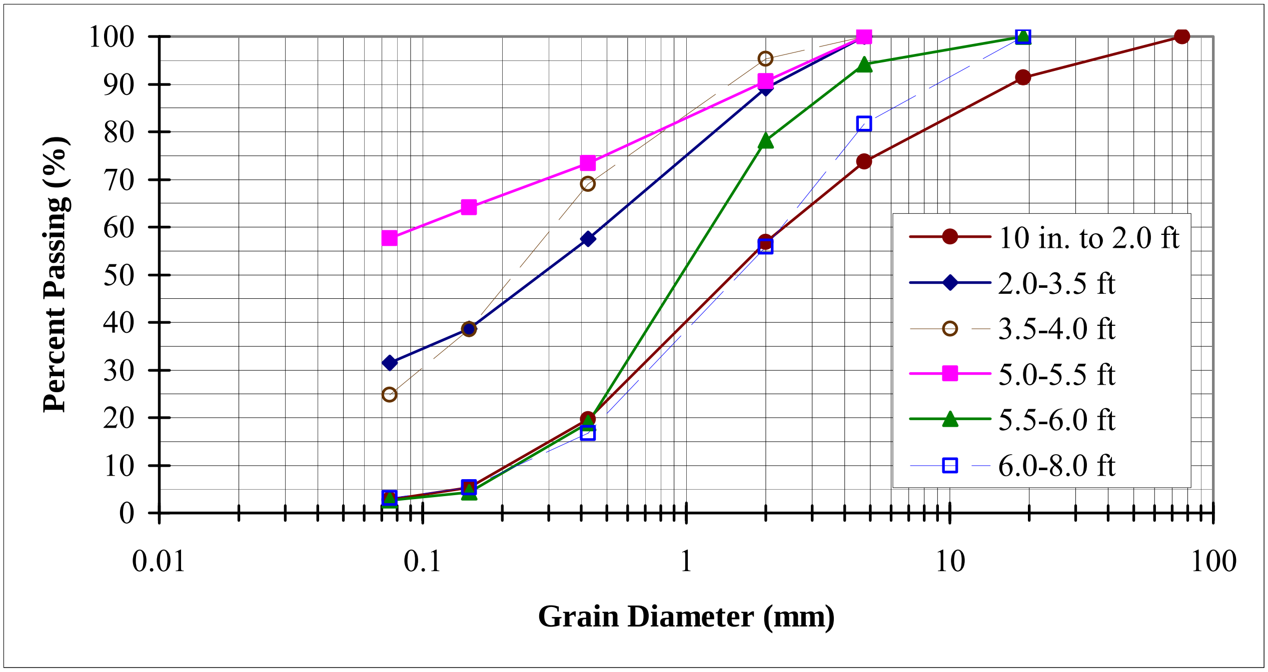

Figure 10. Grain-size distribution of subgrade soils in the FDR test sections at the Kancamagus Highway, NH site.

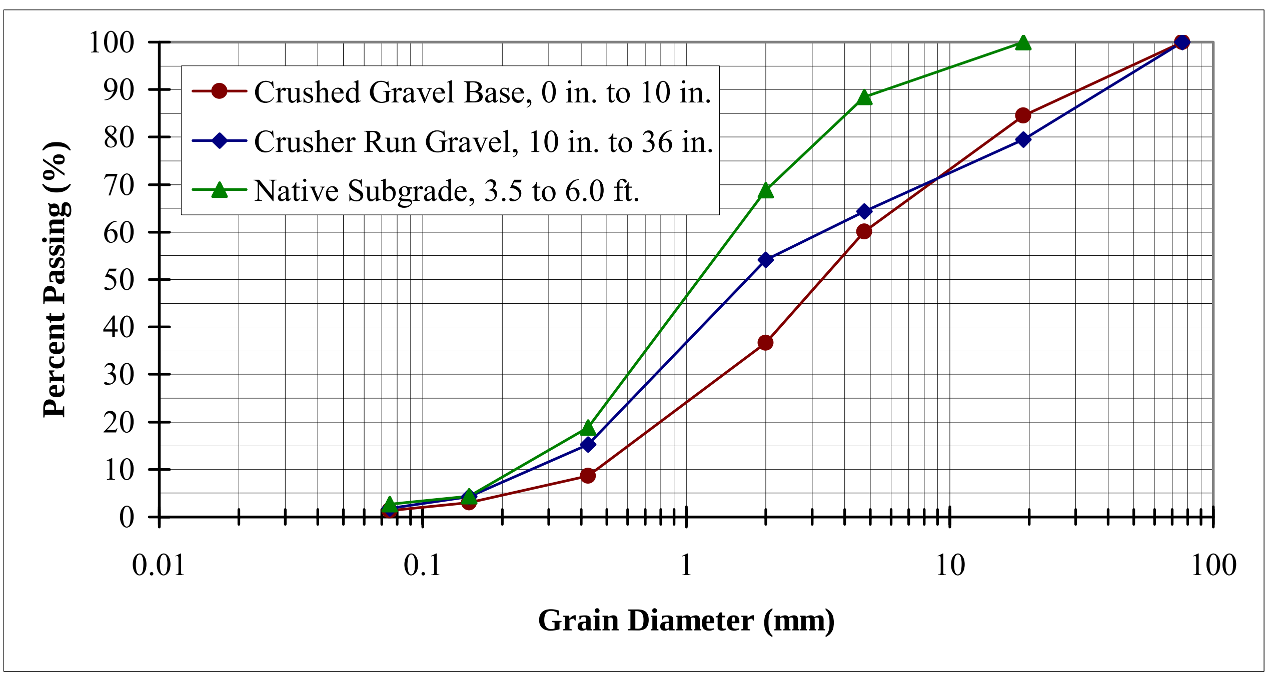

Figure 11. Grain-size distribution of the fill and subgrade soils in the conventional reconstruction test section at the Kancamagus Highway, NH site.

Figures 10 and 11 exemplify the substantial difference in subgrade soils that exist in the FDR test sections as compared to the conventional reconstruction test section. In the FDR sections, the material between about 2.0 and 5.5 feet below existing grade contains a significant amount of fines (between 25 and 58 percent). On the other hand, the soils within that same depth range in the conventional reconstruction section contain less than 3 percent fines. Therefore, it is likely that increased frost-susceptibility resulted from the higher fines content in the subgrade soils beneath the FDR base materials.

As discussed in Section 5 of this report, thermistor readings were obtained by USDA Forest Service personnel at three of the thermistors (one in each test section) approximately every one to two weeks during the 2005-2006 winter/spring monitoring period. The thermistor locations and data obtained during the monitoring period are tabulated in Appendix D, and plots of data obtained on selected dates are presented in Figures 12 through 17. It should be noted that the ambient air temperatures tabulated in Appendix D were measured at the thermistor readout post locations in the shade. Therefore, they are not necessarily representative of the air temperatures that may have existed above the pavement on the roadway.

Data indicate that, although frost had penetrated at least three feet below the top of pavement in all three test sections by mid-January, unusually warm winter temperatures brought most of the base and subgrade temperatures up to almost 32^{o} F during early February, as shown in Figures 12 and 13. Subsequent cold weather brought subsurface temperatures well below freezing again by March 1 (see Figure 14). On that date, the depth of frost penetration was about 42 in. below the top of the pavement in the cement-treated section and greater than 64 in. below the top of the pavement in the conventional reconstruction section. Because the thermistor installed in the untreated FDR section was relatively short, data were not obtained below a depth of about 41 in. in that test section. The base and subgrade soils began to thaw again during the month of March. On March 27, the base materials were all thawed, and the subgrade soils were thawed and/or just on the verge of thawing, as shown in Figure 15.

It can be seen in Figures 12 through 17 that the subsurface temperatures measured in the conventional reconstruction section were consistently lower than those measured in the two FDR test sections. While this may possibly be related to material property differences, it is more likely that the variations resulted from differences in exposure to sunlight. Although all three test sections were located along a relatively straight stretch of roadway, the Forest Service personnel observed that the conventional reconstruction section seemed to be much more shaded than the other two test sections. On the other hand, they also noted that there was not any significant difference in sunlight between the cement-treated and the untreated FDR test sections. In light of those observations, the modest differences in the temperature profiles in the two FDR sections may indicate that the cement provided somewhat of an insulation effect. For example, during freezing periods (January 10, 2006 and March 31, 2006 readings), the temperatures in the cement-treated section were slightly greater than the temperatures at corresponding depths in the untreated FDR section.

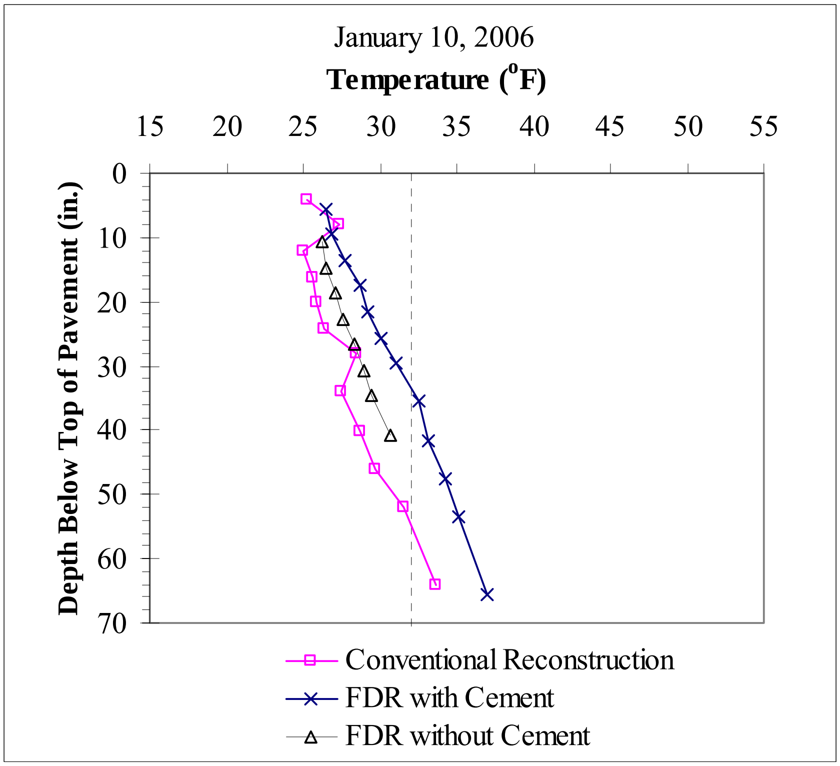

Figure 12. Thermistor data from Kancamagus Highway, NH site: January 10, 2006

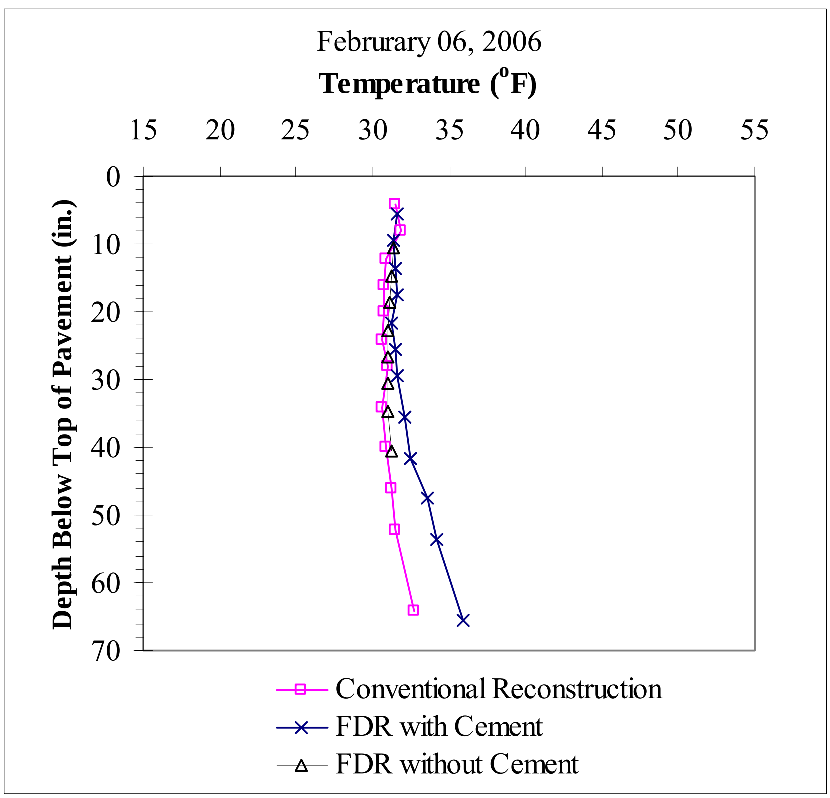

Figure 13. Thermistor data from Kancamagus Highway, NH site: February 6, 2006

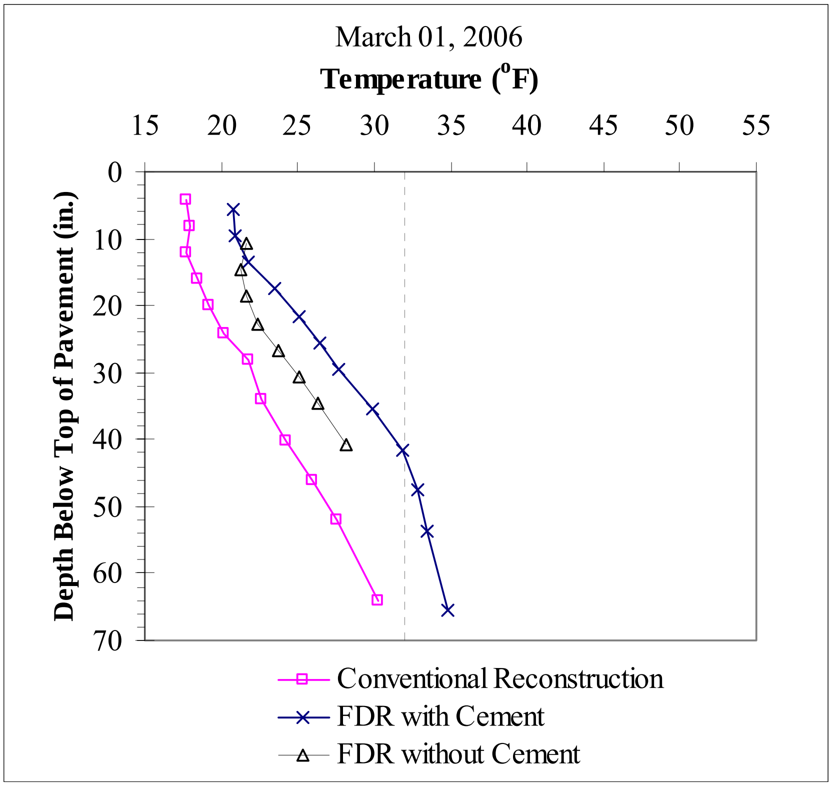

Figure 14. Thermistor data from Kancamagus Highway, NH site: March 1, 2006

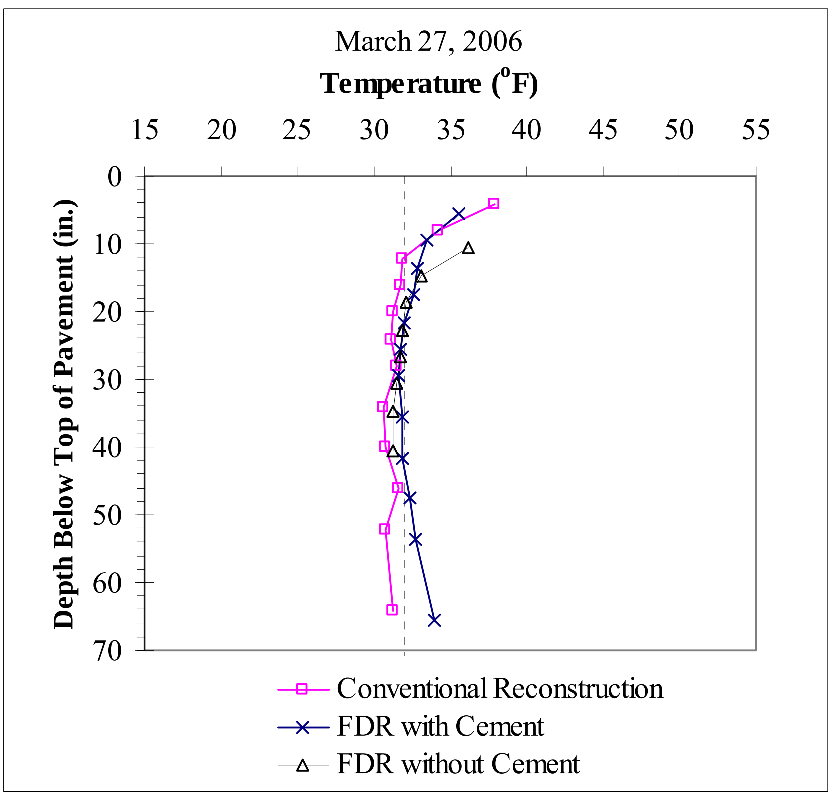

Figure 15. Thermistor data from Kancamagus Highway, NH site: March 27, 2006

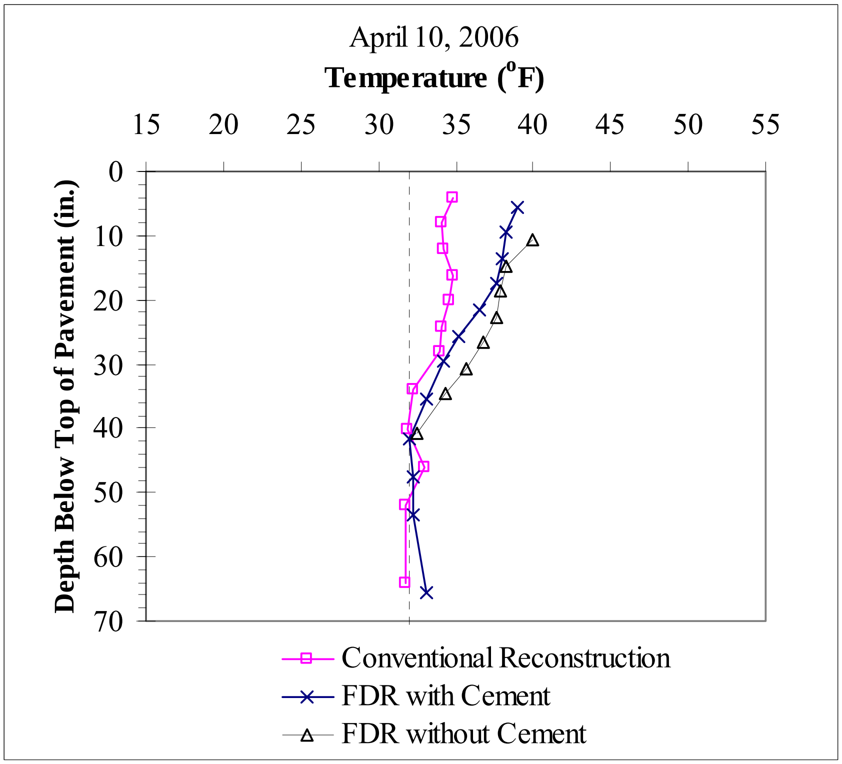

Figure 16. Thermistor data from Kancamagus Highway, NH site: April 10, 2006

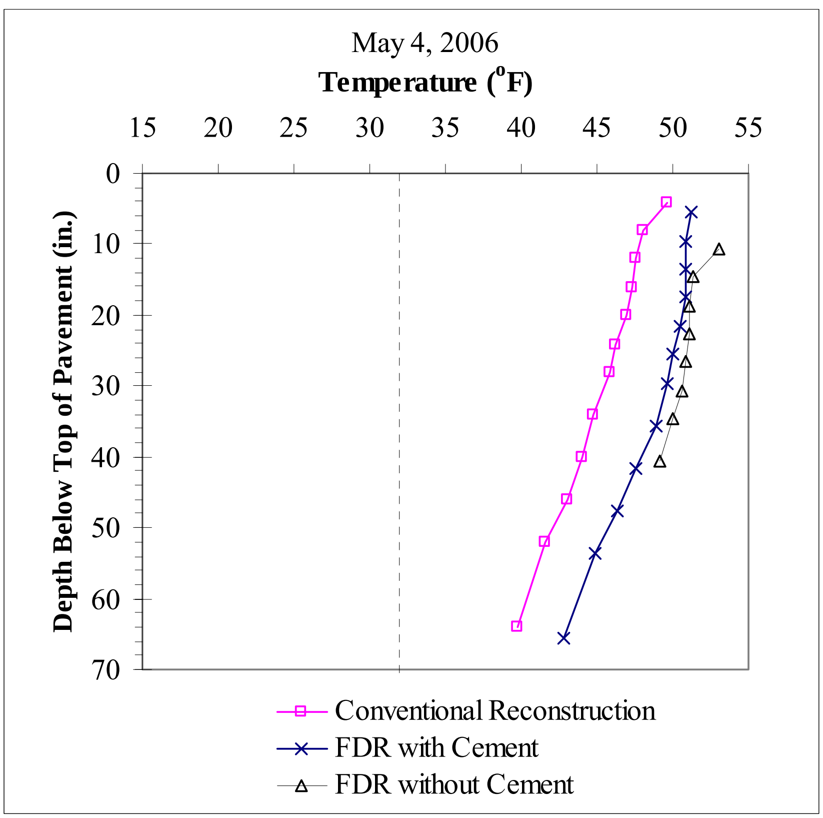

Figure 17. Thermistor data from Kancamagus Highway, NH site: May 4, 2006

As described in Section 5 of this report, FWD testing was conducted at this site as part of an ongoing collaborative research effort led by USDA Forest Service personnel to study the effects of spring thaw on pavement surface and base materials. FWD testing was conducted in October 2005 to provide baseline data just after final paving operations, and then again in March, April, and May 2006 to provide data for the spring thaw study. Testing was performed on an in-kind basis by personnel from Eastern Federal Lands Division of FHWA (October 2005) and by personnel from WPI (March, April, and May 2006). Data from FWD tests were shared with the research team at UMD, who conducted analysis of several deflection-related pavement parameters including adjusted center deflection, area parameter, SCI, shape factor and subgrade modulus. The significance of these parameters and the methods used to compute them are described in Section 5 of this report; results are presented in Figures 18 through 22 and are discussed in the following paragraphs. In Figures 18 through 22, each data point represents the average value of a given parameter computed from the eight locations established in each test section, as described in Section 5.

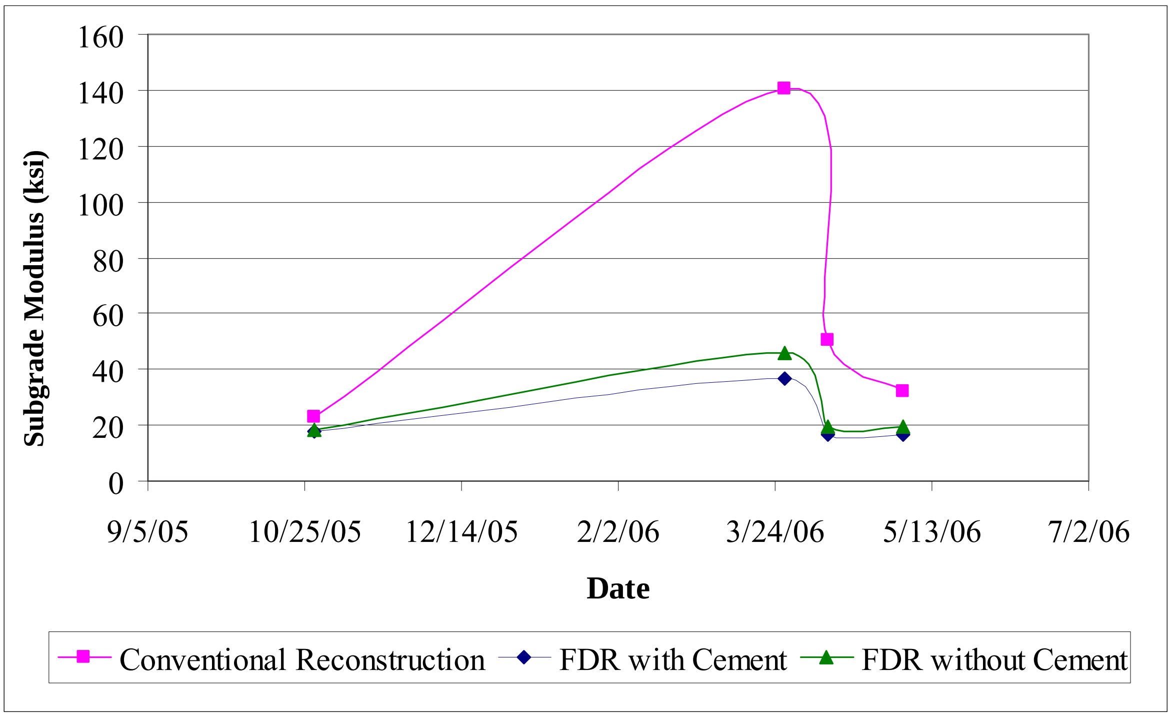

Figure 18. Subgrade modulus values at Kancamagus Highway, NH site

The average subgrade modulus values computed from the FWD deflection data are presented in Figure 18. The modulus values in the two FDR test sections were approximately equal to one another on any given date, whereas the moduli in the conventional reconstruction section tended to be higher than those in the FDR sections. This makes sense, given the higher fines content of the subgrade soils beneath the FDR base materials, as indicated in Figures 10 and 11. The spike in modulus values (in all three test sections) in the March 27, 2006, data is reflective of the fact that the subgrade became stiff as a result of freezing temperatures during much of the winter, as illustrated in Figures 12 through 15.

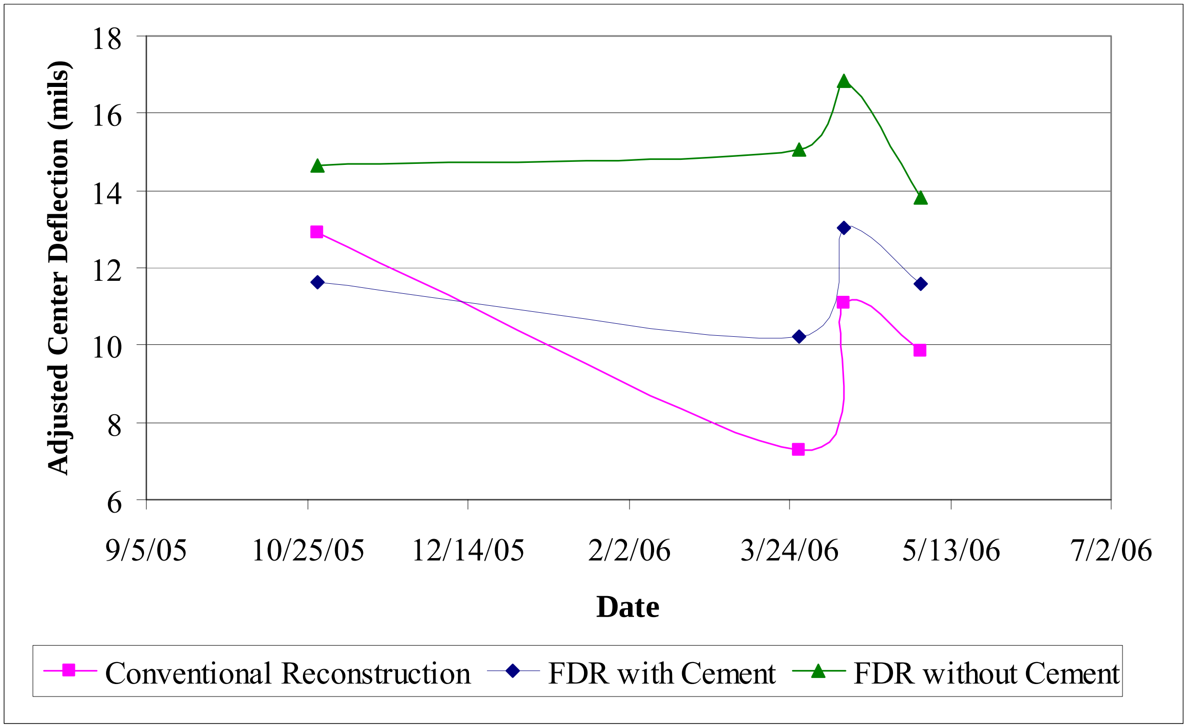

Figure 19. Adjusted center deflection values at Kancamagus Highway, NH site

Average temperature-adjusted center deflection values are presented in Figure 19. As discussed in Section 5, while the outer FWD deflection sensors respond primarily to the subgrade characteristics, the deflections at the inner sensors respond to the combined characteristics of the subgrade and upper pavement layers (FHWA, 1994). Since the subgrade is more or less the same beneath the two FDR test sections, comparison of those two data sets clearly shows the beneficial effect of the cement in stiffening the base layer and thus reducing the magnitude of deflection under loading on any given date. Since the soft fine-grained subgrade soils in the conventional reconstruction section were removed and replaced with select fill, it is likely that the lower deflections generally observed in that test section resulted from the stiffer subgrade soils. The spike in center deflection values measured in all three test sections on April 10, 2005, reflects the fact that the pavement system became weaker just after the base and subgrade materials thawed. The center deflection values then decreased as the base and subgrade soils subsequently recovered strength and stiffness later in the spring.

It is interesting to note that the adjusted center deflection in the conventional reconstruction section was higher than that measured in the cement-treated FDR section on October 28, 2005. This may be reflective of the fact that the conventional crushed gravel base was much more permeable than the cement-treated FDR base material. As described previously, there was a lag of three to four months between base rehabilitation/reconstruction and paving operations (which were conducted in late October), and there were periods of heavy rain that occurred during hurricanes in October 2005. Prior to paving, the crushed gravel base may have allowed more moisture to penetrate into the underlying subgrade and temporarily soften that material.

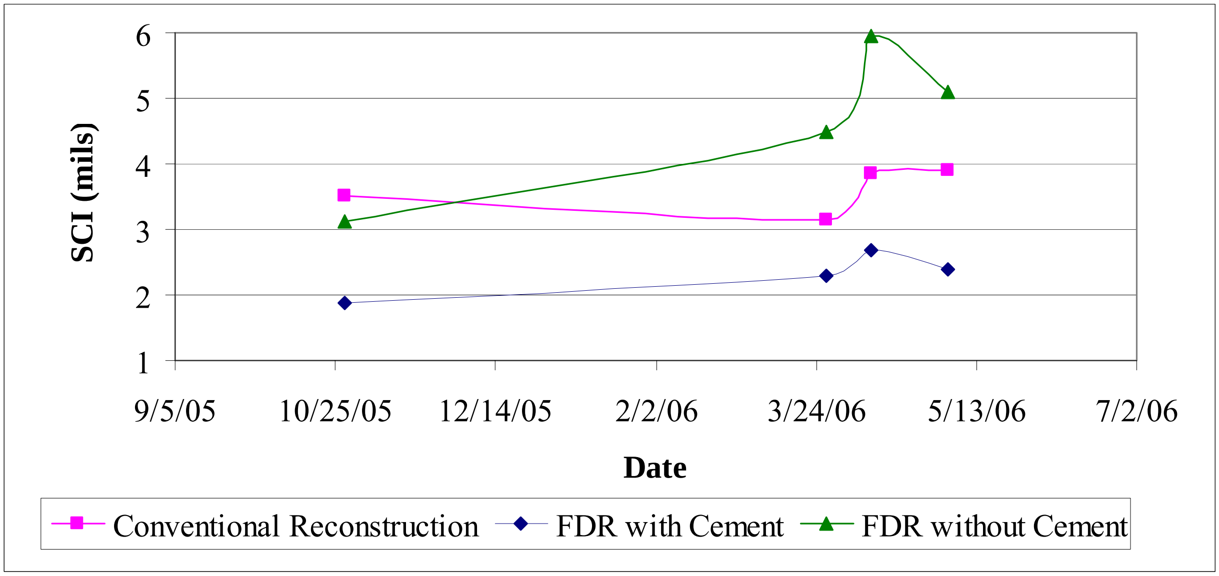

Figure 20. SCI values at Kancamagus Highway, NH site

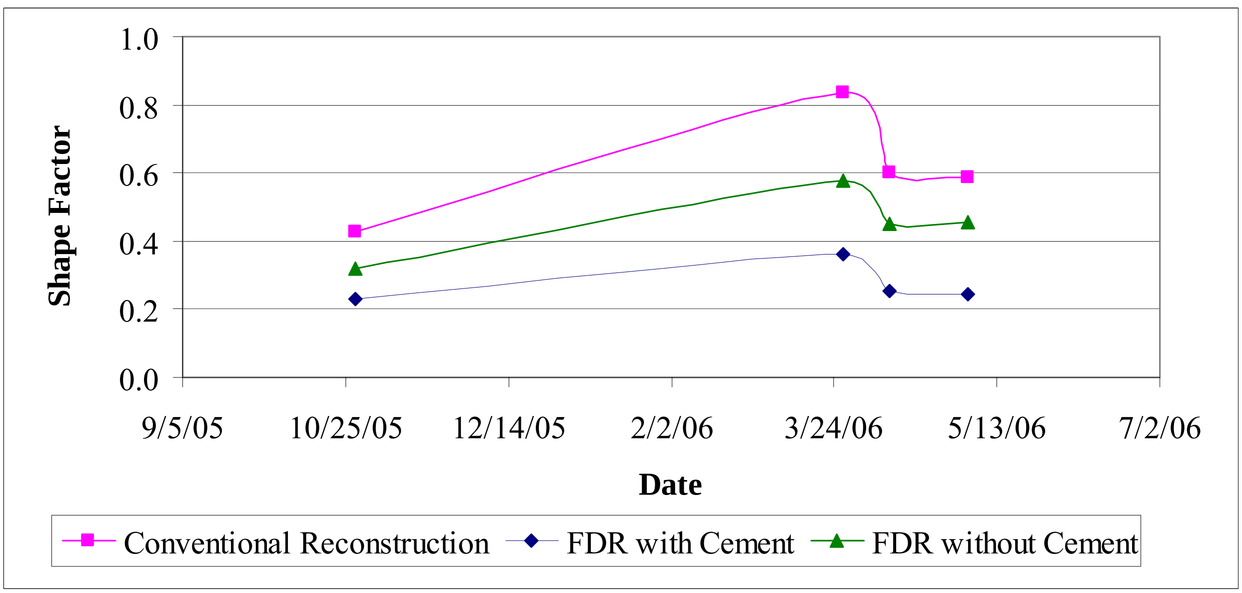

Figure 21. Shape factor values at Kancamagus Highway, NH site

Values of SCI and shape factor are presented in Figures 20 and 21, respectively. As noted previously, the SCI and shape factor are both related to the slope of the deflection basin close to the FWD load plate and are therefore considered to give an indication of the relative stiffness of the upper pavement layers (FHWA, 1994). The greater stiffness of the CTB is indicated by the consistently lower values of SCI and shape factor shown in Figures 20 and 21.

The general shape of the SCI curves shown in Figure 20 are comparable with the shape of adjusted center deflection curves presented in Figure 19, where the increased values on April 10, 2006 are reflective of reduced stiffness that occurred just after the base and subgrade materials thawed. The shape factor curves in Figure 21 show trends that are more similar to the subgrade modulus curves presented in Figure 18, possibly indicating that this parameter is influenced by subgrade stiffness in addition to being influenced by the stiffness of the upper pavement layers.

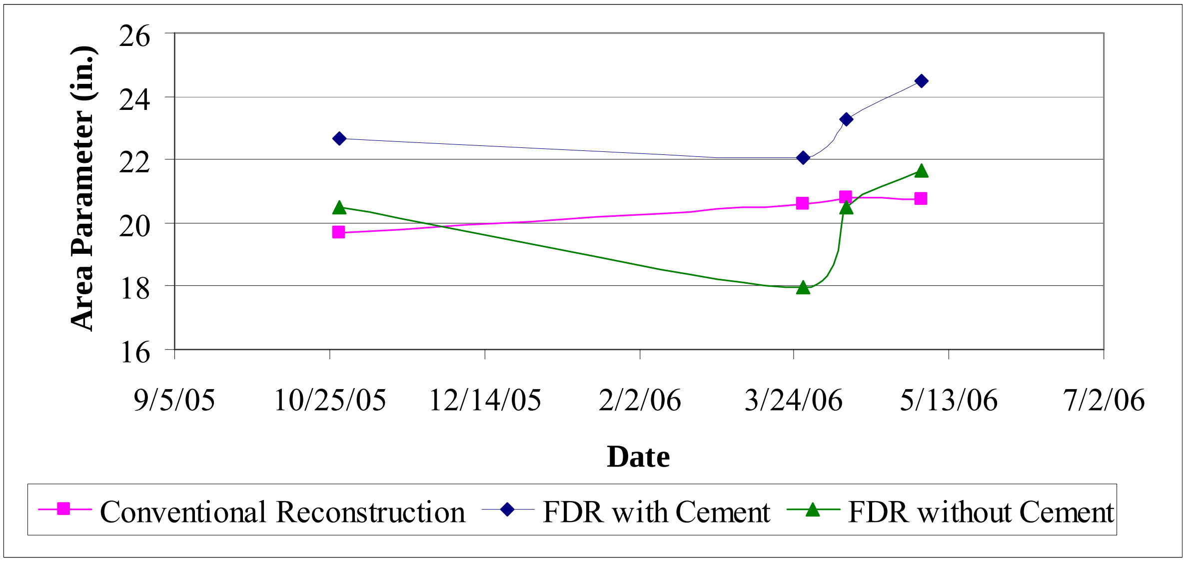

Figure 22. Area parameter values at Kancamagus Highway, NH site

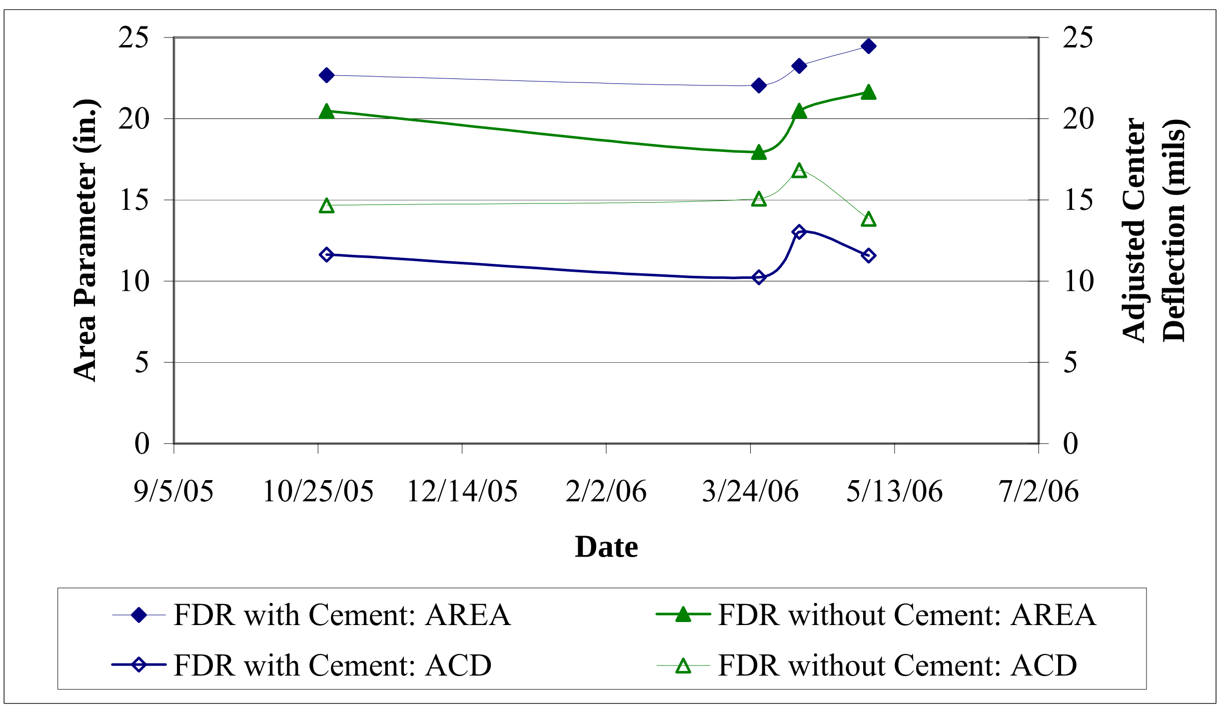

Figure 23. Area parameter and adjusted center deflection values in FDR test sections at Kancamagus Highway, NH site

Area parameter values computed using the FWD-AREA computer program (WSDOT, 1999) are presented in Figure 22. While the shapes of the curves are similar for the two FDR test sections, the trends observed in the conventional reconstruction test section do not follow a similar pattern and cannot be readily explained. The area parameter values obtained in the FDR test sections can be more easily interpreted by considering those values in conjunction with the corresponding adjusted center deflection (ACD) values, plotted together in Figure 23. The increases in both area parameter and center deflection that occur between March 27, 2006 and April 10, 2006 reflect the weakening of the pavement system that occurred during that period. Since the area parameter is normalized by dividing the area under the deflection basin by the adjusted center deflection (see Equation 2), the further increases observed in area parameter between April 10 and May 4, 2006 may be due either to the subsequent reduction in center deflections, and/or to the fact that the pavement system had not fully recovered during that period.

Finally, personnel from the research team visited both the test site in Maine and the test site in New Hampshire during the summer of 2006, approximately one year after construction, to document any signs of pavement distress. The only damage observed was at the test site in Maine, in the vicinity of a culvert that had not been placed deep enough. In the southbound lane at that location, a crack developed above the culvert, and two more cracks developed a couple of feet to the right and left of the culvert. Since no other signs of distress were observed at that site, it is reasonable to assume that those cracks are due to a localized problem involving the depth of the culvert. To this date, there are no other signs of any distress at that test site in Maine or at the test site in New Hampshire.

7. NUMERICAL MODELLING

The addition of cement increases the strength and stiffness of FDR base materials and therefore offers greater structural support to the surface layer and greater protection of the underlying subgrade. However, the use of excessive amounts of cement can produce overly stiff base materials that exhibit brittle behavior under heavy traffic loading; the susceptibility of CTB materials to cracking increases with increasing stiffness.

For design of cement-treated bases, knowledge of the fatigue life of CTB layers is useful, especially in situations in which the base layer will be expected to bridge over weak subgrades. For example, during spring in cold regions, frost-susceptible subgrade soils may exhibit severe thaw weakening and markedly reduced bearing capacities. In this situation, the decreased support beneath the CTB layers permits the occurrence of greater horizontal tensile stress in the CTB layer at its interface with the subgrade. Depending on the magnitude of the induced tensile stress relative to the tensile strength of the CTB material, bottom-up cracking may occur, deteriorating the pavement integrity.

With the advent of computer software available for calculating stresses and strains at specific locations in pavement systems, several mechanistic-empirical models have been developed specifically for predicting the fatigue life of CTB layers. One of the tasks for this research project was to identify models published in the literature for prediction of fatigue cracking in CTB layers, identify specific pavement parameters to which each model is sensitive, identify models that predict consistently higher or lower values than the others, and determine the expected pavement life and mode of failure associated with varying asphalt concrete (AC) and CTB thicknesses and CTB and subgrade modulus values in a parametric study. Descriptions of the numerical models, experimental methodology, and results and analyses are presented in the following sections.

DESCRIPTIONS OF NUMERICAL MODELS

Six mechanistic-empirical models for predicting fatigue of CTB layers were identified in the literature review performed in this research: 1) American Coal Ash Association, 2) Australian, 3) Kohn, 4) National Cooperative Highway Research Program (NCHRP), 5) South African, and 6) Uzan. Each of these numerical models is described in the following sections.

American Coal Ash Association

In the American Coal Ash Association model, which was originally developed for pozzolan-stabilized mixtures, the fatigue life of the CTB layer is related to the stress ratio, or the ratio between the maximum induced tensile stress and the flexural tensile strength, or modulus of rupture, as shown in Equation 7 (Scullion, 1993; ACAA, 1991):

$$N_f = 10^{\left(11.207 - 11.494 \cdot \left(\frac{\sigma_t}{R}\right)\right)} \qquad (7)$$

where N_f = number of repetitions to CTB fatigue failure

σ_t = horizontal tensile stress at bottom of CTB layer, psi

R = flexural tensile strength of CTB layer, psi

Australian

In the Australian method, the fatigue life of a CTB layer is dependent on the modulus of the cement-treated material and the horizontal tensile strain induced by the design load as indicated in Equation 8 (Scullion,1993; AUSTROADS, 1992):

$$N_f = \left(\frac{X}{\varepsilon_t}\right)^{18} \qquad (8)$$

where N_f = number of repetitions to CTB fatigue failure

X = value selected from Table 1

ε_t = horizontal tensile strain at bottom of CTB layer, $\mu\varepsilon$

Table 1 was prepared by Texas Transportation Institute (TTI) personnel as a summary of multiple charts provided in the Austroads Pavement Design Guide to relate the CTB modulus of elasticity, denoted as E_2 in Table 1, to the fatigue life of a CTB layer.

Table 1 *X*-Value for Australian Model

E_2 (ksi)	X
>1000	148
≤ 1000	177
≤ 750	196
≤ 500	228
≤ 250	300

Kohn

Similar to the American Coal Ash Association model, the Kohn model also predicts CTB fatigue life using the stress ratio as shown in Equation 9 (Drenth, 2002; Kohn, 1989):

$$\log(N_f) = 11.782 - 12.121 \cdot \left(\frac{\sigma_t}{R}\right) \tag{9}$$

where N_f = number of repetitions to fatigue cracking of the CTB

σ_t = horizontal tensile stress at bottom of CTB layer, psi

R = flexural tensile strength of CTB layer, psi

National Cooperative Highway Research Program

The NCHRP model predicts fatigue life of chemically stabilized materials following Equation 10 (NCHRP, 2006):

$$\log N_f = \frac{0.972(\beta_{c1}) - \left(\frac{\sigma_t}{R}\right)}{0.0825 \cdot (\beta_{c2})} \tag{10}$$

where N_f = number of repetitions to CTB fatigue failure

R = flexural tensile strength of CTB layer, psi

σ_t = horizontal tensile stress at bottom of CTB layer, psi

β_{c1} = 1.0645 (field calibration factor)

β_{c2} = 0.9003 (field calibration factor)

The values given for the field calibration factors were provided in software developed by TTI in 2005 (TTI, 2005). Alternatively, the values of both factors may be specified as 1.0 (NCHRP, 2006).

South African

The South African model is described in Equations 11 and 12 for strongly cemented and weakly cemented materials, respectively (Scullion, 1993; De Beer, et al., 1989):

$$N_f = 10^{9.1\left(1-\frac{\varepsilon_t}{\varepsilon_b}\right)} \text{ (Unconfined compressive strength (UCS) between 400 and 1700 psi)} \tag{11}$$

where N_f = number of repetitions to CTB fatigue failure

ε_t = horizontal tensile strain at bottom of CTB layer, $\mu\varepsilon$

ε_b = tensile strain at break, $\mu\varepsilon$

$$N_f = 10^{7.19\left(1-\frac{\varepsilon_t}{\varepsilon_b}\right)} \text{ (UCS less than 400 psi)} \tag{12}$$

where N_f = number of repetitions to CTB fatigue failure

ε_t = horizontal tensile strain at bottom of CTB layer, $\mu\varepsilon$

ε_b = tensile strain at break, $\mu\varepsilon$

The tensile strain at break may be estimated from the UCS of the CTB as indicated in Table 2.

Table 2 Tensile Strain at Break

CTB Unconfined Compressive Strength (psi)	Material Type	Tensile Strain at Break ($\mu\varepsilon$)
900-1700	Crushed Stone	145
400-900	Stone/Gravel	120
200-400	Gravel	125
100-200	Gravel	145

Uzan

The Uzan model predicts CTB fatigue life following Equation 13 (TTI, 2005):

$$N_f = \left(\frac{\beta_{c4}}{\left(\frac{\sigma_t}{R}\right)}\right)^{20(\beta_{c3})} \tag{13}$$

where N_f = number of repetitions to CTB fatigue failure

R = flexural tensile strength of CTB layer, psi

σ_t = CTB horizontal tensile stress, psi

β_{c3} = 1.0259 (field calibration factor)

β_{c4} = 1.1368 (field calibration factor)

As with the NCHRP model, the values given for the field calibration factors were provided in software developed by TTI (2005).

PARAMETRIC STUDY: METHODOLOGY

Following completion of the literature review, a parametric study was conducted to identify specific pavement parameters to which each model is sensitive, identify models that predict consistently higher or lower values than the others, and determine the expected pavement life and mode of failure associated with varying AC and CTB thicknesses and CTB and subgrade modulus values. A full-factorial experimental design was utilized in conjunction with a three-layer flexible pavement system in the parametric study, which included the effects of four factors on CTB fatigue life. AC layer thicknesses of 2 and 6 in. and CTB layer thicknesses of 6, 9, and 12 in. were included, as well as CTB modulus values of 500, 750, 1000, 1250, and 1500 ksi and subgrade modulus values of 4, 8, and 12 ksi. The AC modulus was held constant at 500 ksi.

Crossing every level of each factor with every level of every other factor yielded a total of 90 different combinations for evaluation. Computer software was then utilized to calculate the critical stresses and strains needed to determine CTB fatigue life using the models identified in the literature review. Poisson's ratios of 0.35, 0.15, and 0.40 were specified for the AC, CTB, and subgrade, respectively, and the response of each system was determined under an equivalent single axle load (ESAL). This loading configuration was defined in the computer software as a single axle having two tires on each side, where each tire was characterized by a circular footprint having a contact radius of 3.78 in. and a contact pressure of 100 psi (Huang, 1993). The distance between the centers of the wheels on each side of the axle was specified to be 13.5 in. In addition, all layer interfaces were assumed to be fully bonded. Based on the output obtained from the computer simulations, the CTB fatigue life in ESALs was determined for each combination of factors using each numerical model in accordance with the research objectives.

In models requiring the flexural tensile strength of the CTB layer, the specified modulus was related to the 28-day UCS using Equation 14, which was developed from empirical charts published in the literature and the assumption that 70 percent of the 28-day UCS is achieved after a 7-day cure (Huang, 1993):

$$UCS = 0.0028 \cdot E_2 - 1142.6 \tag{14}$$

where $UCS =$ unconfined compressive strength of CTB layer, psi
$E_2 =$ CTB modulus of elasticity, psi

The flexural tensile strength of the CTB layer was then estimated from the UCS computed in Equation 14 using Equation 15 (Kohn, 1989; George, 1990; Mindess et al., 2003):

$$R = 0.2 \cdot UCS \tag{15}$$

where $R =$ flexural tensile strength of CTB layer, psi
$UCS =$ unconfined compressive strength of CTB layer, psi

After the calculations were completed, statistical procedures were utilized to evaluate the sensitivity of model results to specific pavement parameters, including AC thickness, CTB thickness and modulus, and subgrade modulus, as well as two- and three-way interactions between these variables. A backward-selection process was used in conjunction with analysis of variance (ANOVA) to identify the factors to which each model is most sensitive. The null hypothesis in the ANOVA was that the population means associated with different levels of a given factor were equal, while the alternative hypothesis was that the populations means were not equal. The output of each statistical analysis was a *p*-value, or level of significance, for each of the pavement parameters. In the backward-selection process, a full statistical model is initially fit, and then the least significant term, where significance is assessed using the adjusted sum of squares, is eliminated from the model. A new model is then fit without the eliminated factor. This process is repeated until all terms in the model have *p*-values less than 0.15 (Ott, 2001). When the *p*-value is less than or equal to 0.05, which was the tolerable level of error specified in this research, one may conclude that the fatigue model is sensitive to the given parameter (Ott, 2001). To facilitate comparisons of the sensitivities of the models to each parameter, the difference between the fatigue lives computed using the highest and lowest values of each parameter was calculated. Larger differences indicate a greater sensitivity of the model to variability in the given parameter.

To identify those models that predict consistently higher or lower values than the others, research personnel utilized a ranking procedure in which the number of times that a given model predicted the first, second, third, etc. highest CTB fatigue life was reported as a percentage of the 90 total combinations. That is, if a given model predicted the highest CTB fatigue life in all 90 combinations, for example, it would be given a value of 100 percent for first place and 0 percent for second through sixth places.

Finally, based on the results of the sensitivity analyses and rankings, one model was selected for use in determining the expected pavement life and mode of failure associated with varying AC and CTB thicknesses and CTB and subgrade modulus values. The fatigue lives of the AC and subgrade layers were determined using the Asphalt Institute formulations given in Equations 16 and 17, respectively (Huang, 1993):

$$N_f = f_1(\varepsilon_t)^{-f_2}(E_1)^{-f_{33}} \tag{16}$$

where N_f = number of repetitions to AC fatigue failure

ε_t = horizontal tensile strain at bottom of AC layer

E_1 = AC modulus of elasticity, psi

f_1 = 0.0796

f_2 = 3.291

f_3 = 0.854

$$N_d = f_4(\varepsilon_c)^{-f_5} \tag{17}$$

where N_d = number of repetitions to subgrade rutting failure

ε_c = vertical compressive strain at top of subgrade

f_4 = 1.365×10^{-9}

f_5 = 4.477

The fatigue lives of the AC, CTB, and subgrade layers in ESALs were then compared for each combination of factors, and the lowest value was designated as the pavement service life. The layer associated with the lowest fatigue life was identified in each case to indicate the mode of failure.

PARAMETRIC STUDY: RESULTS

The stresses, strains, and deflections computed for each of the 90 simulations are provided in Appendix F (Tables F-1 and F-2) together with the thickness and modulus of the AC and CTB layers and the modulus of the subgrade utilized in each case. The numbers of repetitions to failure of the AC, CTB, and subgrade layers are given in Appendix F (Table F-2), in which entries of "infinite" are given for zero-valued horizontal tensile strains at the bottom of the AC layer.

In preparation for the statistical analyses performed to evaluate the sensitivity of model results to AC thickness, CTB thickness and modulus, as well as two- and three-way interactions between these variables, the numbers of repetitions to failure of the AC, CTB, and subgrade layers were all subjected to a logarithmic transformation to reduce the variability between values. To facilitate the analysis, "infinite" life was assigned a value of 10^{24}, and every number was increased by 1 before the transformation so that the resulting values would all be positive. The ANOVA was then performed on the transformed data, and the results are given in Appendix F (Table F-3), in which hyphens indicate factors that were eliminated in the backward-selection process.

The data indicate that all six models are sensitive to the four main factors, including AC thickness, CTB thickness and modulus, and subgrade modulus, investigated in the analysis. The only two factors not significant in any model are the two-way interaction between AC thickness and subgrade modulus and the two-way interaction between CTB thickness and subgrade modulus. The implication of a significant two-way interaction is that the effect of one factor on the model results depends upon the level of the other factor. That is, for example, the effect of AC thickness on CTB fatigue life depends upon the CTB thickness, and vice-versa, in all of the models. In a three-way interaction, the two-way interaction between any two of the factors in the interaction depends upon the level of the third factor.

While the *p*-values in Appendix F (Table F-3) indicate that model results are sensitive to each of the main factors, further analysis was required to evaluate the degree of sensitivity of each model to each factor, which is quantified in Appendix F (Table F-4) for AC thickness, CTB thickness and modulus, and subgrade modulus. In each table, differences in fatigue lives between the minimum and maximum values of the factor of interest are shown for combinations of other variables when interactions exist. For example, for AC thickness, differences between the minimum and maximum fatigue lives are shown for all possible combinations of CTB thickness and CTB modulus, and the entries are averaged over all of the subgrade modulus values included in the study. However, in the analysis of subgrade values, differences associated with combinations of other factors are not presented due to the comparative lack of interactions with subgrade modulus.

In each case, the average difference was used to rank the relative sensitivity of each model, where a ranking of "1" indicates the highest sensitivity and a ranking of "6" indicates the lowest sensitivity. The data show that the Australian and Uzan models are most sensitive to both AC thickness and CTB thickness, while the Coal Ash Association and Kohn models are least sensitive to these factors. Regarding CTB modulus, the Uzan and NCHRP models are most sensitive, while the South African and Australian models are least sensitive. Finally, the

Australian and Uzan models are most sensitive to subgrade modulus, while the Coal Ash Association and Kohn models are least sensitive. Therefore, in general, the Australian and Uzan models are most sensitive to the evaluated factors, while the Coal Ash Association and Kohn models are least sensitive.

A ranking procedure was also utilized to identify those models that predict consistently higher or lower CTB fatigue lives than the others. Table 3 shows the percentage of occurrences of each ranking from 1 to 6 for each model, where a ranking of 1 indicates the highest predicted fatigue life and a ranking of 6 indicates the lowest predicted fatigue life. The data clearly indicate that the Uzan model most frequently predicts the highest values of CTB fatigue life, while the South African model most frequently predicts the lowest values of CTB fatigue life. Figure 24 provides a visual depiction of the relative values of predicted CTB fatigue lives for each model in the same order presented in Appendix F (Table F-2). Both the sensitivity of the models to changes in input parameters and the relative proximity of model results to each other are represented in the figure.

To investigate the expected pavement life and mode of failure associated with varying AC and CTB thicknesses and CTB and subgrade modulus values, CTB fatigue life predictions from the NCHRP model were compared against the fatigue lives of AC and subgrade layers predicted using Equations 16 and 17 for each of the 90 combinations and shown in Appendix F (Table F-2). The NCHRP model was used for this purpose because of its average sensitivity and CTB fatigue life predictions compared to the other models and because it has been recommended for incorporation in the new American Association of State Highway and Transportation Officials (AASHTO) pavement design guide (NCHRP, 2005).

The pavement life predicted in each case is depicted in Figures 25 and 26 for combinations having AC thicknesses of 2 and 6 in., respectively. For a given simulation, the pavement life was specified as the lowest fatigue life associated with any particular layer. In none of the 90 evaluations did the AC layer ever fail first. The CTB layer failed first in the 18 simulations in which CTB modulus values were 500 ksi, as well as in the two simulations in which the AC and CTB thicknesses were at their minimum values of 2 in. and 6 in., respectively, the CTB modulus was 750 ksi, and the subgrade modulus was either 4 or 8 ksi. Among these 20 simulations, the pavement life exceeded an arbitrary traffic level of 10,000,000 ESALs in only case in which the AC thickness was 6 in., CTB thickness was 12 in., CTB modulus was 500 ksi, and subgrade modulus was 12 ksi. The subgrade failed first in the remaining 70 simulations, among which the pavement life exceeded 10,000,000 ESALs in 62 cases. The eight exceptions were all characterized by an AC thickness of 2 in., and seven had a CTB thickness of 6 in. Among those seven, the simulation having a CTB modulus of 750 ksi and a subgrade modulus of 12 ksi was inadequate, simulations having a CTB modulus of 1000 ksi were inadequate for all subgrade modulus values, simulations having a CTB modulus of 1250 ksi were inadequate for subgrade modulus values of 4 and 8 ksi, and the simulation having a CTB modulus of 1500 ksi and a subgrade modulus of 4 ksi was inadequate. The eighth exception was characterized by a CTB thickness of 9 in., a CTB modulus of 750 ksi, and a subgrade modulus of 4 ksi.

Table 3 Frequency of Highest Predicted CTB Life

Rank	Rank Frequency (%)					
	Australian	Coal Ash Association	Kohn	NCHRP	South African	Uzan
1	20.00	0.00	0.00	3.33	0.00	76.67
2	12.22	0.00	0.00	67.78	14.44	5.56
3	21.11	0.00	46.67	15.56	1.11	15.56
4	5.56	45.56	33.33	8.89	4.44	2.22
5	41.11	45.56	12.22	1.11	0.00	0.00
6	0.00	8.89	7.78	3.33	80.00	0.00
Total	100.0	100.0	100.0	100.0	100.0	100.0

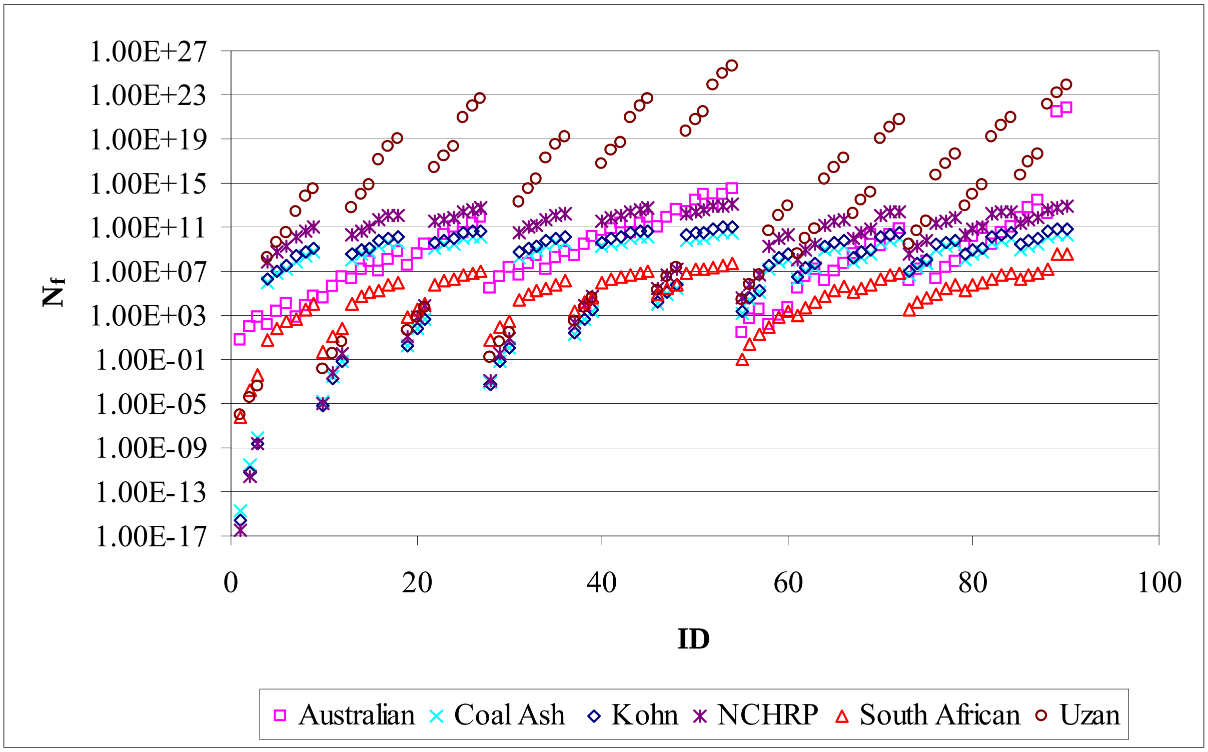

Figure 24. Comparison of predicted CTB fatigue lives.

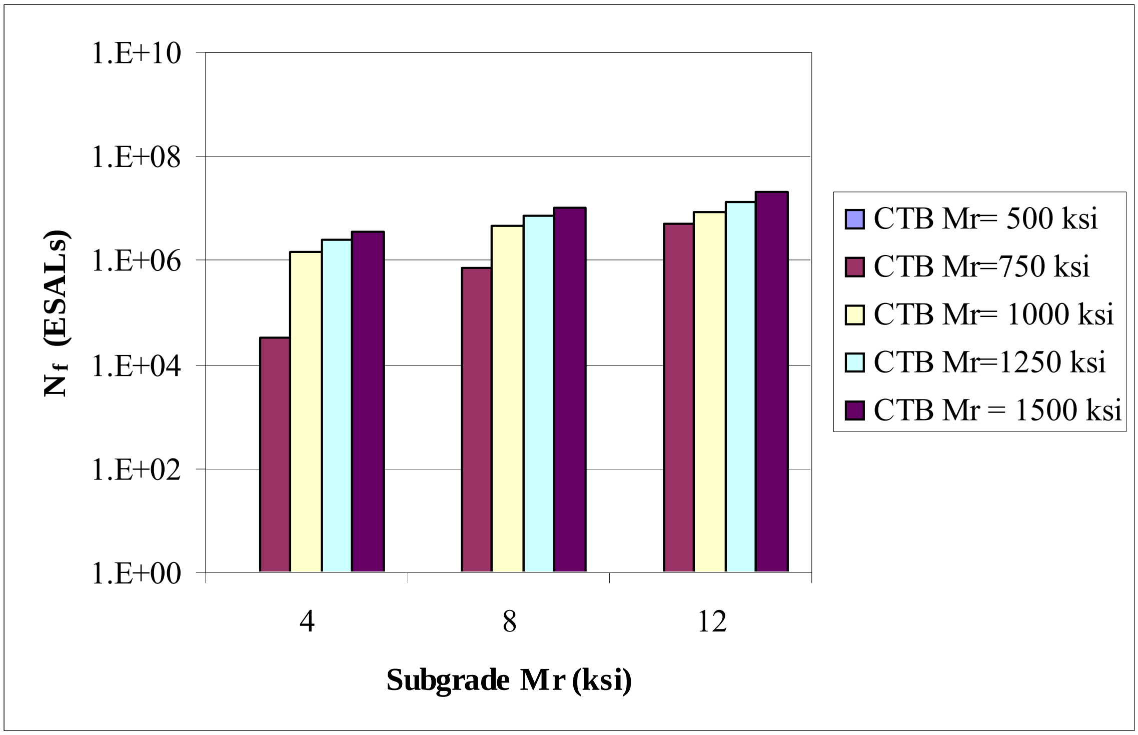

(a) CTB thickness of 6 in.

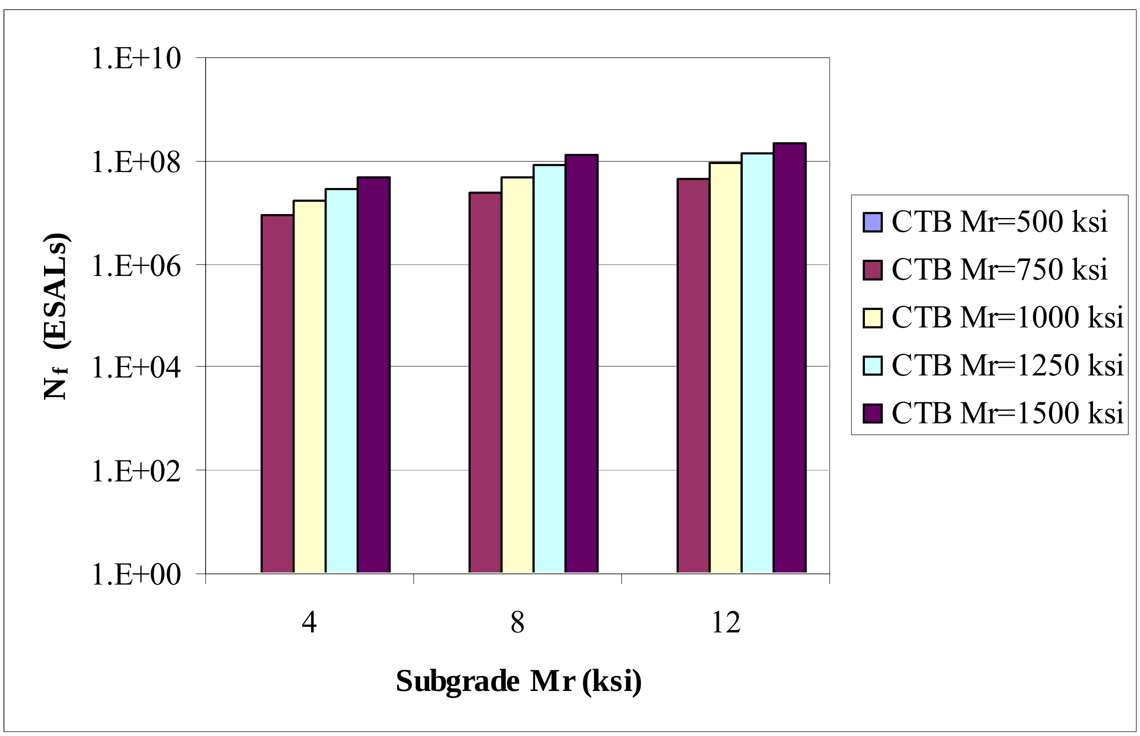

(b) CTB thickness of 9 in.

Figure 25. Pavement life for AC thickness of 2 in.

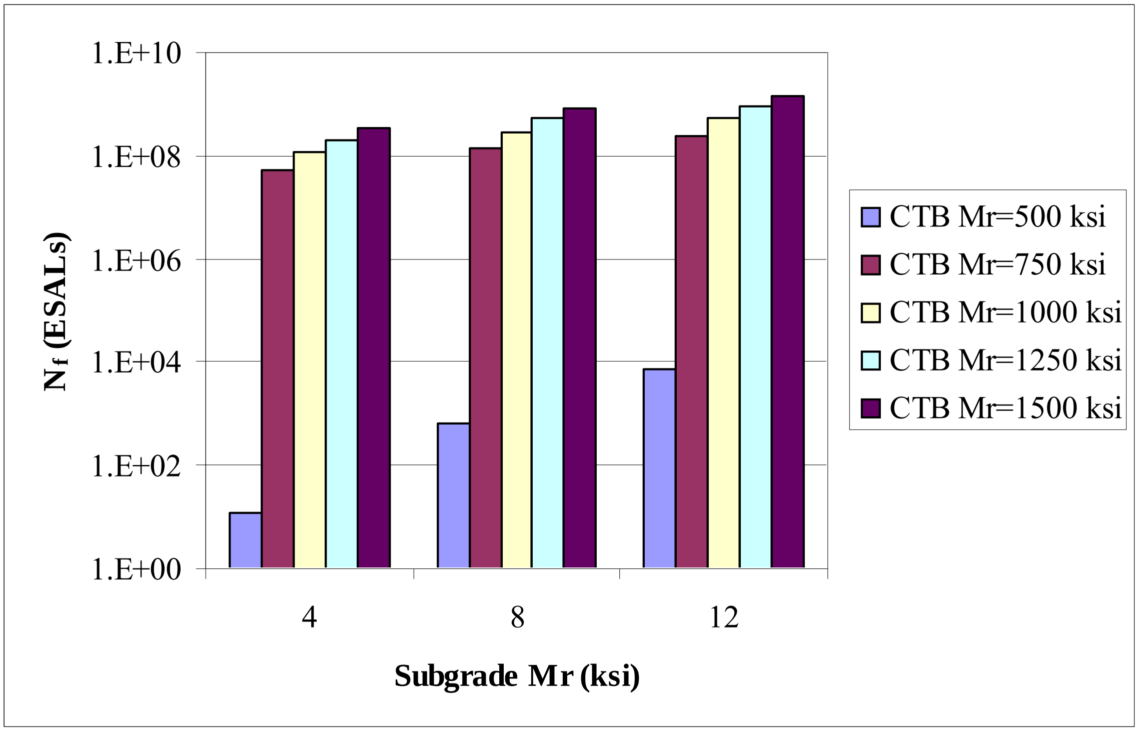

(c) CTB thickness of 12 in.

Figure 25. Pavement life for AC thickness of 2 in., continued.

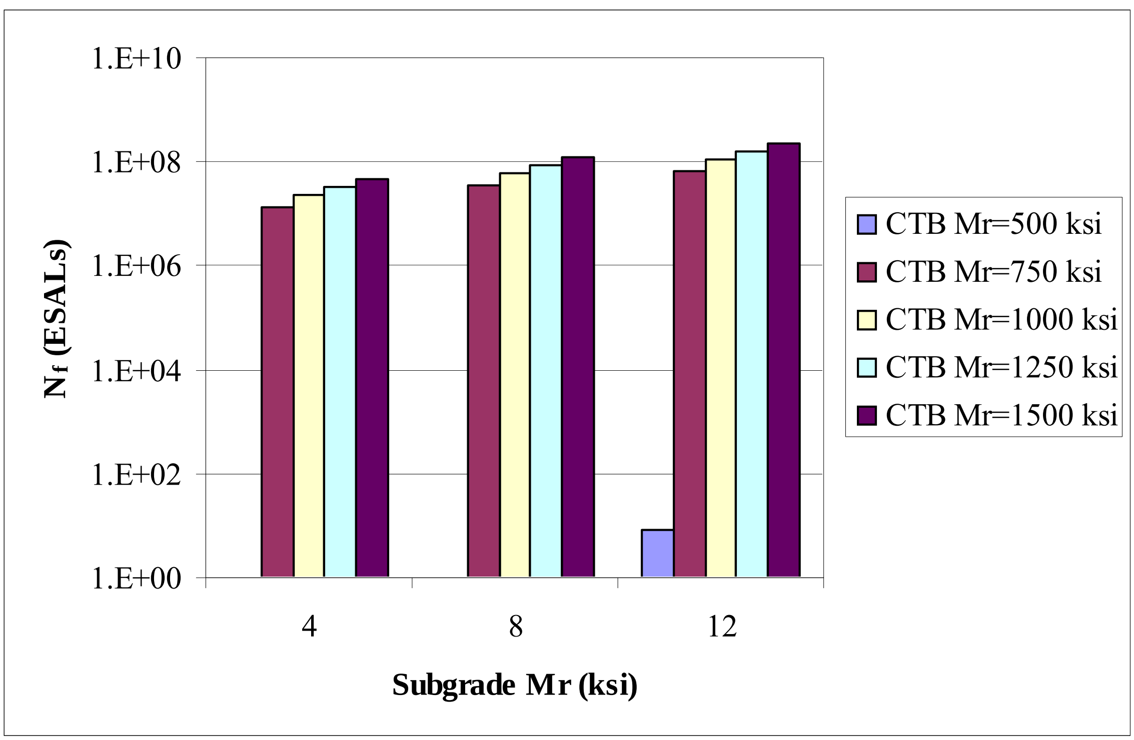

(a) CTB thickness of 6 in.

Figure 26. Pavement life for AC thickness of 6 in.

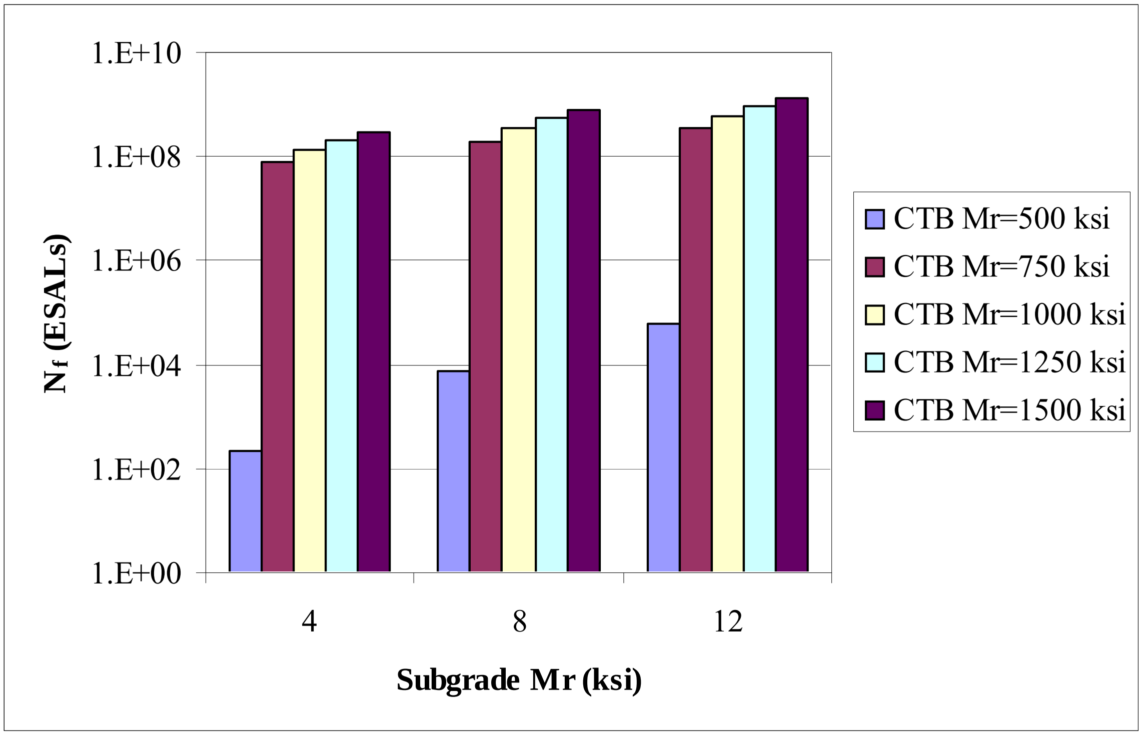

(b) CTB thickness of 9 in.

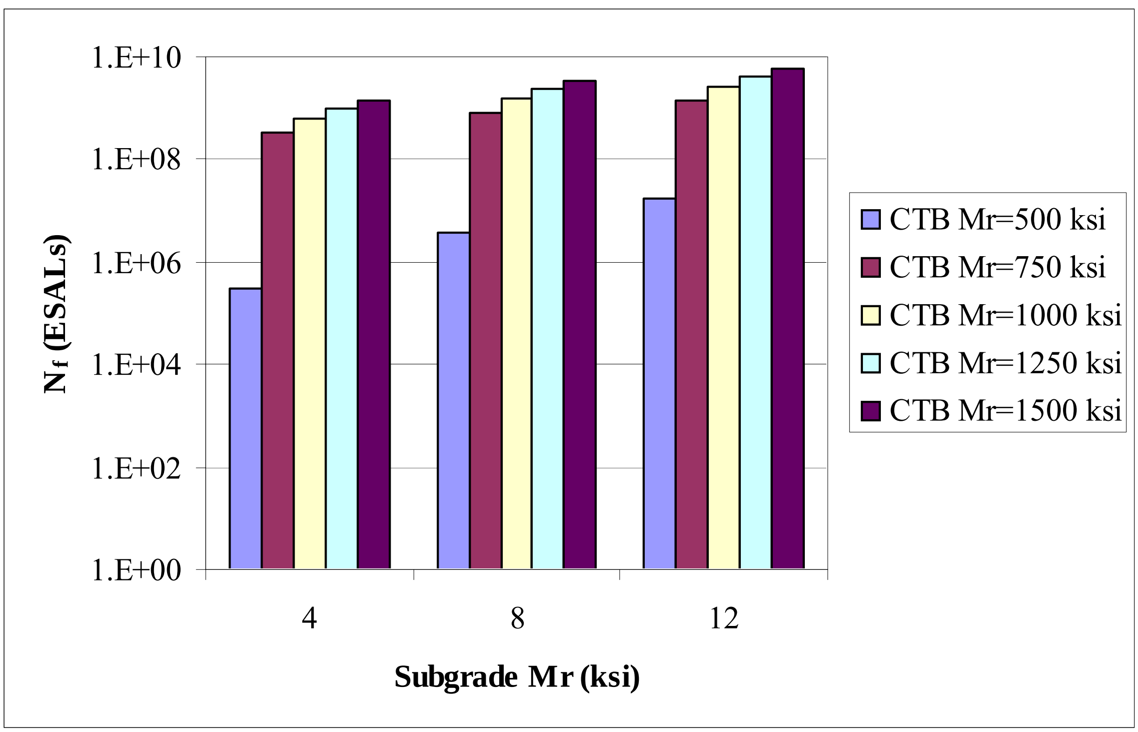

(c) CTB thickness of 12 in.

Figure 26. Pavement life for AC thickness of 6 in., continued.

8. CONCLUSIONS

The major goal in this project was to conduct field and laboratory testing to evaluate cement-stabilized FDR bases with regard to performance in frost areas and under early traffic conditions. Additionally, the scope of this project included evaluation of mechanistic-empirical models for predicting fatigue of CTB layers and development of design charts to predict expected pavement life and mode of failure associated with cement-treated recycled base layers. The ultimate objective of this research is to provide generalized engineering guidelines that can be utilized by local and state transportation agencies so that they can potentially benefit from the significant cost and environmental advantages of FDR with cement-treated base materials.

Literature was reviewed to assess the state-of-the-art in pavement design for frost-affected areas, and a questionnaire survey of state Departments of Transportation was conducted to investigate material and construction specifications and to define current pavement design practices. A general description of the survey is presented in Section 4 of this report, and detailed analysis of the survey is included in Appendix A. Although the results of the survey reveal a variety of practices, the data suggest that many DOTs utilize similar methods for the design and construction of pavements in cold regions. The information obtained in the survey represents a unique compilation of standards of practice that have been developed by DOTs based on years of experience and research in their respective jurisdictions.

After receipt of the completed questionnaire, members of the research team contacted several of the survey respondents and obtained copies of specifications adopted by their respective agencies for construction of cement-stabilized FDR bases. Based upon a review of those specifications and others provided by PCA, a generic set of suggested specifications for construction of cement-treated recycled base layers was developed; these specifications are included in Appendix B.

Laboratory testing was conducted to characterize the properties of CTB materials constructed from RAP and aggregate materials obtained from several locations in New England. The aggregates and RAP were blended in approximately equal proportions by weight, and extensive laboratory testing was performed to evaluate the strength and durability of each blend in the untreated condition and after treatment with various levels of cement. Testing included determinations of particle-size distributions, 7-day UCS values, and moisture susceptibility classifications for the materials.

Results of the laboratory testing suggest that modest amounts of cement can greatly improve the strength and durability of base materials. At a cement content of 4 percent, the UCS of four of the test materials was in the recommended range of 300 to 400 psi, while the UCS values of the other two materials approached the target range at cement contents between 2 and 3 percent. Four of the materials exhibited decreases in final dielectric value with increasing cement content. However, with the other two materials, which were both gap-graded, addition of cement in the range of 1 to 4 percent actually caused the dielectric values to be higher than those exhibited by the untreated specimens; for these materials, cement contents on the order of 6 to 8 percent may be required to achieve satisfactory durability in terms of capillary rise potential. At these comparatively high levels of cement, the use of microcracking in construction should be considered to minimize the occurrence of reflective cracking into the surface layer.

The results of the laboratory testing were used to establish design parameters for two field test sites constructed in the summer of 2005, one on Route 112 (Kancamagus Highway) in New Hampshire and another on Route 2A in Maine. At the New Hampshire site, three test sections were established: one on a section of roadway reconstructed using conventional techniques, and two on sections of roadway rehabilitated using FDR (one with cement stabilization and the other untreated). At the Maine site, data were collected cement-treated FDR sections only; although a section of roadway was left untreated, testing could not be conducted in the control section due to scheduling incompatibility. At both sites, field testing was conducted to characterize the structural properties of CTBs subjected to early trafficking. The New Hampshire test site was also monitored during the 2005-2006 winter and spring to examine variations in performance-related properties that result from seasonal changes in temperature and moisture content.

For field testing, the research team utilized a falling-weight deflectometer (FWD) and a Geogauge at the field test site in New Hampshire. A heavy Clegg hammer was used at the field test site in Maine. Field testing at both sites indicated that a substantial increase in strength and stiffness occurred in the CTB materials during the first two to three days of curing.

At the Kancamagus Highway site, data suggest that early trafficking adversely affected the initial strength gain and base layer stiffness in the cement-treated sections. After two days of curing, the cement-treated WP test areas exhibited FWD modulus values that were 50 percent lower than the corresponding NWP test areas stabilized with cement. However, also after two days of curing, FWD data suggested that the WP and NWP test areas with cement were 200 and 700 percent stiffer, respectively, than the corresponding test areas without cement. The stiffness values measured by the Geogauge were apparently not as sensitive to the early trafficking as the modulus values determined from FWD testing. The cement-treated areas did, however, exhibit reductions in average Geogauge stiffness of about 26 percent under trafficking during the first day of curing and about 11 percent during the following two days. At the standard error rate of 0.05, both the FWD and the Geogauge data show a statistically significant difference between WP and NWP measurements in the cement-treated test section, while the differences between WP and NWP measurements in the untreated test section are not significant.

At the test site in Maine, average CIST values in the NWP locations in two of the three test sections were always larger than average values in corresponding WP locations; however, those differences were statistically significant only for the testing conducted on the day of construction and, for one of those test sections, for the testing conducted after two days of curing. In the third test section at this site, average CIST values measured in the NWP locations were consistently lower than average values in corresponding WP locations.

Therefore, while much of the data suggest that early trafficking reduces the initial strength gain and stiffness of CTB layers, additional research may be warranted to quantify the effects of early traffic. The differences observed in the data collected at these two sites may be related to differences in traffic volume and magnitude. At the New Hampshire site, there was much more heavy truck traffic on the newly constructed base due to construction activities both east and west of the test sections.

Data were collected at the Kancamagus Highway site during the 2005-2006 winter and spring to study variations in performance-related properties that result from seasonal changes in temperature and moisture content. During the monitoring period, subsurface temperature profiles indicate that frost penetrated at least 42 inches below the top of the pavement in the cement-treated FDR section and greater than 64 inches below the top of the pavement in the conventional reconstruction section.

Data from FWD tests were used to compute several deflection-related pavement parameters, including adjusted center deflection, area parameter, SCI, shape factor, and subgrade modulus. Plots of SCI, shape factor, and area parameter illustrate the beneficial effect of cement in stiffening the base layer. The spike in center deflection and SCI values measured in all three test sections in April, 2006, reflects the fact that the pavement system became weaker just after the base and subgrade materials thawed. Those values then decreased as the base and subgrade soils subsequently recovered strength and stiffness later in the spring. Subgrade modulus values in the conventional reconstruction section were consistently higher than those in the two FDR test sections (where subgrade modulus values were approximately equal). Since the soft fine-grained subgrade soils in the conventional reconstruction section were removed and replaced with select fill, it is likely that the higher subgrade modulus values and the lower adjusted center deflection values generally observed in that test section resulted from the improved subgrade soils.

In mid-February 2006, optical survey measurements showed that, while heave in the conventional reconstruction section appeared to be negligible, a substantial amount of heave occurred in both of the FDR test sections. Although there is no obvious explanation for why the cement-treated section heaved slightly more than the untreated FDR section, it is likely that the differences between the conventional reconstruction section and the two FDR sections resulted from differences in the underlying subgrade soils. Therefore, while cement can be extremely beneficial in stiffening reclaimed base layers and bridging over subgrade soils that may become weakened during spring thaw, it will not reduce the heave associated with frost-susceptible subgrade soils. Because of this fact, if a CTB will be exposed to frost heaving subgrade soils, it is imperative that the CTB be designed such that it does not exhibit brittle behavior, which can lead to cracking.

As such, one of the tasks associated with this research project was to identify models published in the literature for prediction of fatigue cracking in CTB layers, identify specific pavement parameters to which each model is sensitive, identify models that predict consistently higher or lower values than the others, and determine the expected pavement life and mode of failure associated with varying AC and CTB thicknesses and CTB and subgrade modulus values in a parametric study. Six mechanistic-empirical models for predicting fatigue of CTB layers were identified in the literature review performed in this research: 1) American Coal Ash Association, 2) Australian, 3) Kohn, 4) NCHRP, 5) South African, and 6) Uzan. A full-factorial experimental design was utilized in conjunction with a three-layer flexible pavement system in the parametric study, which included 90 different combinations of AC thickness, CTB thickness and modulus, and subgrade modulus. Computer software was utilized to calculate the critical stresses and strains needed to determine AC, CTB, and subgrade fatigue life using the models identified in the literature review, and statistical and ranking procedures were both employed to address the research objectives.

The results of the ANOVA indicate that the results of all six models are sensitive to the four main factors, including AC thickness, CTB thickness and modulus, and subgrade modulus, investigated in the analysis. The data show that the Australian and Uzan models are most sensitive to both AC thickness and CTB thickness, while the Coal Ash Association and Kohn models are least sensitive to these factors. Regarding CTB modulus, the Uzan and NCHRP models are most sensitive, while the South African and Australian models are least sensitive. Finally, the Australian and Uzan models are most sensitive to subgrade modulus, while the Coal Ash Association and Kohn models are least sensitive. Therefore, in general, the Australian and Uzan models are most sensitive to the evaluated factors, while the Coal Ash Association and Kohn models are least sensitive. In addition, the data clearly indicate that the Uzan model most frequently predicts the highest values of CTB fatigue life, while the South African model most frequently predicts the lowest values of CTB fatigue life.

The NCHRP model was used for investigating the pavement life and mode of failure associated with each combination in the parametric study because of its average sensitivity and CTB fatigue life predictions compared to the other models and because it has been recommended for incorporation in the new AASHTO pavement design guide. In none of the 90 evaluations did the AC layer ever fail first. The CTB layer failed first in the 18 simulations in which CTB modulus values were 500 ksi, as well as in the two simulations in which the AC and CTB thicknesses were at their minimum values of 2 in. and 6 in., respectively, the CTB modulus was 750 ksi, and the subgrade modulus was either 4 or 8 ksi. The subgrade failed first in the remaining 70 simulations.

Although the sensitivity to specific parameters and relative proximity of model results to each other could be evaluated in this research, the true accuracy of the models could not be assessed. Field performance data are needed for validating these models; as a remarkable degree of variability exists among their predictions, some may be more applicable to certain traffic, materials, and climatic conditions than others. Furthermore, knowledge of seasonal variation in CTB layer properties would be needed to effectively utilize the charts prepared in this research for pavement design.

In summary, results of this research suggest that modest amounts of cement can greatly improve the strength and durability of base materials, which should in turn increase their resistance to frost damage. The design charts provided in Section 7 of this report can be used as an aid to predict expected pavement life and mode of failure associated with varying AC and CTB thicknesses and varying CTB and subgrade modulus values. Suggested construction specifications are included in Appendix B, and appropriate quality control should be provided in the field to assure that the CTB performs well over its intended life. Exposure to early traffic may reduce the initial strength gain and stiffness in cement-treated bases, particularly if that traffic consists of heavily-loaded construction traffic. On the other hand, CTB test sections studied in this project all exhibit satisfactory performance after one year of service, despite their exposure to early traffic. Finally, future research is warranted to better quantify changes in CTB layer properties that result from variations in temperature and moisture conditions during different seasons. Such field performance data are needed for validating the models described herein and for effectively utilizing the associated charts for pavement design.

9. ACKNOWLEDGEMENTS

The authors wish to thank Maureen Kestler (USDA Forest Service), Carolina Carbó (New England Region of the Road Recycling Council), and Dr. David Luhr and Wayne Adaska (PCA) for technical support throughout the project. Dr. Rajib Mallick (WPI) and Christopher Chang (Eastern Federal Lands Division of FHWA) are acknowledged for conducting the FWD testing. The assistance provided by the New Hampshire and Maine Departments of Transportation with regard to coordinating work at the field test sites is also greatly appreciated. Finally, the authors wish to thank J. Sylvester (USDA Forest Service), Christopher Berini and Charles Smith (CRREL), family members Charles Miller and Rand Kmiec, BYU graduate students Ash Brown and Aimee Birdsall, and UMD research assistants Joe Iaccarino, Aly Fahmy, Justin Yaitanes, and David Guerriero for their assistance with laboratory and field testing performed in this research.

10. REFERENCES

Al-Amoudi, O. S. B., I. M. Asi, H. I. A.-A. Wahhab, and Z. A. Khan (2002). *Clegg Hammer-California-Bearing Ratio Correlations*. Journal of Materials in Civil Engineering, Vol. 14, No. 6, November/December 2002, pp. 512-522.

American Association of State Highway and Transportation Officials (AASHTO). (1998). *Standard Specifications f Sampling and Testing*, 19th Ed., Washington, DC.

American Coal Ash Association (ACAA). (1993). *Flexible Pavement Manual: Recommended Practice—Coal Fly Ash in Pozzolanic Stabilized Mixtures for Flexible Pavement Systems,* Aurora, CO.

American Concrete Institute (ACI). (1990). *State-of-the-Art Report on Soil Cement*, PUB: ACI 230R-90, ACI Committee 230, Farmington Hills, MI.

Asphalt Recycling and Reclaiming Association (2001). *Basic Asphalt Recycling Manual*, PUB: NHIO1-022, USA.

AUSTROADS (1992). *Pavement Design—A Guide to the Structural Design of Road Pavements*, PUB: AP-17/92, The Kelvin Press Pty Limited, Sydney, Australia.

Carbó, C., and L. Fernandez Luco (2001). *A Comprehensive Criteria to Optimize Full Depth Recycling Mixture Proportions*, First International Symposium on Subgrade Stabilization and In-situ Pavement Recycling Using Cement. 1-4 October, 2001, Salamanca, Spain.

Chakrabarti, S., J. Kodikara, and L. Pardo (2001). *An Overview of Stabilization Methods and Performance of Local Government Roads in Australia*, First International Symposium on Subgrade Stabilization and In-situ Pavement Recycling Using Cement. 1-4 October, 2001, Salamanca, Spain.

De Beer, M., Kleyn, E. G., and Horak, E. (1989). *Behavior of Cementitious Gravel Pavements with Thin Asphalt Surfacings*, PUB: RR649, Department of Roads and Transport Technology, Council for Industrial and Scientific Research, South Africa.

Drenth, K.P. (2002). *Pavement Design Considerations Regarding the Introduction of the A380*, Federal Aviation Administration Airport Technology Transfer Conference. May 2002.

Federal Highway Administration (1994). Publication No. FHWA-HI-94-021. *National Highway Institute Course No. 13127: Pavement Deflection Analysis*, Washington, D.C.

Federal Highway Administration (2000). *Highway Statistics 2000 Table HM-51*, Washington, D.C.

Fiedler, S., C. Nelson, E. F. Berkman, and A. DiMillio (1998). *Soil Stiffness Gauge for Soil Compaction Control*. Public Roads, Vol. 61, No. 5, March/April 1998. http://www.tfhrc.gov/pubrds/marapr98/soil.htm. Accessed July 30, 2004.

Freitag, D. R., and T. McFadden (1997). *Introduction to Cold Regions Engineering*. American Society of Civil Engineers, New York, NY.

George, K. P. (1990). *Characterization and Structural Design of Cement-Treated Base*. In Transportation Research Record 1288 (pp. 78-87), TRB, National Research Council, Washington, D.C.

Guthrie, W. S., S. Sebesta, and T. Scullion (2002). *Selecting Optimum Cement Contents for Stabilizing Aggregate Base Materials.* Report 4920-2, Texas Transportation Institute, Texas A&M University System, College Station, Texas.

Guthrie, W. S., T. B. Young, B. J. Blankenagle, and D. A. Cooley (2005). *Early-Age Strength Assessment of Cement-Treated Base Material.* In Transportation Research Record 1936 (pp. 12-19), Transportation Research Board, National Research Council, Washington, D.C.

Huang, Y. H. (1993) *Pavement Analysis and Design*. Prentice Hall, Inc., Upper Saddle River, NJ.

Humboldt Manufacturing Company (2000). *GeoGauge User Guide*, version 3.8, Norridge, IL.

Humboldt Manufacturing Company (2002). *Test Results: Specification Validation for Pre-Cracked Portland Cement Treated Base Utilizing the Humboldt GeoGauge*. Norridge, IL.

Janoo, V. (2002). *Performance of Base/Subbase Materials Under Frost Action*. In Cold Regions Engineering, American Society of Civil Engineers, Reston, VA, pp. 299-310.

Kestler, M. A., and R. L. Berg (2004). *Framework for Evaluation of a Cost-Effective Method for Placing and Removing Seasonal Load Restrictions on Low Volume Roads: The Portable Falling Weight Deflectometer*. In Proceedings of the American Society of Civil Engineers Twelfth International Specialty Conference on Cold Regions Engineering. CD-ROM. Edmonton, Alberta, Canada.

Kohn, S. D. (1989). *Development of a Thickness Design Procedure for Stabilized Layers under Rigid Airfield Pavements*, Fourth International Conference on Concrete Pavement Design and Rehabilitation. April, 1989, Purdue University, Lafayette, IN.

Lafayette Instrument (2004), Lafayette, IN. *Clegg Impact Soil Tester*, http://www.licmef.com/clegg.htm. Accessed July 30, 2004.

Lay, R. D. (2005). *Development of a Frost Heave Apparatus*. M.S. thesis, Department of Civil and Environmental Engineering, Brigham Young University, Provo, Utah.

Litzka, J., and W. Haslehner, *Cold In-Place Recycling on Low Volume Roads in Austria*, proceedings of the 6th International Conference on Low Volume Roads, Minnesota, June 1995, USA.

Luhr, David R., Adaska, Wayne S., Halsted, Gregory E. (2005). *Guide to Full-Depth Reclamation with Cement,* Publication EB234, Portland Cement Association (PCA), Skokie, Illinois.

Mackay, M. H., D. K. Hein, and J. J. Emery (1992). *Evaluation of Frost Action Mitigation Procedures for Highly Frost-Susceptible Soils*. In Transportation Research Record 1362, TRB, National Research Council, Washington, DC, pp. 79-89.

Mallick, R.B., P.S. Kandhal, E.R.Brown, R.L. Bradbury, and E.J. Kearney (2002). *Development of a Rational and Practical Mix Design System for Full Depth Reclaimed (FDR) Mixes*, Final Report for Project No. 00-373, Funded by the Recycled Materials Resource Center (RMRC) at the University of NH.

Mindess, S., J. F. Young, and D. Darwin. (2003). *Concrete*, Second Edition. Prentice Hall, Inc., Upper Saddle River, NJ.

National Cooperative Highway Research Program (NCHRP) (1974). *Synthesis of Highway Practice 26*: *Roadway Design*. TRB, National Research Council, Washington, DC.

National Cooperative Highway Research Program (NCHRP). (2006), Washington, DC. *NCHRP 1-37A Design Guide*, http://www.trb.org/mepdg/guide.htm. Accessed June 17, 2006.

Newcomb, D. E. (1986). *Development and Evaluation of a Regression Method to Interpret Dynamic Pavement Deflections*. PhD Dissertation, University of Washington, Seattle, Washington.

Ott, R. L., and M. Longnecker. (2001). *An Introduction to Statistical Methods and Data Analysis*, Fifth Edition. Duxbury, Pacific Grove, CA.

Portland Cement Association (PCA). (1992). *Soil-Cement Laboratory Handbook*. Publication EB052.07S, Skokie, Illinois.

Portland Cement Association (PCA). (2001). *Thickness Design for Soil-Cement Pavements*, PUB: EB068.02, Skokie, IL.

Portland Cement Association (PCA). (2003). *Reflective Cracking in Cement Stabilized Pavements*. Publication IS537, Skokie, Illinois.

Prusinski, J., *Recycling Flexible Pavements with Cement: Diverse Methods Produce Durable Pavements*, Soil-Cement and Other Construction Practices in Geotechnical Engineering, Proceedings of Geo-Denver 2000 American Society of Engineers. August 5-8, 2000, Denver, Colorado, USA.

Robinson, D.A., S.B. Jones, J.M. Wraith, D. Or, and S.P. Friedman (2003). *Advances in Dielectric and Electrical Conductivity Measurement Using Time Domain Reflectometry: Simultaneous Measurement of Water Content and Bulk Electrical Conductivity in Soils and Porous Media*. Vadose Zone Journal 2:444–475. Soil Science Society of America, Madison, WI.

Salem Tool Company (2003). *Corps Style Dual Mass Dynamic Cone Penetrometer: Application and Maintenance Manual*. Salem, MI.

Scullion, T (1993). *Review of Existing CTB Thickness Design Procedures*, Technical Memorandum. Texas Department of Transportation Cooperative Research Program. September, 1993.

Scullion, T., and Saarenketo, T. (1997). "*Using Suction and Dielectric Measurements as Performance Indicators for Aggregate BaseMaterials*." Transportation Research Record 1577, TRB, National Research Council, Washington, D.C., 37-44.

Scullion, T., Sebesta, S., Harris, J. P., and Syed, I. (2000). *A Balanced Approach to Selecting the Optimal Cement Content for Soil-Cement Bases*. Report 404611-1, Texas Transportation Institute, Texas A&M University System, College Station, Texas.

Scullion, T. (2002). "*Field Investigation: Pre-cracking of Soil-cement Bases to Reduce Reflection Cracking.*" Transportation Research Board 81st Annual Meeting Compendium of Papers, CD-ROM, Transportation Research Board, National Research Council, Washington, D.C.

Sebesta, S. (2005). *Use of Microcracking to Reduce Shrinkage Cracking in Cement Treated Bases*. In Transportation Research Board 83rd Annual Meeting Compendium of Papers. CD-ROM. Transportation Research Board, National Research Council, Washington, D.C.

Seyfried, M. S., and M. D. Murdock (2004). *Measurement of Soil Water Content with a 50-MHz Soil Dielectric Sensor*. Journal of the Soil Science Society of America V. 68:394–403, Madison, WI.

Sommer, H. (2001). *Strength and Durability Requirements for Cement-Stabilized Materials*, First International Symposium on Subgrade Stabilization and In-situ Pavement Recycling Using Cement. 1-4 October, 2001, Salamanca, Spain.

Syed, I., Scullion, T., and Harris, J. P. (1999). "Durability of recycled and stabilized pavement materials." *Recent Advances in the Characterization of Transportation Geo-Materials*, E. Tutumluer and A. T. Papagiannakis, Eds., American Society of Civil Engineers, Reston, Va., 25-36.

Texas Transportation Institute (TTI). (2005). Cement-Treated Base Design Software, College Station, TX.

Von Quintus, H. L, and A. L. Simpson (2002). *Back-Calculation of Layer Parameters for LTPP Test Sections, Volume II: Layered Elastic Analysis for Flexible and Rigid Pavements*. Publication FHWA-RD-01-113. FHWA, U.S. Department of Transportation. http://www.tfhrc.gov/pavement/ltpp/pdf/01113.pdf. Accessed November 15, 2004.

Washington State Department of Transportation (WSDOT). (1995). *Pavement Guide, Volume 3: Pavement Analysis Computer Software and Case Studies*, Olympia, Washington.

Washington State Department of Transportation (WSDOT). (1999). *Development of a Computer Program for the Determination of the Area Value and Subgrade Modulus using the Dynatest FWD*, Olympia, Washington.

Appendix A

Results of Survey:
State of the Practice for Design and Construction of Pavements in Cold Regions

INTRODUCTION

As discussed in Section 4 of this report, a detailed questionnaire survey was conducted of 23 state departments of transportation (DOTs) and an agency in Sweden to investigate the state of the practice concerning the design and construction of pavements in cold regions. The survey included 20 questions specifically addressing material specifications, identification of frost-susceptible soils, stabilization techniques, geosynthetics, full-depth recycling, and spring load restrictions and winter premiums. Most of these questions had multiple-choice answers, but others required short-answer responses. The following sections present the survey questions and a summary of the results obtained for each question. The 20 survey questions are presented in three different sections: climate, design and construction, and policies.

CLIMATE

This section discusses the results of two questions addressing the climate in the regions of the different respondents.

Question 1. What is the typical air freezing index for the weather in your jurisdiction?

Figure 1 shows that the air freezing indices reported by the responding agencies range from negligible to 3000ºF-days. Eight surveys were received without a response.

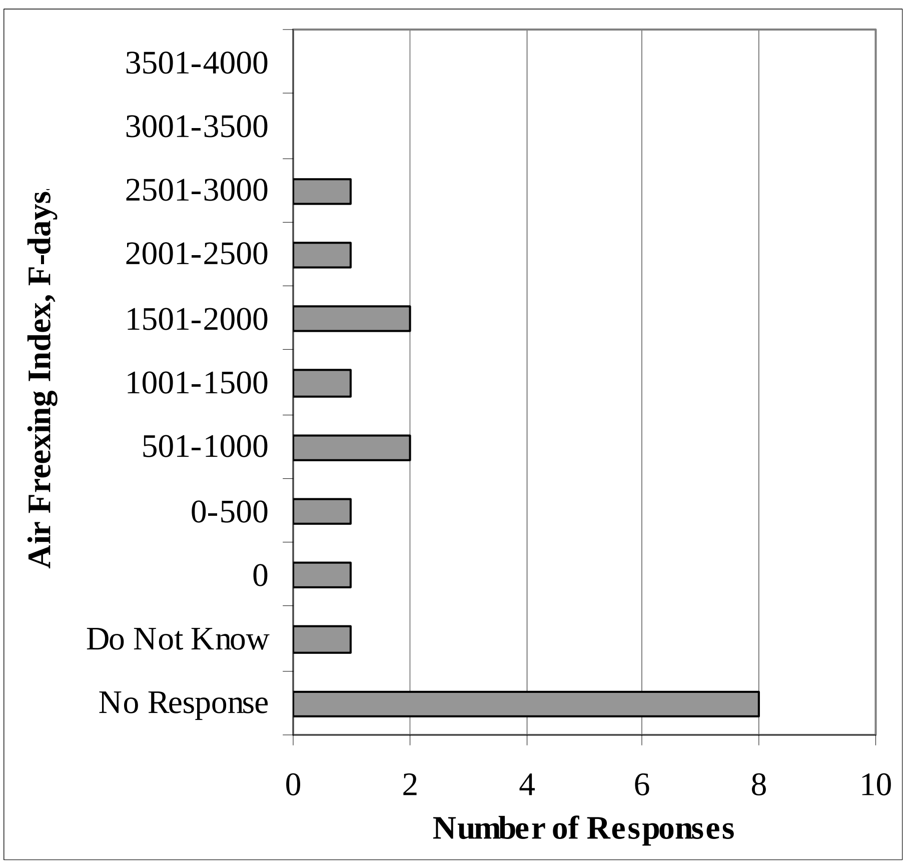

FIGURE 1 Average air freezing indices.

Question 2. What is the typical depth of frost penetration in your area?

The respondents to this question generally answered with both a minimum and a maximum penetration depth for their respective regions. Figure 2 shows the minimum and maximum values of frost penetration depth. Values for minimum and maximum frost penetration depths ranged from 0 ft to 8 ft and from 0 ft to greater than 10 ft, respectively. Only one survey participant did not respond.

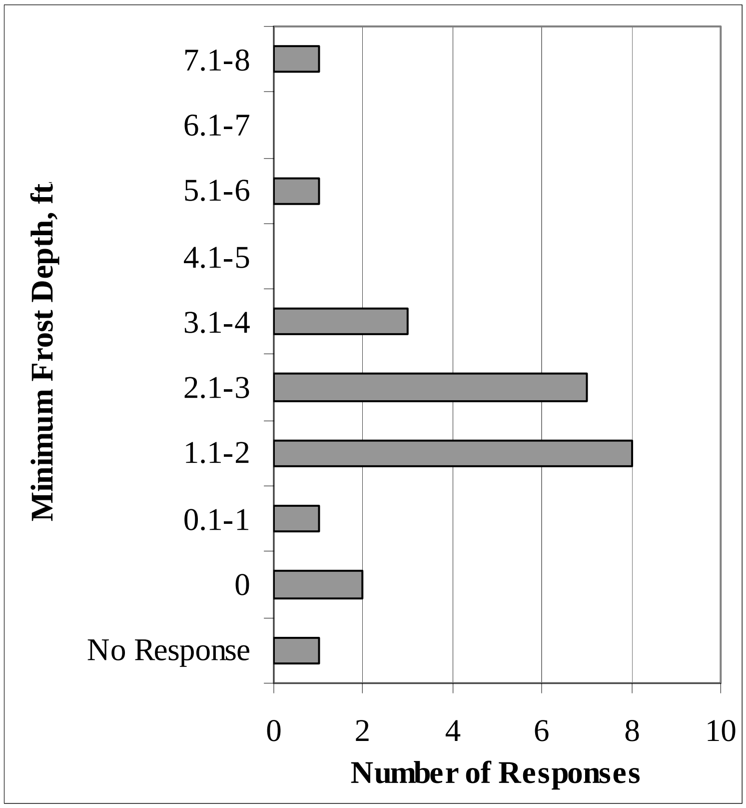

(a) Minimum frost penetration depths.

FIGURE 2 Frost penetration depths.

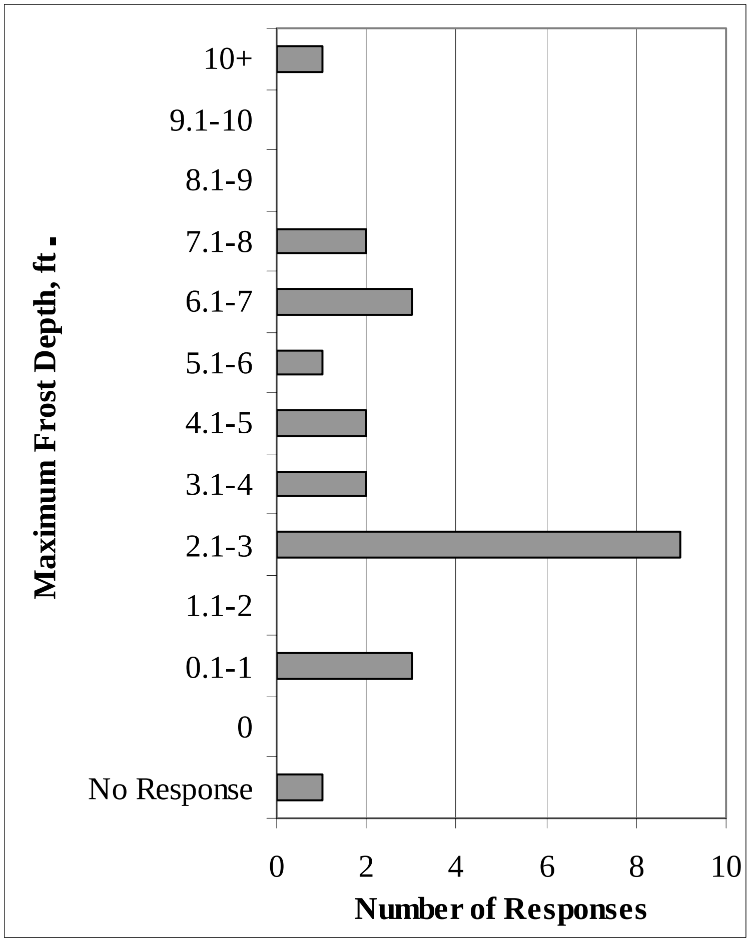

(b) Maximum frost penetration depths.

FIGURE 2 Frost penetration depths, continued.

DESIGN AND CONSTRUCTION

This section discusses the results of the 15 questions regarding design and construction of roadways included in the survey.

Question 1: What kind of pavement design methodology do you use for areas that experience frost action?

As indicated in Figure 3, the pavement design methodologies listed as choices in the survey included mechanistic, reduced subgrade strength, limited subgrade frost penetration, complete protection, American Concrete Pavement Association (ACPA), Portland Cement Association (PCA), National Stone Association (NSA), Asphalt Institute (AI), and American Association of State and Highway Transportation Officials (AASHTO) procedures. The AASHTO method is used more frequently than the other methodologies. Four of the agencies that responded do not consider frost action in their pavement designs. Responses in the “Other” category include placing 2 ft of expanded foam followed by 6 in. of granular base course for areas that experience frost action. Minnesota, New York, Pennsylvania, Arizona, Vermont, and

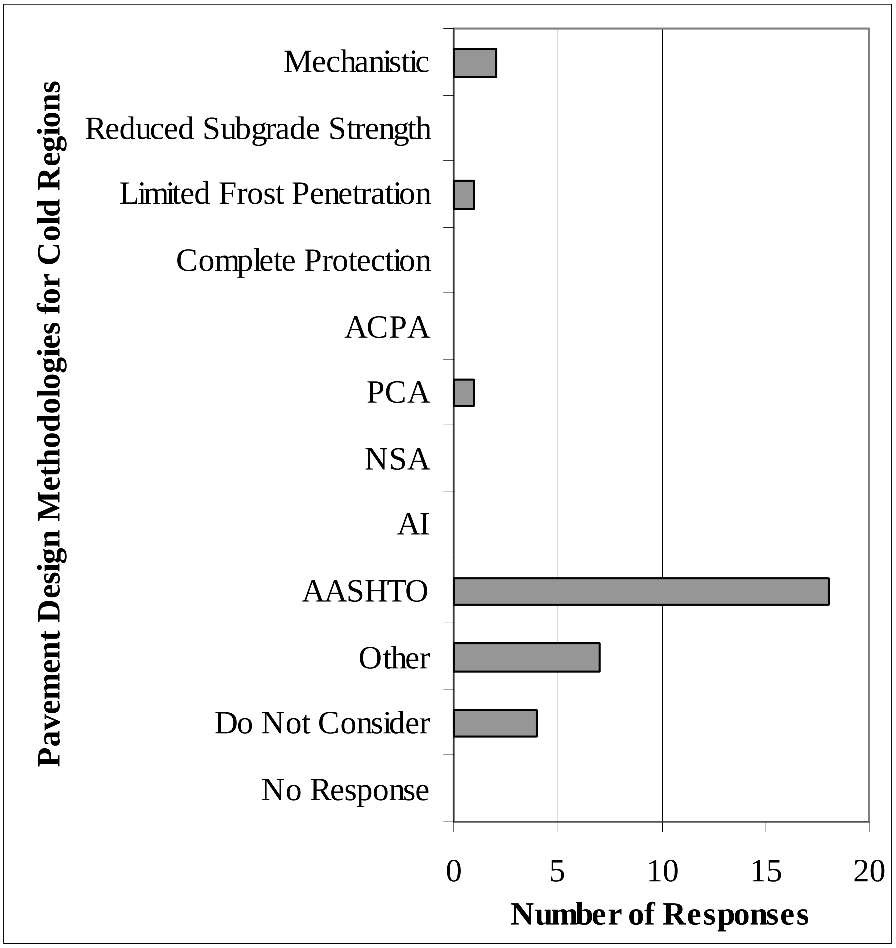

FIGURE 3 Pavement design methodologies used.

Sweden each had specific in-house methodologies that were included in the “Other” response category.

Question 2: What are the layer types and thicknesses of a typical flexible (asphalt) highway pavement in your jurisdiction?

Of the 24 survey respondents, 22 reported that they use HMA for their highway pavements. The remaining two survey participants did not respond. As indicated by 12 of the surveys, dense-graded aggregate is the most commonly used base material for flexible highway pavements. The next most commonly used base material is stabilized base, which is routinely specified by five of the respondents. Crushed aggregate is utilized by four respondents. Two respondents indicated the use of existing material, gravel, or asphalt, and one respondent indicated the use of sand or RAP.

Thirteen responses were received regarding the type of subbase materials generally used in flexible pavement sections. Twelve of the 13 respondents indicated the use of granular material for subbases, while three of the respondents indicated the use of stabilized layers as subbases. The remaining respondents indicated that a subbase layer is not used as part of the flexible highway pavement sections in their jurisdiction.

Figure 4 shows the typical thicknesses used by the respondents for asphalt, base, and subbase layers in flexible highway pavements. Although the thicknesses of the asphalt, base, and subbase vary widely among the respondents, the survey results indicate that 4 in. to 6 in. of HMA, 5 in. to 8 in. of base material, and 7 in. to 12 in. of subbase material are the most commonly specified.

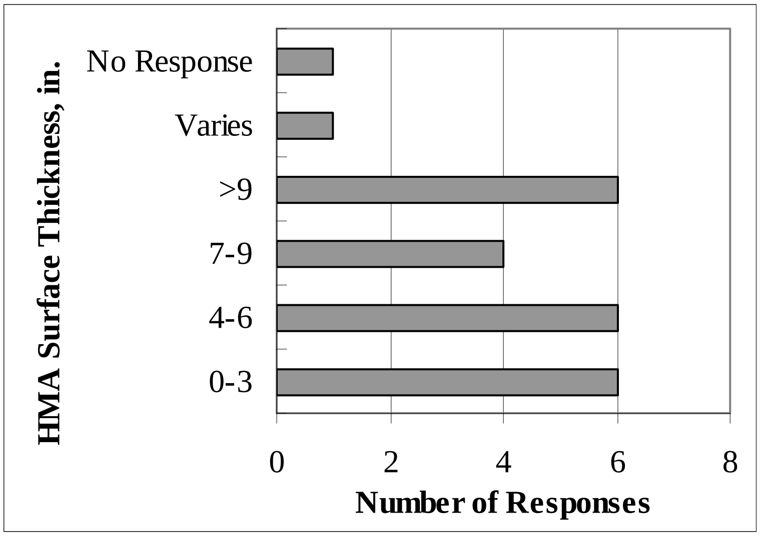

(a) HMA surface thickness.

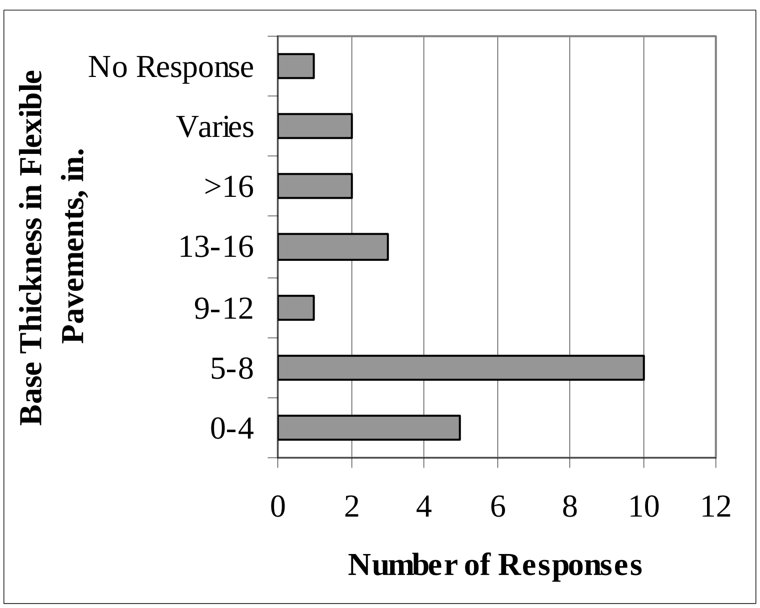

(b) Base thickness.

FIGURE 4 Layer thicknesses in flexible highway pavements.

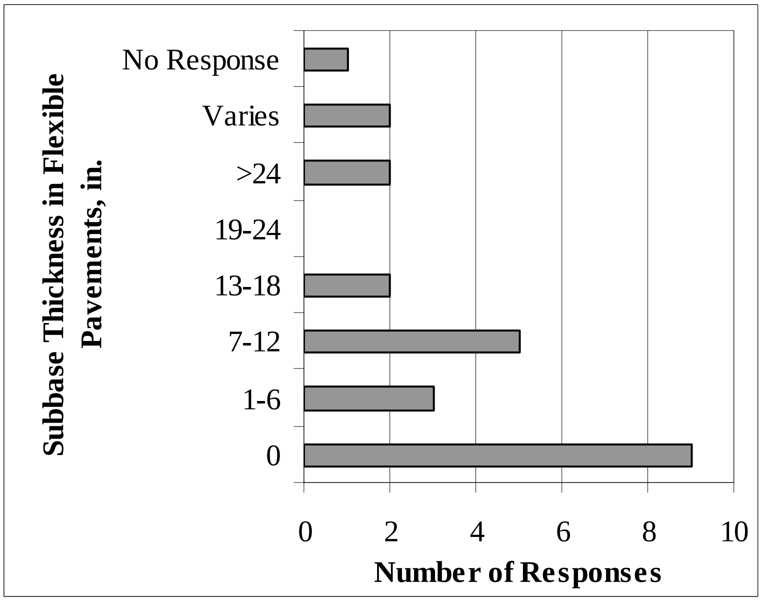

(c) Subbase thickness.

FIGURE 4 Layer thicknesses in flexible highway pavements, continued.

Question 3: What are the types and thicknesses of a typical rigid (concrete) highway pavement in your jurisdiction?

Of the 24 survey respondents, nine reported the use of rigid pavement sections for their highways; the remaining 15 survey participants did not address this question. Of the eight responses received concerning the use of base materials, two indicated the use of granular material, while two of the respondents reported the use of crushed aggregate. Stabilized base, cement-treated base, lean concrete, and asphalt bases were each used by at least one respondent.

Of the surveys received, six included information regarding subbase layers. Three of the six survey respondents indicated that subbase layers are not typically used in rigid pavement sections in their jurisdictions. Two responses indicated the use of granular subbases, while the remaining respondent reported the use of chemically-treated subbases.

Figure 5 shows the typical Portland cement concrete (PCC), base, and subbase thicknesses used in rigid highway pavements. Although the frequency of use is essentially equal across the base and subbase thickness categories, the data show that a PCC thickness of between 9 in. and 12 in. is most commonly specified.

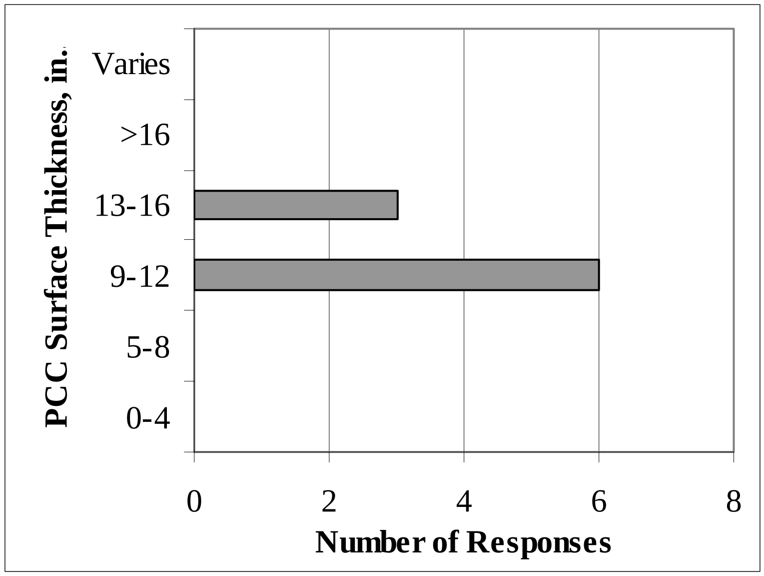

(a) PCC surface thickness.

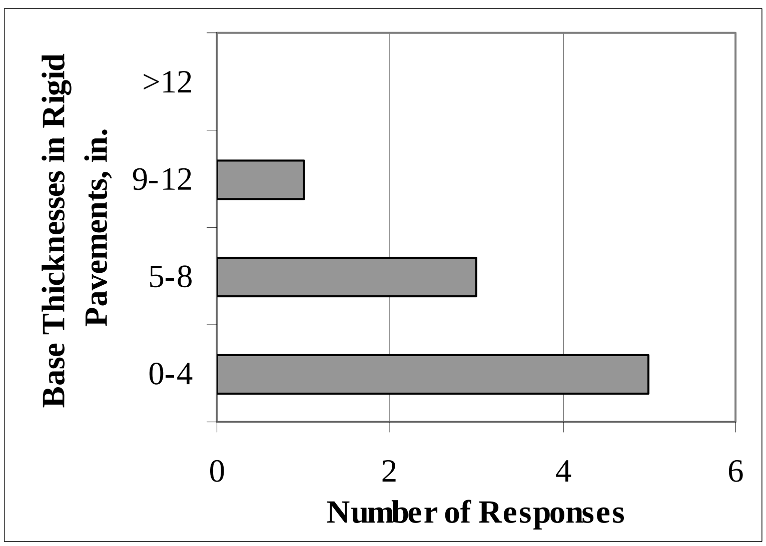

(b) Base thickness.

FIGURE 5 Layer thicknesses in rigid highway pavements.

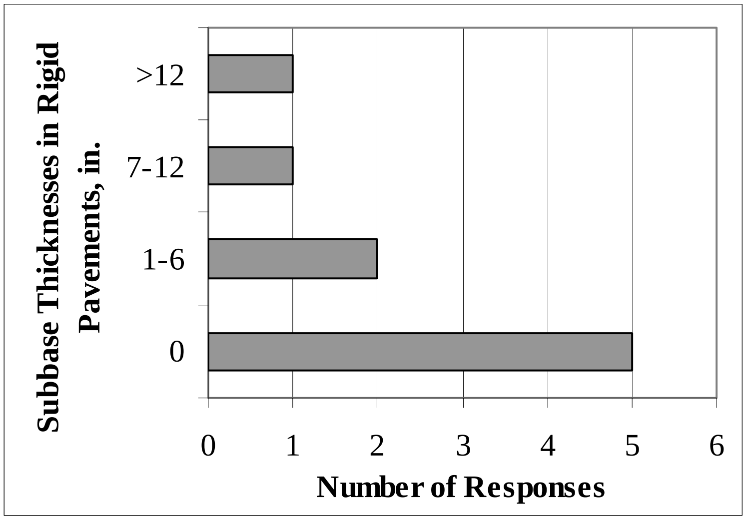

(c) Subbase thickness.

FIGURE 5 Layer thicknesses in rigid highway pavements, continued.

Question 4: How do you determine whether a given aggregate base or subgrade material is frost susceptible?

Figure 6 shows that the most commonly used methods for identifying frost-susceptible soils are field experience, laboratory testing, and particle-size distribution. Responses for “Other” were received from an agency that is currently conducting research to upgrade the existing method, as well as from an agency that uses solely granular bases to reduce the need to identify frost-susceptible soils.

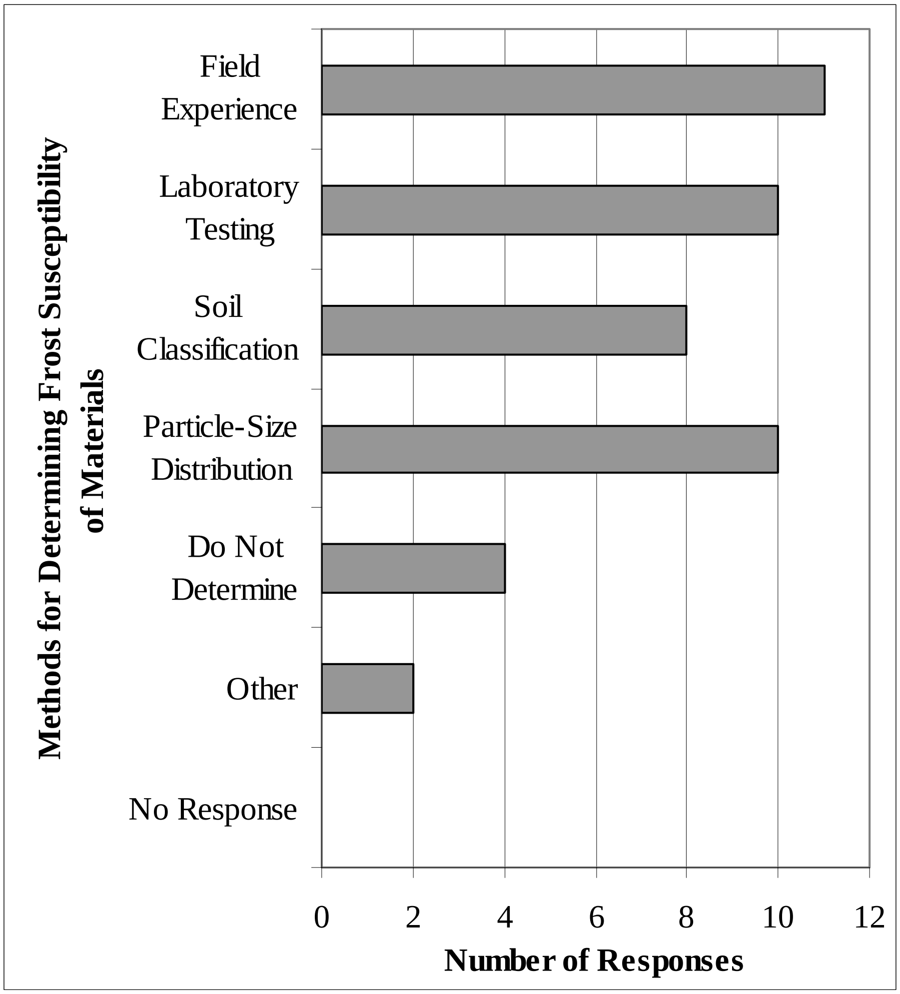

FIGURE 6 Methods used to determine if a material is frost-susceptible.

Question 5: For pavement construction on frost-susceptible subgrades or reconstruction of pavements that previously exhibited frost susceptibility, what pavement construction approaches do you use?

Figure 7 displays the pavement construction practices used in areas characterized by frost-susceptible soils. Excavation and replacement of the frost-susceptible soils is the most frequently cited method of constructing pavements on frost-susceptible subgrades. Only one survey participant did not respond. The response "Other" includes reinforcement with steel nets, bituminous-treated bases, underdrains, rock subgrade fragmentation, and broken rock trenches. Figure 8 presents the depths of excavation and replacement typically specified by the agencies that employ this method. All three of the respondents who cited the use of subgrade processing to remove large stones indicated removal of stones larger than 12 in. in diameter.

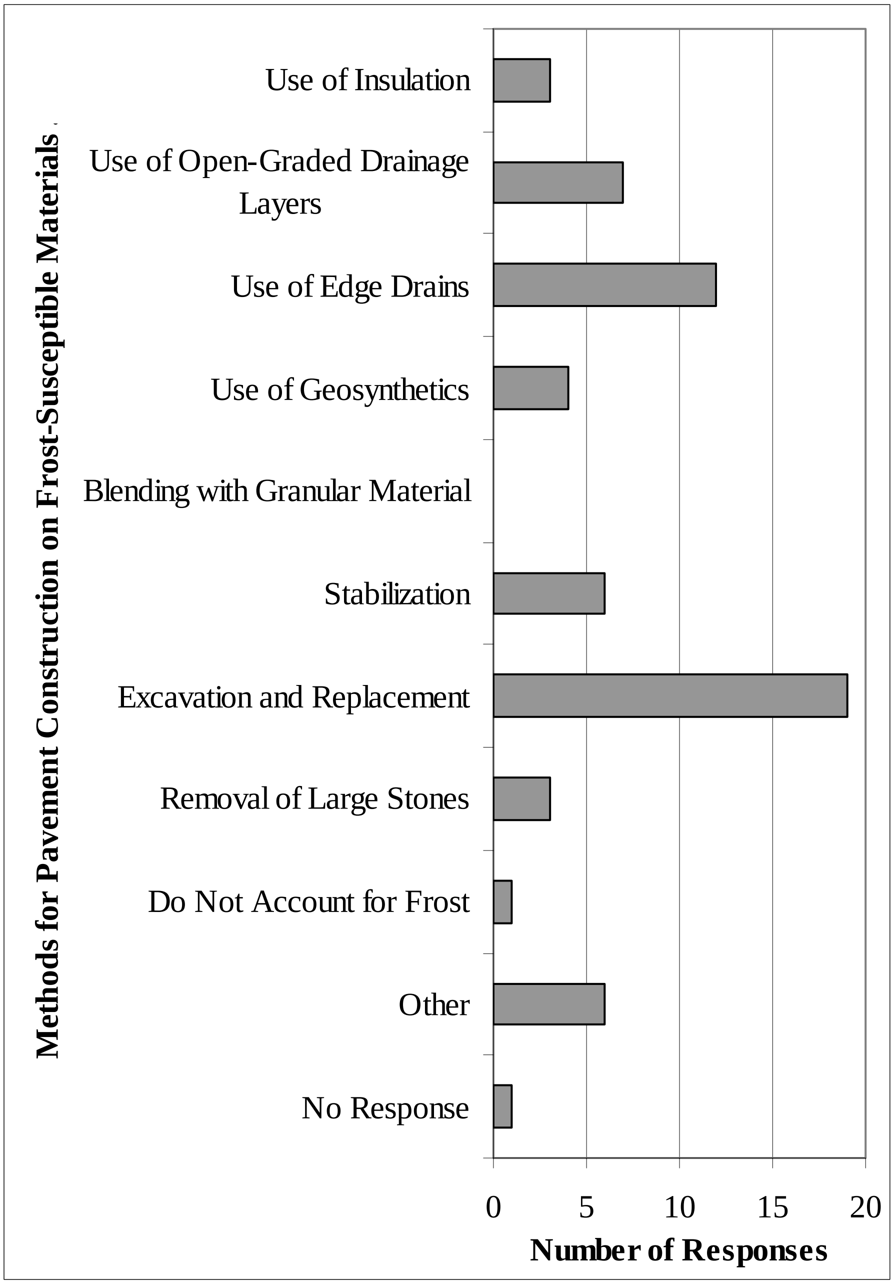

FIGURE 7 Construction methods used for frost-susceptible materials.

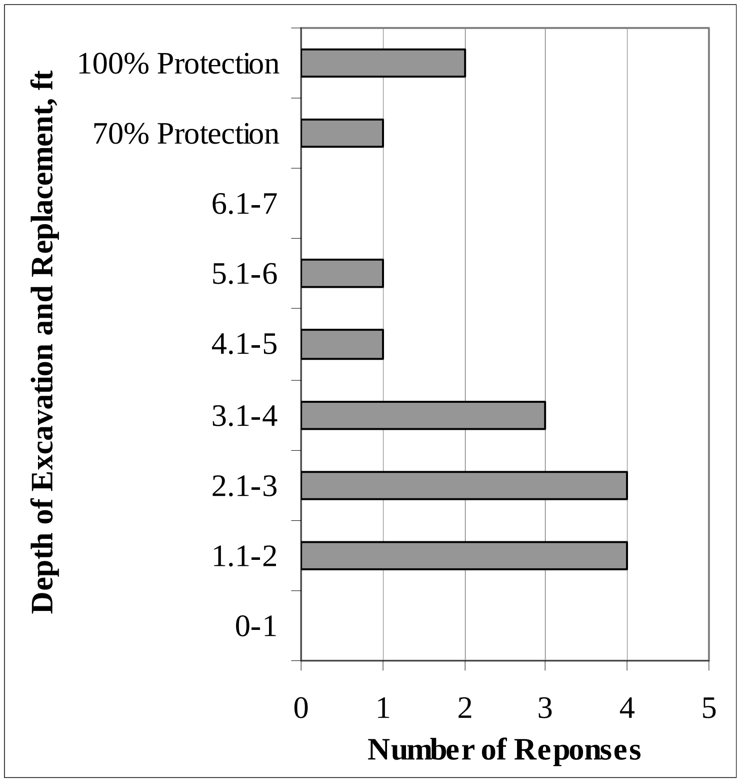

FIGURE 8 Depth of excavation and replacement generally used.

Question 6: When stabilization is selected, which types of stabilizers do you most commonly use?

Figure 9 clearly indicates that Portland cement and lime are the two most commonly used stabilizers. Snake oil, any of various proprietary admixtures, was the only choice not cited by a respondent. The responses for “Other” include that stabilization was used only for constructability purposes and that 1 to 2 percent cement was added to all treated materials. Seven survey respondents did not respond.

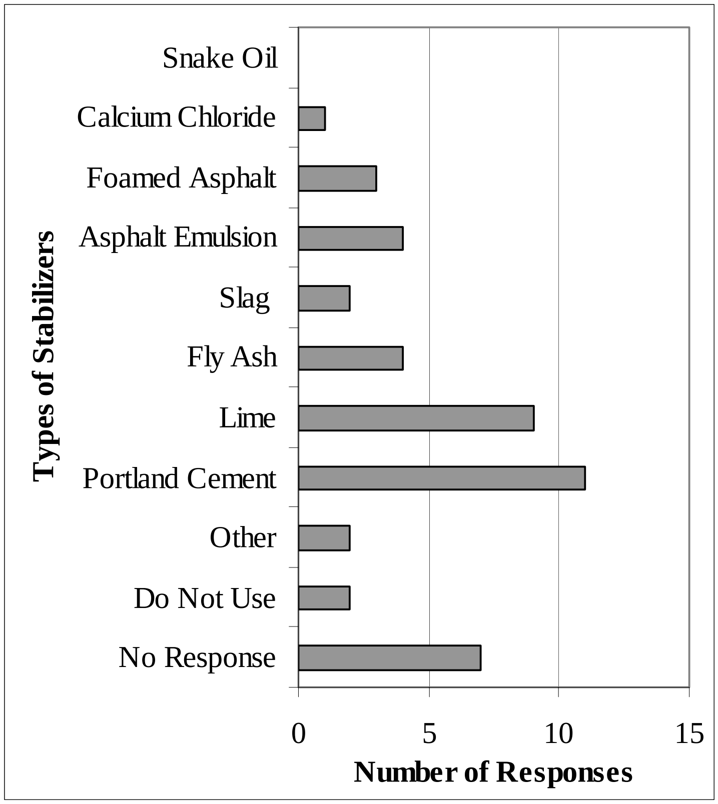

FIGURE 9 Stabilizers most commonly used.

Question 7: How do you determine the optimum amount of chemical stabilizer to add to a given base or subgrade material?

As shown in Figure 10, field experience and unconfined compressive strength (UCS) are the most commonly cited methods for determining the optimum amount of chemical stabilizer to add to a base or subgrade material. Agencies that use UCS for determining lime content all use different target strength values in selecting the optimum content. For example, while one agency specifies strength values of greater than 50 psi at 3 days, another agency requires strengths greater than 60 psi at 7 days. A third agency adds sufficient lime to achieve an increase of 50 psi over the untreated soil strength. Target UCS values for cement stabilization ranged from 3-day values between 100 psi and 150 psi and 7-day values between 125 psi and 750 psi. The responses for "Other" include plasticity index reduction, indirect tensile strength, Virginia DOT in-house testing procedure, Eades and Grimm procedure, 10 percent by weight, pH test for lime, and the Wirtgen process for foamed asphalt. Seven survey respondents did not respond to the question.

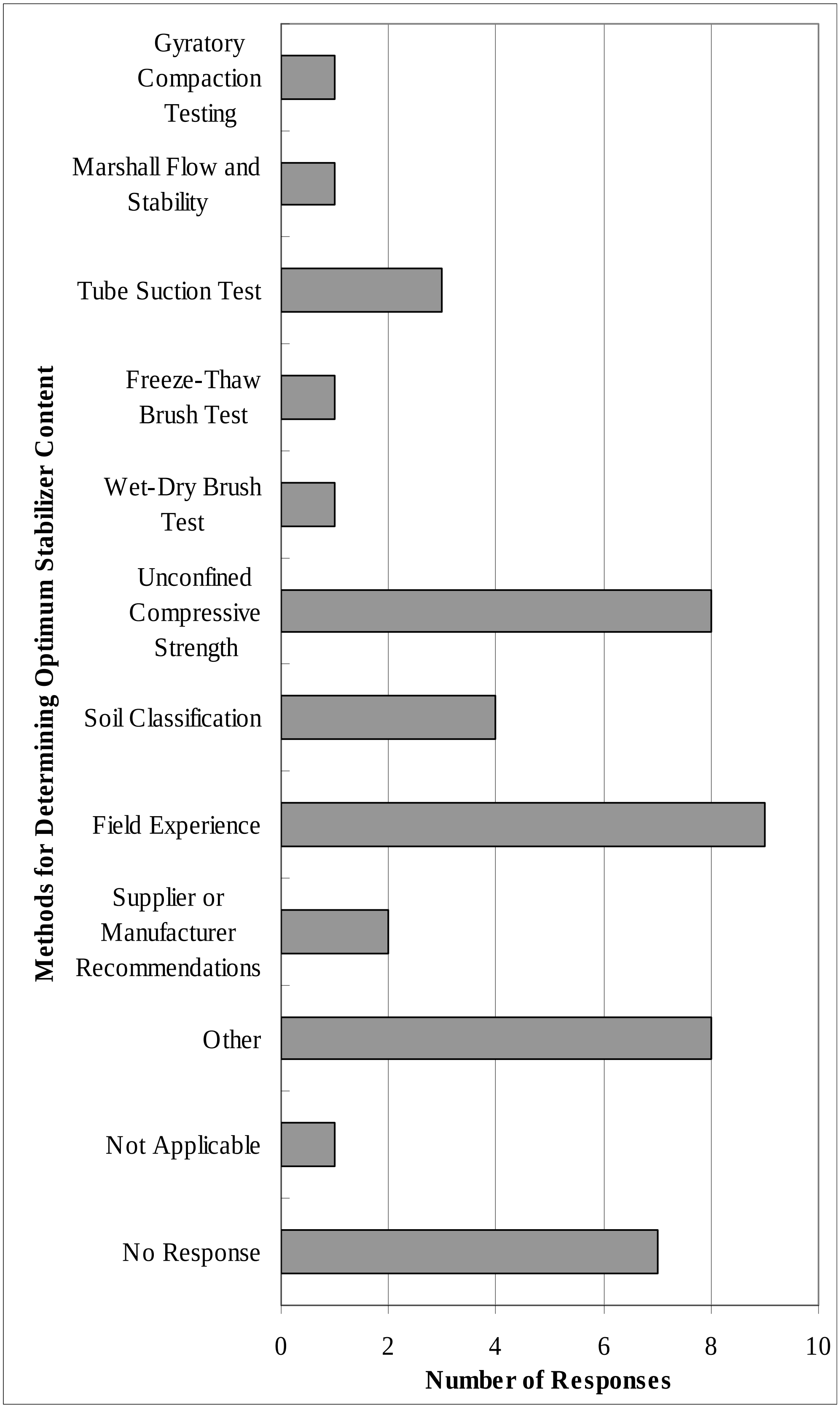

FIGURE 10 Methods used to determine optimum amount of chemical stabilizer.

Question 8: When geosynthetics (geogrids in particular) are used in the pavement structure, do you permit thinner surface or base layers compared to pavement structures not designed with geosynthetics?

Of the 24 surveys received, one did not respond, six indicated that they do permit thinner pavement sections to be constructed when geosynthetics are incorporated in the design, and 17 indicated that they do not allow thinner pavement sections. Of the respondents that indicated that they do not allow thinner pavement sections, many indicated that they do not have research supporting the effectiveness of geosynthetics. One participant explained that he had tried geosynthetics twice in the past, but both sections had failed. Many of the agencies that do not allow thinner pavement sections do apparently use geosynthetics in problematic areas and for constructability purposes, however. Those that do permit the use of thinner pavement sections reported increasing the subgrade R-value by 10 points in design, reducing subbase thicknesses by 6 in., and using Spectrapave software for designing with geogrids.

Question 9: For full-depth recycling of asphalt pavements, what is the typical weight ratio of reclaimed asphalt pavement (RAP) to aggregate base material that you use in the mixture with the underlying base material? For example, a blend of 40 percent RAP and 60 percent base would be a ratio of 40:60.

The most common answer to this question was that full-depth recycling is not used. However, as shown in Figure 11, agencies that do utilize this technique indicate that the typical RAP content is 50 percent, which corresponds to a 50:50 ratio of RAP to base, or that it varies by project. Three survey participants did not respond to the question.

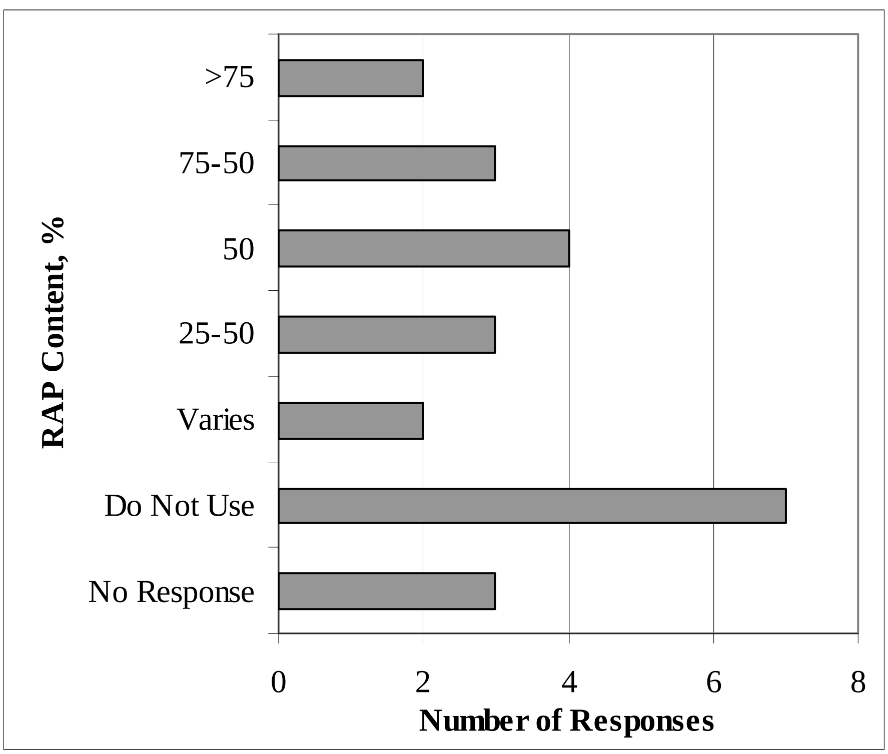

FIGURE 11 RAP content used.

Question 10: For construction of full-depth-recycled asphalt pavements, what other materials specifications or processing specifications do you utilize?

Twenty-five survey participants responded to this question, eight of whom indicated that the question was not applicable. Five survey participants did not respond. Among the remaining respondents, seven indicated the use of in-house specifications. Other responses indicated individual requirements for specific gradations and/or the use of Portland cement, crushed stone, gravel, or asphalt.

Question 11: Overall, what are your observations regarding the performance of pavements constructed using the full-depth recycling process in your jurisdiction?

Three of the 16 agencies indicated that the performance of full-depth recycled pavements was very good, and nine agencies indicated good performance. Two agencies judged the performance as satisfactory, and four agencies indicated poor performance. Only one agency did not respond.

Question 12: In construction of cement-treated pavement layers, what procedures do you follow to minimize shrinkage cracking of layers? For example, please address pre-cracking procedures, if used, the type and timing of sealing, the timing of surface layer paving, use of granular layers or other features to resist reflective cracking into the surface, and other relevant practices.

Ten of the respondents indicated that the question was not applicable, and three did not respond. Of the answers received, curing seal was the most common, as indicated by five respondents. Maintaining moisture levels and using minimum amounts of Portland cement were reported by four respondents. Using geogrids, requiring lower UCS values, pre-cracking, and only stabilizing the subbase layer were all responses given. One of the respondents indicated that they did not require any method for minimizing shrinkage cracking.

Questions 13: Following construction of a cement-treated pavement layer, what methods or specifications are used to certify that the layer can be opened to traffic?

Figure 12 indicates that specifying a curing time is the method most frequently used by the survey respondents. Seven survey participants did not respond to the question. Curing times of 3 days and 7 days are most common as indicated by three respondents for each curing time. A two-day curing time is used by one agency, while another agency requires that paving occur within two days of placing the cement-treated layer.

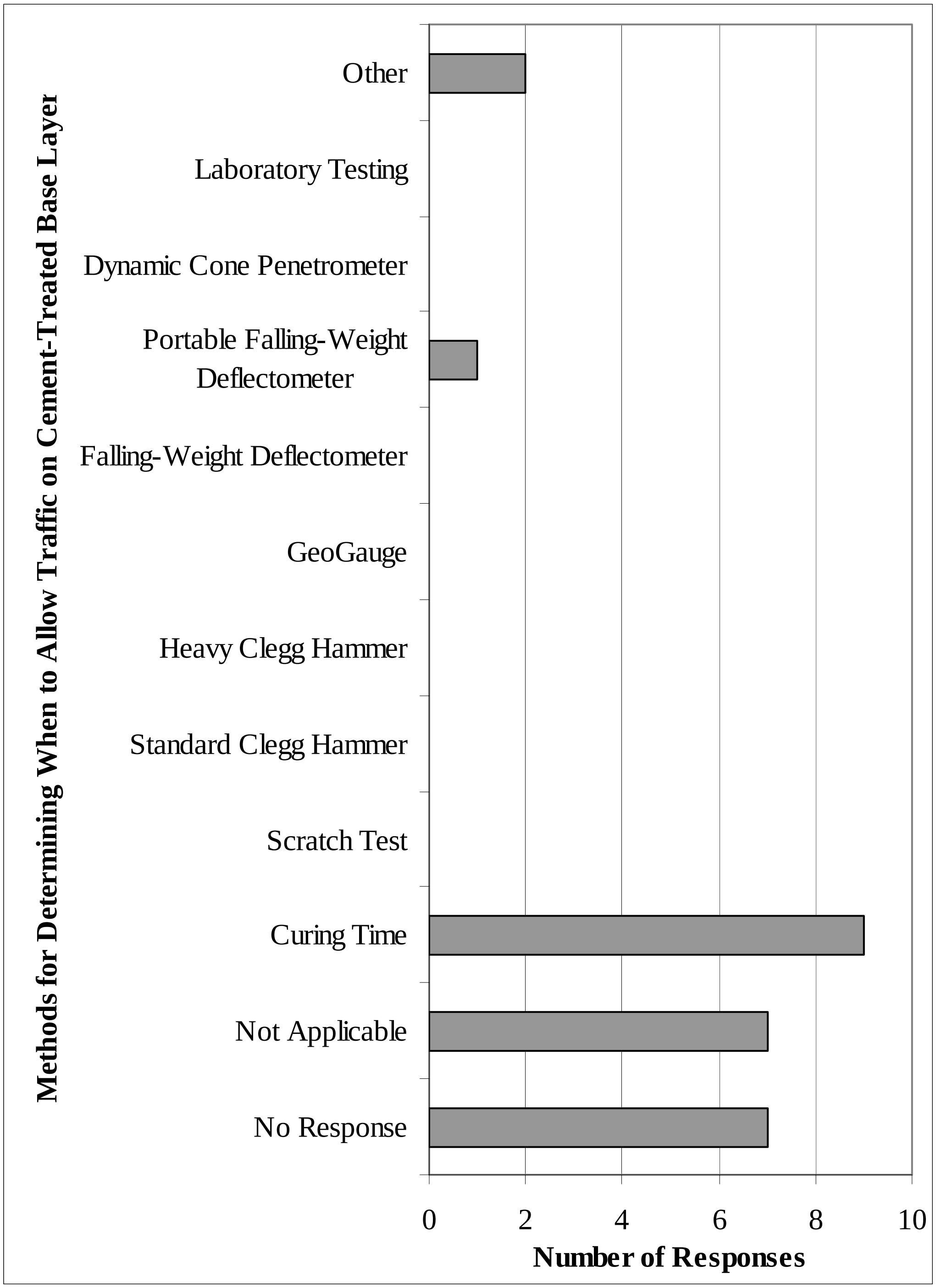

FIGURE 12 Methods used to determine when to open a cement-treated pavement layer to traffic.

Question 14: Overall, what are your observations regarding the performance of pavements constructed using chemically or mechanically stabilized layers in your jurisdiction?

Two survey respondents reported very good performance, and five respondents reported good performance. Six participants indicated satisfactory performance. Only one agency reported poor performance of stabilized layers. Four survey participants did not respond

Question 15: Do you have pavement projects scheduled for the upcoming construction season that will utilize full-depth recycling in conjunction with cement stabilization?

Only five agencies indicated plans to utilize full-depth recycling in conjunction with cement stabilization during the next construction season. Only two survey participants did not respond.

POLICIES

This section discusses responses to the two survey questions that addressed spring and winter pavement loading policies.

Question 1: Do you require spring load restrictions for pavements in your jurisdiction?

Thirteen of the 23 agencies that responded to the question reported that they do not require spring load restrictions in their jurisdictions. Ten of the agencies indicated that they do require some type of spring load restriction. Of the agencies that do require spring load restrictions, past experience was the most common method used to determine the timing and duration of the restrictions, as listed by four respondents. Computer modeling and use of a predetermined period of time were methods listed by two and three surveys, respectively. In addition, evaluation of snow melt, soil temperature, and air temperature were cited as methods used by different agencies to determine both the timing and duration of the spring load restrictions.

Question 2: Do you permit winter load premiums?

Only two of the 24 agencies surveyed allow a winter load premium. One survey participant did not respond to the question.

Appendix B:

Suggested Construction Specifications for Full-Depth Reclamation with Cement-Treated Base

NOTE:

The construction guidelines included in this appendix were developed by David R. Luhr, Wayne S. Adaska and Gregory E. Halsted (PCA, 2005).

1. GENERAL

1.1 Description. Full-depth reclamation (FDR) shall consist of pulverizing and mixing the existing asphalt pavement and base course material with portland cement soil and water to produce a dense, hard cement-treated base. It shall be proportioned, mixed, placed, compacted and cured in accordance with these specifications; and shall conform to the lines, grades, thicknesses, and typical cross sections shown in the plan.

1.2 Caveat. These specifications are intended to serve as a guide to format and content for normal FDR construction. Most projects have special features or requirements that should be incorporated in the project documents.

2. MATERIALS

2.1 Recycled Asphalt Pavement (RAP) and Base Material. Shall consist of the existing asphalt pavement, existing base course material and/or subgrade material. The base course and subgrade material shall not contain roots, topsoil or any material deleterious to its reaction with cement. The particle distribution of the processed material shall be such that 100% passes the 3-in. (75 mm) sieve, 95% passes a 2-in. (50 mm) sieve, and at least 55% passes a No. 4 (4.75 mm)sieve.

2.2 Portland Cement. Shall comply with the latest specifications for portland cement (ASTM C 150, ASTM C 1157, or AASHTO M 85) or blended hydraulic cements (ASTM C595, ASTM C 1157, or AASHTO M 240).

2.3 Water. Water shall be free from substances deleterious to the hardening of the cement treated material.

2.4 Pozzolans. If used, pozzolans including fly ash, slag, and silica fume shall comply with the appropriate specifications (ASTM C 618, AASHTO M 295 for fly ash; ASTM C 989, AASHTO M 302 for slag; and ASTM C 1240 for silica fume).

3. EQUIPMENT

3.1 Description FDR may be constructed with any machine or combination of machines or equipment that will produce a satisfactory product meeting the requirements for pulverization, cement and water application, mixing, compacting, finishing, and curing as provided in these specifications.

3.2 Mixing Methods. Mixing shall be accomplished in place, using single-shaft or multiple-shaft mixers. Agricultural disks or motor graders are not acceptable mixing equipment.

3.3 Cement Proportioning. Cement can be added in a dry or a slurry form. If applied in slurry form, the slurry mixer and truck shall be capable of completely dispersing the cement in the water to produce a uniform slurry, and shall continuously agitate the slurry once mixed.

3.4 Application of Water. Water may be applied through the mixer or with water trucks equipped with pressure-spray bars.

3.5 Compaction. The processed material shall be compacted with one or a combination of the following: tamping or grid roller, pneumatic-tire roller, steel-wheel roller, vibratory roller, or vibrating-plate compactor.

4. CONSTRUCTION REQUIREMENTS

4.1 General

4.1.1 Preparation of Subgrade. Before processing begins, the area to be processed shall be graded and shaped to lines and grades as shown in the plans or as directed by the engineer. During this process any unsuitable soil or material shall be removed and replaced with acceptable material. Any manholes, valve covers or other buried structures shall be protected from damage prior to processing. The subgrade shall be firm and able to support without yielding or subsequent settlement the construction equipment and the compaction of the FDR material. Soft or yielding subgrade shall be corrected and made stable before construction proceeds.

4.1.2 Mixing and Placing. FDR processing shall not commence when the soil aggregate or subgrade is frozen, or when the air temperature is below 40^{o}F. Moisture in the base course material at the time of cement application shall not exceed the quantity that will permit a uniform and intimate mixture of the pulverized asphalt, base material and cement during mixing operations, and shall be within 2% of the optimum moisture content for the processed material at start of compaction.

The operation of cement application, mixing, spreading and compacting shall be continuous and completed within 2 hours from the start of mixing. Any processed material that has not been compacted and finished shall not be left undisturbed for longer that 30 minutes.

4.2 Pulverization/Mixing

4.2.1 Preparation. The surface of the pavement prior to mixing shall be at an elevation so that, when mixed with cement and water and recompacted to the required density, the final elevation will be as shown in the plans or as directed by the engineer. The material in place and surface conditions shall be approved by the engineer before the next phase of construction is begun.

4.2.2 Scarifying. Before cement is applied, initial pulverization or scarification may be required to the full depth of mixing. Scarification and pre-pulverization is a requirement for the following conditions:

1) When the processed material is more than 3% above or 3% below optimum moisture content. When the material is below optimum moisture content, water shall be added. The pre-pulverized material shall be sealed and properly drained at the end of the day or if rain is expected.

2) For slurry application of cement, initial scarification shall be done to provide a method to uniformly distribute the slurry over the processed material without excessive runoff or ponding.

4.2.3 Application of Cement. The specified quantity of cement shall be applied uniformly in a manner which minimizes dust and is satisfactory to the engineer. If cement is applied as a slurry, the time from first contact or cement with water to application on the soil shall not exceed 60 minutes. The time from slurry placement on the soil to start of mixing shall not exceed 30 minutes.

4.2.4 Mixing. Mixing shall begin as soon as possible after the cement has been spread and shall continue until a uniform mixture is produced. The mixed material shall meet the following gradation conditions:

1) The final mixture (bituminous surface, granular base and subgrade soil) shall be pulverized such that 100% passes the 3-in. (75 mm) sieve, 95% passes the 2 in. (50 mm) sieve and at least 55 % passes the No. 4 (4.75 mm) sieve. No more than 50% of the final mixed material shall be made of the existing bituminous material unless approved by the engineer and included in a mixture design. Additional material can be added to the top, or from the subgrade to improve the mixture gradation, as long as this material was included in the mixture design.

2) The final pulverization test shall be made at the conclusion of mixing operations. Mixing shall be continued until the product is uniform in color, meets gradation requirements, and is at the required moisture content throughout. The entire operation of cement spreading, water application, and mixing shall result in a uniform pulverized asphalt, soil, cement, and water mixture for the full design depth and width.

4.3 Compaction. The processed material shall be uniformly compacted to a minimum of 98% of maximum density based on a moving average of five consecutive tests with no individual test below 96%. Field density of compacted material can be determined by 1) Nuclear method in the direct transmission mode (ASTM D 2922, AASHTO T 238); 2) Sand cone method (ASTM D 1556, AASHTO T 191); or rubber balloon method (ASTM D 2167 or AASHTO T 205). Optimum moisture and maximum density shall be determined prior to start of construction and also in the field during construction by a moisture-density test (ASTM D 558 or AASHTO T 134).

At the start of compaction, the moisture content shall be within 2% of the specified optimum moisture. No section shall be left undisturbed for longer than 30 minutes during compaction operations. All compaction operations shall be completed within 2 hours from start of mixing.

4.4 Finishing. As compaction nears completion, the surface of the FDR material shall be shaped to the specified lines, grades, and cross sections. If necessary or as required by the engineer, the surface shall be lightly scarified or broom-dragged to remove imprints left by equipment or to prevent compaction planes. Compaction shall then be continued until uniform and adequate density is obtained. During the finishing process the surface shall be kept moist by means of water spray devices that will not erode the surface. Compaction and finishing shall be done in such a manner as to produce dense surface free of compaction planes, cracks, ridges, or loose material. All finishing operations shall be completed within 4 hours from start of mixing.

4.5 Curing. Finished portions of the FDR base that are traveled on by equipment used in constructing an adjoining section shall be protected in such a manner as to prevent equipment from marring or damaging completed work.

After completion of final finishing, the surface shall be cured by application of a bituminous or other approved sealing membrane, or by being kept continuously moist for a period of 7 days with a water spray that will not erode the surface of the FDR base. If curing material is used, it shall be applied as soon as possible, but not later than 24 hours after completing finishing operations. The surface shall be kept continuously moist prior to application of curing material.

For bituminous curing material, the soil-cement surface shall be dense, free of all loose and extraneous materials, and shall contain sufficient moisture to prevent excessive penetration of the bituminous material. The bituminous material shall be uniformly applied to the surface of the completed cement treated material. The exact rate and temperature of application for complete coverage, without undue runoff, shall be specified by the engineer.

Should it be necessary for construction equipment or other traffic to use the bituminous-covered surface before the bituminous material has dried sufficiently to prevent pickup, sufficient sand cover shall be applied before such use.

Sufficient protection from freezing shall be given the cement treated material for 7 days after its construction or as approved by the engineer.

4.6 Traffic. Completed portions of FDR base can be opened immediately to low-speed local traffic and to construction equipment, provided the curing material or moist curing operations are not impaired, and provided the FDR base is sufficiently stable to withstand marring or permanent deformation. The section can be opened up to all traffic after the FDR base has received a curing compound or subsequent surface, and is sufficiently stable to withstand marring or permanent deformation. If continuous moist curing is employed in lieu of a curing compound or subsequent surfacing within 7 days, the soil-cement can be opened to all traffic after the 7-day moist curing period, provided the FDR base has hardened sufficiently to prevent marring or permanent deformation.

4.7 Surfacing. Subsequent pavement layers (asphalt, chip-seal or concrete) can be placed any time after finishing, as long as the soil-cement is sufficiently stable to support the required construction equipment without marring or permanent distortion of the surface.

4.8 Maintenance. The contractor shall maintain the cement treated material in good condition until all work is completed and accepted. Such maintenance shall be done by the contractor at his own expense.

Maintenance shall include immediate repairs of any defects that may occur. If it is necessary to replace any processed material, the replacement shall be for the full depth, with vertical cuts, using either cement treated material or concrete. No skin patches will be permitted.

5. INSPECTION AND TESTING

5.1 Description. The engineer, with the assistance and cooperation of the contractor, shall make such inspections and tests as he deems necessary to ensure the conformance of the work to the contract documents. These inspections and tests may include, but shall not be limited to, (1) Obtaining test samples of the cement treated material and its individual components at all stages of processing and after completion and (2) Observing the operation of all equipment used on the work. Only those materials, machines, and methods meeting the requirements of the contract documents shall be approved by the engineer.

All testing of processed material or its individual components, unless otherwise provided specifically in the contract documents, shall be in accordance with the latest applicable ASTM or AASHTO, specifications in effect as of the date of advertisement for bids on the project.

6. MEASUREMENT AND PAYMENT

6.1 Measurement. This work will be measured (1) in square yards (square meters) of completed and accepted cement treated base course as determined by the specified lines, grades, and cross sections shown on the plans and (2) in tons (tonnes) or cwt of cement incorporated into the cement treated base course in accordance with the instructions of the engineer.

6.2 Payment. This work will be paid for at the contract unit price per square yard (square meter) of cement treated base course and at the contract unit price per ton (tonne) or cwt of cement furnished, multiplied by the quantities obtained in accordance with Section 6.1. Such payment shall constitute full reimbursement for all work necessary to complete the cement treated base course, including watering, curing, inspection and testing assistance, and all other incidental operations.

Appendix C:

Supplementary Information and Data from Soil Moisture Probes

NOTE:

A total of six soil moisture sensors ("Hydra Probes") manufactured by Stevens Water Monitoring Systems, Inc. were installed at the test site on the Kancamagus Highway (Rt. 112) in NH. All of the moisture sensors were installed between wheel paths (approximately six feet off centerline) in the eastbound lane of Route 112. The locations (station, elevation, and depth below top of pavement) of the soil moisture sensors are tabulated in the beginning of this Appendix. Baseline data obtained from the moisture sensors is included at the end of this Appendix.

Locations of Soil Moisture Sensors

I.D.	Approx. Station	Test Section	Elev. Sensor (ft)	Elev. Top Pavement (ft)	Depth Below Top of Pave-ment (in)	Comments
1A	46+87	Conventional Reconstruction	1227.37	1228.23	10.3	Sensor in "select material" just below gravel base
1B	46+87	Conventional Reconstruction	1224.69	1228.23	42.5	Sensor in Subgrade
2A	58+95	FDR with Cement	1224.47	1225.10	7.6	Sensor in Base
2B	58+95	FDR with Cement	1223.47	1225.10	19.6	Sensor in Subgrade
3B	60+65	FDR without Cement	1224.23	1225.43	14.4	Sensor in Subgrade
3A	61+05	FDR without Cement	1225.04	1225.43	4.7	Sensor in Base

Moisture Probe 1A

Date	Er	Ei
06/28/05	10.4770	1.1998
08/16/05	7.7630	1.5070
08/17/05	7.7330	1.5440
09/01/05	7.7149	1.8067
10/11/05	7.6300	1.9300
11/25/05	7.4010	1.3600
12/28/05	4.4080	0.4000
04/23/06	7.0860	2.5200

Moisture Probe 1B

Date	Er	Ei
06/28/05	6.4711	0.8015
08/16/05	5.5290	0.3470
08/17/05	5.4400	0.3700
09/01/05	5.2644	0.3656
10/11/05	5.6500	0.3700
11/25/05	5.1630	0.2260
12/28/05	3.3810	0.2170
04/23/06	5.0920	1.2100

Moisture Probe 2A

Date	Er	Ei
06/28/05	8.1820	7.5725
08/16/05	7.4860	5.2870
08/17/05		
09/01/05	7.4145	4.8718
10/11/05	7.0480	4.2200
11/25/05	4.3840	1.2150
12/28/05	4.3220	1.0320
04/23/06	6.4130	3.1050

Moisture Probe 2B

Date	Er	Ei
06/28/05	4.0855	0.5857
08/16/05	3.8260	0.5350
08/17/05	3.7390	0.5730
09/01/05	3.6817	0.5826
10/11/05	3.6342	0.5266
11/25/05	3.4750	0.3910
12/28/05	2.7760	0.2860
04/23/06	3.8230	1.2660

Moisture Probe 3A

Date	Er	Ei
06/28/05		
08/16/05	5.1970	1.0780
08/17/05	5.1990	1.0790
09/01/05	6.1534	0.4524
10/11/05	5.7335	0.2784
11/25/05	3.3680	0.1670
12/28/05	3.4840	0.1050
04/23/06	6.0540	4.3730

Moisture Probe 3B

Date	Er	Ei
06/28/05	4.8059	0.4545
08/16/05	5.0500	0.5990
08/17/05	5.0510	0.5990
09/01/05	4.9586	0.5713
10/11/05	4.9370	0.5043
11/25/05	3.6060	0.2290
12/28/05	3.4990	0.2310
04/23/06	5.0210	0.7460

NOTE:

Er = Real component of the complex dielectric constant

Ei = Imaginary component of the complex dielectric constant

Appendix D:

Supplementary Information and Data from Thermistors

NOTE:

A total of six thermistors were installed at the test site on the Kancamagus Highway (Rt. 112) in NH. All thermistors were installed between wheel paths (approximately six feet off centerline) in the eastbound lane of Route 112. The approximate locations (station numbers) and the depths of the individual temperature gauges relative to the top of the pavement are tabulated in the beginning of this Appendix. Temperature data obtained by USDA Forest Service personnel at three of the thermistors (one in each test section) during the 2005-2006 winter/spring monitoring period is included at the end of this Appendix.

Thermistor in Conventional Reconstruction Test Section

Location A	Thermistor # T-6	Sta. 46+62	Elev. Top of Pavement (ft) = 1228.36	
	Channel	Depth below Top Probe (in)	Depth below Top Pavement (in)	Elevation (ft)
	2	1.5	4.1	1228.015
	3	5.5	8.1	1227.682
	4	9.5	12.1	1227.348
	5	13.5	16.1	1227.015
	6	17.5	20.1	1226.682
	7	21.5	24.1	1226.348
	8	25.5	28.1	1226.015
	9	31.5	34.1	1225.515
	10	37.5	40.1	1225.015
	11	43.5	46.1	1224.515
	12	49.5	52.1	1224.015
	13	61.5	64.1	1223.015

Thermistor in FDR with Cement Test Section

	Thermistor # T-2	Sta. 58+95	Elev. Top of Pavement (ft) = 1225.10	
	Channel	Depth below Top Probe (in)	Depth below Top Pavement (in)	Elevation (ft)
	2	1.5	9.1	1224.342
	3	5.5	13.1	1224.008
	4	9.5	17.1	1223.675
	5	13.5	21.1	1223.342
	6	17.5	25.1	1223.008
	7	21.5	29.1	1222.675
	8	25.5	33.1	1222.342
	9	31.5	39.1	1221.842
	10	37.5	45.1	1221.342
	11	43.5	51.1	1220.842
	12	49.5	57.1	1220.342
	13	61.5	69.1	1219.342

Thermistor in FDR with Cement Test Section

Location B	Thermistor # T-1	Sta. 59+37	Elev. Top of Pavement (ft) = 1225.12	
	Channel	Depth below Top Probe (in)	Depth below Top Pavement (in)	Elevation (ft)
	2	1.5	5.56	1224.657
	3	5.5	9.56	1224.323
	4	9.5	13.56	1223.99
	5	13.5	17.56	1223.657
	6	17.5	21.56	1223.323
	7	21.5	25.56	1222.99
	8	25.5	29.56	1222.657
	9	31.5	35.56	1222.157
	10	37.5	41.56	1221.657
	11	43.5	47.56	1221.157
	12	49.5	53.56	1220.657
	13	61.5	65.56	1219.657

Thermistor in FDR without Cement Test Section

	Thermistor # T-4	Sta. 60+65	Elev. Top of Pavement (ft) = 1225.43	
	Channel	Depth below Top Probe (in)	Depth below Top Pavement (in)	Elevation (ft)
	2	1.5	57.66	1220.625
	3	5.5	61.66	1220.292
	4	9.5	65.66	1219.958
	5	13.5	69.66	1219.625
	6	17.5	73.66	1219.292
	7	21.5	77.66	1218.958
	8	25.5	81.66	1218.625
	9	31.5	87.66	1218.125

Thermistor in FDR without Cement Test Section

Location C	Thermistor # T-3	Sta. 60+65	Elev. Top of Pavement (ft) = 1225.43	
	Channel	Depth below Top Probe (in)	Depth below Top Pavement (in)	Elevation (ft)
	2	1.5	10.66	1224.542
	3	5.5	14.66	1224.208
	4	9.5	18.66	1223.875
	5	13.5	22.66	1223.542
	6	17.5	26.66	1223.208
	7	21.5	30.66	1222.875
	8	25.5	34.66	1222.542
	9	31.5	40.66	1222.042

Thermistor in FDR without Cement Test Section

	Thermistor # T-5	Sta. 61+05	Elev. Top of Pavement (ft) = 1225.43	
	Channel	Depth below Top Probe (in)	Depth below Top Pavement (in)	Elevation (ft)
	2	1.5	4.74	1225.035
	3	5.5	8.74	1224.702
	4	9.5	12.74	1224.368
	5	13.5	16.74	1224.035
	6	17.5	20.74	1223.702
	7	21.5	24.74	1223.368
	8	25.5	28.74	1223.035
	9	31.5	34.74	1222.535

Date:	10-Jan-06		
	Temp. at location		
Channel	**A**	**B**	**C**
Air	36.7	36.5	37.7
1	25.6	26.6	26.5
2	25.2	26.5	26.2
3	27.3	26.9	26.5
4	25.0	27.7	27.1
5	25.6	28.7	27.6
6	25.9	29.2	28.3
7	26.3	30.1	28.9
8	28.5	31.1	29.5
9	27.5	32.5	30.7
10	28.7	33.1	
11	29.7	34.3	
12	31.6	35.1	
13	33.6	37.0	

Date:	6-Feb-06		
	Temp. at location		
Channel	**A**	**B**	**C**
Air	28.8	29.8	29.4
1	31.5	31.8	31.5
2	31.5	31.6	31.4
3	31.8	31.4	31.3
4	30.9	51.5	31.1
5	30.8	31.6	31.0
6	30.7	31.2	31.0
7	30.6	31.5	31.0
8	31.0	31.6	31.0
9	30.6	32.1	31.2
10	30.9	32.5	
11	31.3	33.6	
12	31.5	34.2	
13	32.7	35.9	

Date:	14-Feb-06		
	Temp. at location		
Channel	**A**	**B**	**C**
Air	34.5	35.4	35.7
1	25.8	24.8	24.0
2	24.3	23.7	24.6
3	22.3	23.4	23.7
4	20.7	24.1	23.9
5	21.2	25.7	24.6
6	21.8	26.8	25.7
7	22.6	28.0	26.8
8	23.6	29.2	27.8
9	24.7	31.3	29.4
10	26.2	32.4	
11	28.0	33.4	
12	29.9	34.0	
13	32.3	35.6	

Date:	23-Feb-06		
	Temp. at location		
Channel	**A**	**B**	**C**
Air	32.4	32.5	33.5
1	25.3	26.5	26.4
2	24.8	26.3	26.2
3	25.2	26.4	26.3
4	23.8	27.1	26.8
5	24.2	28.2	27.4
6	24.6	28.8	28.1
7	25.1	29.5	28.7
8	26.1	30.0	29.2
9	26.1	31.2	30.1
10	27.0	32.1	
11	27.4	33.1	
12	29.1	33.6	
13	31.2	35.1	

Date:	1-Mar-06		
	Temp. at location		
Channel	A	B	C
Air	20.6	21.7	22.2
1	17.6	21.3	21.4
2	17.7	20.8	21.7
3	18.0	20.9	21.3
4	17.7	21.8	21.7
5	18.4	23.5	22.4
6	19.2	25.1	23.7
7	20.2	26.4	25.1
8	21.8	27.7	26.3
9	22.6	29.9	28.2
10	24.2	31.8	
11	26.0	32.8	
12	27.6	33.4	
13	30.2	34.8	

Date:	8-Mar-06		
	Temp. at location		
Channel	A	B	C
Air	39.9	39.3	42.3
1	28.7	30.4	28.7
2	27.4	29.2	29.3
3	25.0	28.5	28.3
4	23.5	28.5	28.1
5	23.6	29.1	28.3
6	23.9	29.5	28.8
7	24.3	29.6	29.2
8	25.1	29.9	29.3
9	25.1	30.7	29.8
10	25.8	31.5	
11	26.6	32.5	
12	27.4	33.0	
13	29.3	34.4	

Date:	14-Mar-06		
	Temp. at location		
Channel	A	B	C
Air	45.8	47.5	48.6
1	37.4	36.2	33.2
2	35.3	34.3	34.4
3	32.8	32.6	32.5
4	30.9	31.7	31.6
5	30.5	31.6	31.3
6	30.2	31.3	31.1
7	29.9	31.0	31.0
8	29.5	30.9	30.8
9	29.3	31.2	30.8
10	29.3	31.6	
11	30.9	32.4	
12	29.5	32.8	
13	30.3	34.1	

Date:	22-Mar-06		
	Temp. at location		
Channel	A	B	C
Air	34.6	35.0	35.8
1	33.4	31.9	31.5
2	31.8	31.8	31.4
3	29.7	31.7	31.4
4	28.1	31.7	31.3
5	27.9	31.8	31.4
6	28.0	31.7	31.4
7	28.3	31.4	31.4
8	28.6	31.3	31.2
9	29.0	31.6	31.2
10	29.6	31.7	
11	30.7	32.4	
12	30.4	32.8	
13	31.1	34.1	

Date:	27-Mar-06		
	Temp. at location		
Channel	A	B	C
Air	43.7	41.9	47.8
1	40.1	38.5	33.9
2	37.9	35.5	36.2
3	34.2	33.5	33.1
4	31.8	32.9	32.1
5	31.7	32.6	31.9
6	31.3	32.0	31.7
7	31.1	31.7	31.5
8	31.5	31.6	31.3
9	30.6	31.9	31.3
10	30.7	31.9	
11	31.6	32.3	
12	30.7	32.7	
13	31.2	34.0	

Date:	10-Apr-06		
	Temp. at location		
Channel	A	B	C
Air	45.1	50.8	50.2
1	36.7	40.6	38.6
2	34.8	39.0	40.0
3	34.1	38.2	38.2
4	34.2	38.0	37.9
5	34.8	37.6	37.6
6	34.6	36.5	36.8
7	34.1	35.2	35.7
8	33.9	34.2	34.3
9	32.3	33.1	32.5
10	31.9	32.0	
11	33.0	32.2	
12	31.8	32.3	
13	31.8	33.1	

Date:	4-May-06		
	Temp. at location		
Channel	A	B	C
Air	57.2	65.8	66.0
1	50.9	52.1	51.8
2	49.6	51.2	53.1
3	48.1	50.8	51.4
4	47.6	50.8	51.1
5	47.3	50.9	51.1
6	46.9	50.5	50.9
7	46.2	50.0	50.6
8	45.9	49.6	50.0
9	44.7	48.9	49.2
10	44.0	47.5	
11	43.0	46.3	
12	41.6	44.9	
13	39.7	42.8	

Appendix E:

Results of Statistical Analysis of Field Data

Results of Statistical Analysis of Data from NH Field Test Site

Geogauge Stiffness (% Difference) FDR with CTB

Date	N	Mean Diff. (%)	Std. Dev.	Std. Err.	t-stat	df	p-value	lower 95%	upper 95%
6/22/05	20	27.61	22.37	5.00	5.52	19	0.000	17.15	38.08
6/23/05	20	10.18	13.06	2.92	3.49	19	0.002	4.07	16.30
6/24/05	14	8.09	12.64	3.38	2.39	13	0.032	0.79	15.39

Geogauge Stiffness (% Difference) FDR without Cement

Date	N	Mean Diff. (%)	Std. Dev.	Std. Err.	t-stat	df	p-value	lower 95%	upper 95%
6/23/05	8	0.03	15.66	5.54	0.01	7	0.996	-13.06	13.12

FWD Base Modulus (% Difference) FDR with CTB

Date	N	Mean Diff. (%)	Std. Dev.	Std. Err.	t-stat	df	p-value	lower 95%	upper 95%
6/22/05	7	210.39	58.93	22.28	9.44	6	0.000	155.88	264.89
6/23/05	7	117.62	78.57	29.70	3.96	6	0.007	44.95	190.28
6/24/05	7	129.82	29.83	11.28	11.51	6	0.000	102.23	157.41

FWD Base Modulus (% Difference) FDR without Cement

Date	N	Mean Diff. (%)	Std. Dev.	Std. Err.	t-stat	df	p-value	lower 95%	upper 95%
6/22/05	4	4.86	33.55	16.77	0.29	3	0.791	-48.52	58.24
6/23/05	7	-19.71	25.83	9.76	-2.02	6	0.090	-43.59	4.18

Results of Statistical Analysis of Data from Maine Field Test Site

Clegg Impact Value (% Difference): Location 1A

Date	N	Mean Diff. (%)	Std. Dev.	Std. Err.	t-stat	df	p-value	lower 95%	upper 95%
8/1/05	5	20.51	15.33	6.86	2.99	4	0.040	1.47	39.55
8/2/05	5	11.06	24.03	10.75	1.03	4	0.361	-18.78	40.90
8/3/05	5	16.85	42.05	18.81	0.90	4	0.421	-35.36	69.07
8/4/05	5	20.09	31.59	14.13	1.42	4	0.228	-19.13	59.31

Clegg Impact Value (% Difference): Location 1B

Date	N	Mean Diff. (%)	Std. Dev.	Std. Err.	t-stat	df	p-value	lower 95%	upper 95%
8/2/05	5	-20.63	6.98	3.12	-6.61	4	0.003	-29.29	-11.96
8/3/05	5	-4.17	27.94	12.49	-0.33	4	0.755	-38.86	30.52

Clegg Impact Value (% Difference): Location 2

Date	N	Mean Diff. (%)	Std. Dev.	Std. Err.	t-stat	df	p-value	lower 95%	upper 95%
8/3/05	7	13.57	10.17	3.84	3.53	6	0.012	4.16	22.97
8/4/05	7	18.57	25.43	9.61	1.93	6	0.102	-4.95	42.09
8/5/05	7	40.30	36.57	13.82	2.92	6	0.027	6.48	74.13

Appendix F

Results of Numerical Modeling

TABLE F-1 Results of Computer Simulations

ID	Asphalt Concrete Thickness (in.)	Asphalt Concrete Modulus (psi)	CTB Thickness (in.)	CTB Modulus (psi)	Subgrade Modulus (psi)	Horizontal Tensile Stress at Bottom of CTB, σ_t	Horizontal Tensile Strain at Bottom of CTB, ε_t	Horizontal Tensile Strain at Bottom of AC, ε_t	Vertical Compressive Strain at Top of Subgrade, ε_v	Surface Deflection (in.)
1	2	500,000	6	500,000	4,000	116.44	2.09E-04	0.00E+00	6.04E-04	0.0317
2	2	500,000	6	500,000	8,000	97.60	1.77E-04	0.00E+00	4.70E-04	0.0196
3	2	500,000	6	500,000	12,000	86.50	1.58E-04	0.00E+00	4.02E-04	0.0148
4	2	500,000	6	1,000,000	4,000	150.29	1.34E-04	0.00E+00	4.37E-04	0.0278
5	2	500,000	6	1,000,000	8,000	128.48	1.16E-04	0.00E+00	3.42E-04	0.0172
6	2	500,000	6	1,000,000	12,000	115.71	1.05E-04	0.00E+00	2.94E-04	0.0130
7	2	500,000	6	1,500,000	4,000	173.21	1.03E-04	0.00E+00	3.60E-04	0.0256
8	2	500,000	6	1,500,000	8,000	149.45	8.93E-05	0.00E+00	2.82E-04	0.0159
9	2	500,000	6	1,500,000	12,000	135.58	8.15E-05	0.00E+00	2.43E-04	0.0121
10	2	500,000	9	500,000	4,000	72.07	1.28E-04	0.00E+00	3.69E-04	0.0240
11	2	500,000	9	500,000	8,000	61.53	1.11E-04	0.00E+00	2.89E-04	0.0152
12	2	500,000	9	500,000	12,000	55.23	1.00E-04	0.00E+00	2.50E-04	0.0117
13	2	500,000	9	1,000,000	4,000	90.33	7.99E-05	0.00E+00	2.54E-04	0.0204
14	2	500,000	9	1,000,000	8,000	78.61	7.01E-05	0.00E+00	2.03E-04	0.0130
15	2	500,000	9	1,000,000	12,000	71.64	6.42E-05	0.00E+00	1.77E-04	0.0100
16	2	500,000	9	1,500,000	4,000	101.72	5.98E-05	0.00E+00	2.03E-04	0.0185
17	2	500,000	9	1,500,000	8,000	89.42	5.29E-05	0.00E+00	1.63E-04	0.0118
18	2	500,000	9	1,500,000	12,000	82.07	4.88E-05	0.00E+00	1.42E-04	0.0091
19	2	500,000	12	500,000	4,000	49.14	8.67E-05	0.00E+00	2.47E-04	0.0194
20	2	500,000	12	500,000	8,000	42.49	7.55E-05	0.00E+00	1.99E-04	0.0125
21	2	500,000	12	500,000	12,000	38.45	6.88E-05	0.00E+00	1.73E-04	0.0097
22	2	500,000	12	1,000,000	4,000	60.28	5.29E-05	0.00E+00	1.67E-04	0.0162
23	2	500,000	12	1,000,000	8,000	53.07	4.69E-05	0.00E+00	1.35E-04	0.0105
24	2	500,000	12	1,000,000	12,000	48.75	4.32E-05	0.00E+00	1.19E-04	0.0081
25	2	500,000	12	1,500,000	4,000	66.99	3.91E-05	0.00E+00	1.31E-04	0.0143
26	2	500,000	12	1,500,000	8,000	59.45	3.49E-05	0.00E+00	1.06E-04	0.0094
27	2	500,000	12	1,500,000	12,000	54.99	3.24E-05	0.00E+00	9.37E-05	0.0073
28	6	500,000	6	500,000	4,000	64.08	1.14E-04	2.22E-05	3.19E-04	0.0222
29	6	500,000	6	500,000	8,000	55.16	9.90E-05	2.17E-05	2.55E-04	0.0141
30	6	500,000	6	500,000	12,000	49.76	8.99E-05	2.14E-05	2.22E-04	0.0109
31	6	500,000	6	1,000,000	4,000	84.63	7.50E-05	0.00E+00	2.38E-04	0.0200
32	6	500,000	6	1,000,000	8,000	74.14	6.62E-05	6.06E-07	1.92E-04	0.0128
33	6	500,000	6	1,000,000	12,000	67.82	6.09E-05	1.34E-06	1.68E-04	0.0099
34	6	500,000	6	1,500,000	4,000	99.76	5.89E-05	0.00E+00	2.03E-04	0.0189
35	6	500,000	6	1,500,000	8,000	88.02	5.23E-05	0.00E+00	1.64E-04	0.0121
36	6	500,000	6	1,500,000	12,000	81.02	4.87E-05	0.00E+00	1.43E-04	0.0094
37	6	500,000	9	500,000	4,000	44.26	7.79E-05	1.23E-05	2.20E-04	0.0181
38	6	500,000	9	500,000	8,000	38.43	6.81E-05	1.36E-05	1.78E-04	0.0117
39	6	500,000	9	500,000	12,000	34.89	6.22E-05	1.44E-05	1.56E-04	0.0092
40	6	500,000	9	1,000,000	4,000	57.49	5.05E-05	0.00E+00	1.60E-04	0.0163
41	6	500,000	9	1,000,000	8,000	50.71	4.47E-05	0.00E+00	1.30E-04	0.0105
42	6	500,000	9	1,000,000	12,000	46.65	4.13E-05	0.00E+00	1.15E-04	0.0082
43	6	500,000	9	1,500,000	4,000	67.02	3.92E-05	0.00E+00	1.34E-04	0.0153
44	6	500,000	9	1,500,000	8,000	59.47	3.49E-05	0.00E+00	1.09E-04	0.0099
45	6	500,000	9	1,500,000	12,000	54.99	3.24E-05	0.00E+00	9.59E-05	0.0077

TABLE F-1 Results of Computer Simulations, Continued

ID	Asphalt Concrete Thickness (in.)	Asphalt Concrete Modulus (psi)	CTB Thickness (in.)	CTB Modulus (psi)	Subgrade Modulus (psi)	Horizontal Tensile Stress at Bottom of CTB, σ_t	Horizontal Tensile Strain at Bottom of CTB, ε_t	Horizontal Tensile Strain at Bottom of AC, ε_t	Vertical Compressive Strain at Top of Subgrade, ε_v	Surface Deflection (in.)
46	6	500,000	12	500,000	4,000	32.26	5.64E-05	1.04E-05	1.61E-04	0.0155
47	6	500,000	12	500,000	8,000	28.13	4.94E-05	1.20E-05	1.31E-04	0.0101
48	6	500,000	12	500,000	12,000	25.63	4.53E-05	1.30E-05	1.16E-04	0.0080
49	6	500,000	12	1,000,000	4,000	41.38	3.61E-05	0.00E+00	1.15E-04	0.0138
50	6	500,000	12	1,000,000	8,000	36.62	3.20E-05	0.00E+00	9.39E-05	0.0090
51	6	500,000	12	1,000,000	12,000	33.78	2.97E-05	0.00E+00	8.31E-05	0.0070
52	6	500,000	12	1,500,000	4,000	47.70	2.77E-05	0.00E+00	9.41E-05	0.0129
53	6	500,000	12	1,500,000	8,000	42.48	2.47E-05	0.00E+00	7.72E-05	0.0084
54	6	500,000	12	1,500,000	12,000	39.37	2.30E-05	0.00E+00	6.83E-05	0.0066
55	2	500,000	6	750,000	4,000	133.91	2.E-04	0.00E+00	5.01E-04	0.0294
56	2	500,000	6	750,000	8,000	114.84	1.E-04	0.00E+00	3.91E-04	0.0182
57	2	500,000	6	750,000	12,000	102.81	1.25E-04	0.00E+00	3.36E-04	0.0137
58	2	500,000	6	1,250,000	4,000	162.67	1.13E-04	0.00E+00	3.93E-04	0.0266
59	2	500,000	6	1,250,000	8,000	139.79	1.00E-04	0.00E+00	3.08E-04	0.0165
60	2	500,000	6	1,250,000	12,000	126.42	9.13E-05	0.00E+00	2.65E-04	0.0125
61	2	500,000	9	750,000	4,000	82.77	9.75E-05	0.00E+00	2.96E-04	0.0220
62	2	500,000	9	750,000	8,000	71.25	8.50E-05	0.00E+00	2.36E-04	0.0139
63	2	500,000	9	750,000	12,000	64.56	7.75E-05	0.00E+00	2.05E-04	0.0107
64	2	500,000	9	1,250,000	4,000	96.57	6.82E-05	0.00E+00	2.25E-04	0.0194
65	2	500,000	9	1,250,000	8,000	84.52	6.01E-05	0.00E+00	1.80E-04	0.0124
66	2	500,000	9	1,250,000	12,000	77.33	5.51E-05	0.00E+00	1.57E-04	0.0095
67	2	500,000	12	750,000	4,000	55.57	6.52E-05	0.00E+00	1.97E-04	0.0174
68	2	500,000	12	750,000	8,000	48.59	5.73E-05	0.00E+00	1.59E-04	0.0113
69	2	500,000	12	750,000	12,000	44.39	5.26E-05	0.00E+00	1.40E-04	0.0088
70	2	500,000	12	1,250,000	4,000	63.98	4.49E-05	0.00E+00	1.46E-04	0.0153
71	2	500,000	12	1,250,000	8,000	56.58	3.99E-05	0.00E+00	1.19E-04	0.0099
72	2	500,000	12	1,250,000	12,000	52.19	3.69E-05	0.00E+00	1.04E-04	0.0077
73	6	500,000	6	750,000	4,000	75.43	8.93E-05	6.18E-06	2.68E-04	0.0208
74	6	500,000	6	750,000	8,000	65.63	7.83E-05	6.93E-06	2.16E-04	0.0133
75	6	500,000	6	750,000	12,000	59.74	7.17E-05	7.39E-06	1.88E-04	0.0103
76	6	500,000	6	1,250,000	4,000	92.62	6.57E-05	0.00E+00	2.18E-04	0.0194
77	6	500,000	6	1,250,000	8,000	81.50	5.82E-05	0.00E+00	1.76E-04	0.0124
78	6	500,000	6	1,250,000	12,000	74.80	5.37E-05	0.00E+00	1.54E-04	0.0096
79	6	500,000	9	750,000	4,000	51.56	6.04E-05	8.16E-07	1.82E-04	0.0170
80	6	500,000	9	750,000	8,000	45.23	5.33E-05	2.58E-06	1.48E-04	0.0110
81	6	500,000	9	750,000	12,000	41.42	4.90E-05	3.65E-06	1.30E-04	0.0086
82	6	500,000	9	1,250,000	4,000	62.56	4.39E-05	0.00E+00	1.45E-04	0.0157
83	6	500,000	9	1,250,000	8,000	55.38	3.90E-05	0.00E+00	1.18E-04	0.0102
84	6	500,000	9	1,250,000	12,000	51.10	3.62E-05	0.00E+00	1.04E-04	0.0079
85	6	500,000	12	750,000	4,000	37.33	4.34E-05	1.05E-06	1.32E-04	0.0144
86	6	500,000	12	750,000	8,000	32.87	3.84E-05	2.79E-06	1.08E-04	0.0094
87	6	500,000	12	750,000	12,000	30.18	3.54E-05	3.85E-06	9.54E-05	0.0074
88	6	500,000	12	1,250,000	4,000	44.77	3.12E-05	0.00E+00	1.03E-04	0.0133
89	6	500,000	12	1,250,000	8,000	39.77	9.58E-06	0.00E+00	8.43E-05	0.0086
90	6	500,000	12	1,250,000	12,000	36.79	9.08E-06	0.00E+00	7.47E-05	0.0068

TABLE F-2 Model Results

ID	Asphalt Concrete N_f	CTB N_f						Subgrade N_d
		Australian	Coal Ash Association	Kohn	NCHRP	South African	Uzan	
1	Infinite	4.67E+00	1.62E-15	2.E-16	3.01E-17	7.29E-07	7.41E-07	3.52E+05
2	Infinite	9.34E+01	2.61E-11	6.E-12	2.55E-12	1.58E-04	2.77E-05	1.08E+06
3	Infinite	7.11E+02	7.85E-09	3.E-09	2.04E-09	3.76E-03	3.30E-04	2.17E+06
4	Infinite	1.46E+02	9.90E+05	2.E+06	6.71E+07	4.76E+00	1.55E+08	1.49E+06
5	Infinite	2.11E+03	5.65E+06	1.E+07	5.15E+08	6.90E+01	3.87E+09	4.47E+06
6	Infinite	1.25E+04	1.57E+07	4.E+07	1.70E+09	3.33E+02	3.32E+10	8.78E+06
7	Infinite	7.06E+02	8.94E+07	2.E+08	1.31E+10	4.45E+02	2.41E+12	3.56E+06
8	Infinite	8.86E+03	2.50E+08	7.E+08	4.37E+10	3.12E+03	4.98E+13	1.06E+07
9	Infinite	4.66E+04	4.56E+08	1.E+09	8.82E+10	9.73E+03	3.67E+14	2.06E+07
10	Infinite	3.12E+04	1.31E-05	6.E-06	1.21E-05	5.75E-01	1.40E-02	3.20E+06
11	Infinite	4.52E+05	2.95E-03	2.E-03	6.91E-03	1.12E+01	3.58E-01	9.54E+06
12	Infinite	2.78E+06	7.50E-02	6.E-02	3.06E-01	6.62E+01	3.28E+00	1.84E+07
13	Infinite	1.65E+06	1.19E+08	3.E+08	1.83E+10	1.22E+04	5.35E+12	1.70E+07
14	Infinite	1.75E+07	3.03E+08	8.E+08	5.47E+10	5.04E+04	9.24E+13	4.64E+07
15	Infinite	8.45E+07	5.28E+08	1.E+09	1.05E+11	1.18E+05	6.21E+14	8.66E+07
16	Infinite	1.20E+07	1.97E+09	6.E+09	4.91E+11	2.21E+05	1.34E+17	4.68E+07
17	Infinite	1.10E+08	3.36E+09	1.E+10	9.16E+11	6.03E+05	1.88E+18	1.24E+08
18	Infinite	4.73E+08	4.62E+09	1.E+10	1.33E+12	1.09E+06	1.09E+19	2.28E+08
19	Infinite	3.62E+07	1.72E+00	2.E+00	1.20E+01	6.14E+02	3.60E+01	1.94E+07
20	Infinite	4.35E+08	5.26E+01	6.E+01	6.59E+02	4.01E+03	7.13E+02	5.12E+07
21	Infinite	2.35E+09	4.19E+02	5.E+02	7.50E+03	1.24E+04	5.54E+03	9.40E+07
22	Infinite	2.73E+09	1.31E+09	4.E+09	3.03E+11	5.99E+05	2.14E+16	1.13E+08
23	Infinite	2.46E+10	2.33E+09	7.E+09	5.96E+11	1.44E+06	2.94E+17	2.88E+08
24	Infinite	1.05E+11	3.28E+09	1.E+10	8.92E+11	2.44E+06	1.67E+18	5.11E+08
25	Infinite	2.51E+10	8.87E+09	3.E+10	2.86E+12	4.41E+06	7.04E+20	3.33E+08
26	Infinite	1.98E+11	1.23E+10	4.E+10	4.18E+12	8.13E+06	8.15E+21	8.44E+08
27	Infinite	7.58E+11	1.49E+10	5.E+10	5.25E+12	1.17E+07	4.03E+22	1.48E+09
28	2.22E+09	2.62E+05	7.96E-04	5.E-04	1.49E-03	6.32E+00	1.56E-01	6.12E+06
29	2.41E+09	3.33E+06	7.80E-02	6.E-02	3.20E-01	7.84E+01	3.37E+00	1.67E+07
30	2.53E+09	1.89E+07	1.25E+00	1.E+00	8.27E+00	3.60E+02	2.79E+01	3.14E+07
31	Infinite	5.11E+06	1.87E+08	5.E+08	3.11E+10	2.46E+04	2.03E+13	2.26E+07
32	3.13E+14	4.85E+07	4.33E+08	1.E+09	8.30E+10	8.79E+04	3.07E+14	5.95E+07
33	2.28E+13	2.18E+08	7.17E+08	2.E+09	1.50E+11	1.89E+05	1.91E+15	1.09E+08
34	Infinite	1.60E+07	2.15E+09	6.E+09	5.42E+11	2.54E+05	1.99E+17	4.63E+07
35	Infinite	1.35E+08	3.57E+09	1.E+10	9.83E+11	6.57E+05	2.60E+18	1.21E+08
36	Infinite	4.98E+08	4.83E+09	1.E+10	1.40E+12	1.11E+06	1.42E+19	2.20E+08
37	1.55E+10	2.48E+08	2.11E+01	2.E+01	2.26E+02	2.68E+03	3.08E+02	3.26E+07
38	1.11E+10	2.79E+09	4.23E+02	5.E+02	7.58E+03	1.39E+04	5.59E+03	8.36E+07
39	9.25E+09	1.44E+10	2.62E+03	4.E+03	6.40E+04	3.75E+04	4.07E+04	1.51E+08
40	Infinite	6.46E+09	1.64E+09	5.E+09	3.94E+11	8.57E+05	5.68E+16	1.34E+08
41	Infinite	5.64E+10	2.81E+09	8.E+09	7.43E+11	1.96E+06	7.44E+17	3.39E+08
42	Infinite	2.35E+11	3.88E+09	1.E+10	1.09E+12	3.21E+06	4.12E+18	6.00E+08
43	Infinite	2.49E+10	8.86E+09	3.E+10	2.85E+12	4.40E+06	6.98E+20	2.97E+08
44	Infinite	1.97E+11	1.23E+10	4.E+10	4.18E+12	8.12E+06	8.10E+21	7.57E+08
45	Infinite	7.58E+11	1.49E+10	5.E+10	5.25E+12	1.17E+07	4.04E+22	1.33E+09

TABLE F-2 Model Results, Continued

ID	Asphalt Concrete N_f	CTB N_f						Subgrade N_d
		Australian	Coal Ash Association	Kohn	NCHRP	South African	Uzan	
46	2.76E+10	8.42E+10	1.01E+04	2.E+04	3.11E+05	9.93E+04	2.03E+05	1.32E+08
47	1.69E+10	8.90E+11	8.43E+04	1.E+05	3.74E+06	3.17E+05	3.36E+06	3.26E+08
48	1.30E+10	4.36E+12	3.06E+05	6.E+05	1.69E+07	6.38E+05	2.28E+07	5.73E+08
49	Infinite	2.75E+12	5.92E+09	2.E+10	1.78E+12	6.88E+06	4.84E+19	5.98E+08
50	Infinite	2.30E+13	8.65E+09	3.E+10	2.77E+12	1.23E+07	5.92E+20	1.46E+09
51	Infinite	9.21E+13	1.09E+10	4.E+10	3.62E+12	1.73E+07	3.11E+21	2.52E+09
52	Infinite	1.29E+13	2.04E+10	7.E+10	7.59E+12	2.31E+07	7.49E+23	1.45E+09
53	Infinite	9.70E+13	2.56E+10	9.E+10	9.89E+12	3.53E+07	8.06E+24	3.53E+09
54	Infinite	3.63E+14	2.93E+10	1.E+11	1.16E+13	4.55E+07	3.83E+25	6.08E+09
55	Infinite	3.23E+01	1.47E+03	2.E+03	3.27E+04	9.08E-02	2.13E+04	8.16E+05
56	Infinite	5.32E+02	2.06E+04	3.E+04	7.17E+05	2.63E+00	4.99E+05	2.47E+06
57	Infinite	3.48E+03	1.09E+05	2.E+05	5.04E+06	1.91E+01	4.84E+06	4.89E+06
58	Infinite	1.22E+02	1.74E+07	4.E+07	1.93E+09	9.72E+01	4.22E+10	2.40E+06
59	Infinite	1.08E+03	6.30E+07	2.E+08	8.68E+09	6.30E+02	9.45E+11	7.17E+06
60	Infinite	5.93E+03	1.33E+08	3.E+08	2.09E+10	2.33E+03	7.44E+12	1.40E+07
61	Infinite	2.87E+05	1.73E+06	3.E+06	1.29E+08	9.56E+02	4.13E+08	8.57E+06
62	Infinite	3.43E+06	8.52E+06	2.E+07	8.34E+08	5.86E+03	8.96E+09	2.37E+07
63	Infinite	1.81E+07	2.15E+07	5.E+07	2.46E+09	1.74E+04	6.76E+10	4.49E+07
64	Infinite	1.13E+06	7.12E+08	2.E+09	1.49E+11	6.58E+04	1.87E+15	2.95E+07
65	Infinite	1.10E+07	1.40E+09	4.E+09	3.29E+11	2.12E+05	2.88E+16	7.93E+07
66	Infinite	5.24E+07	2.10E+09	6.E+09	5.28E+11	4.37E+05	1.78E+17	1.46E+08
67	Infinite	4.05E+08	7.44E+07	2.E+08	1.06E+10	1.02E+05	1.47E+12	5.35E+07
68	Infinite	4.07E+09	1.95E+08	5.E+08	3.27E+10	3.18E+05	2.31E+13	1.39E+08
69	Infinite	1.90E+10	3.49E+08	9.E+08	6.45E+10	6.28E+05	1.48E+14	2.49E+08
70	Infinite	2.12E+09	4.44E+09	1.E+10	1.27E+12	1.92E+06	8.73E+18	2.04E+08
71	Infinite	1.77E+10	6.73E+09	2.E+10	2.07E+12	3.95E+06	1.09E+20	5.17E+08
72	Infinite	7.11E+10	8.61E+09	3.E+10	2.76E+12	6.06E+06	5.70E+20	9.11E+08
73	1.51E+11	1.41E+06	4.78E+06	1.E+07	4.24E+08	3.14E+03	2.78E+09	1.33E+07
74	1.03E+11	1.49E+07	1.85E+07	4.E+07	2.07E+09	1.53E+04	4.83E+10	3.54E+07
75	8.37E+10	7.27E+07	4.18E+07	1.E+08	5.37E+09	3.98E+04	3.32E+11	6.54E+07
76	Infinite	2.26E+06	8.90E+08	3.E+09	1.93E+11	9.55E+04	4.41E+15	3.36E+07
77	Infinite	2.01E+07	1.66E+09	5.E+09	4.01E+11	2.82E+05	6.07E+16	8.81E+07
78	Infinite	8.56E+07	2.42E+09	7.E+09	6.23E+11	5.41E+05	3.53E+17	1.61E+08
79	1.18E+14	1.59E+09	1.29E+08	3.E+08	2.02E+10	2.04E+05	6.81E+12	7.53E+07
80	2.66E+12	1.51E+10	3.10E+08	8.E+08	5.62E+10	5.68E+05	1.00E+14	1.91E+08
81	8.55E+11	6.80E+10	5.26E+08	1.E+09	1.04E+11	1.05E+06	6.10E+14	3.40E+08
82	Infinite	3.19E+09	4.81E+09	1.E+10	1.39E+12	2.22E+06	1.38E+19	2.07E+08
83	Infinite	2.62E+10	7.19E+09	2.E+10	2.23E+12	4.47E+06	1.69E+20	5.28E+08
84	Infinite	1.04E+11	9.15E+09	3.E+10	2.96E+12	6.78E+06	8.78E+20	9.31E+08
85	5.14E+13	6.08E+11	9.25E+08	3.E+09	2.02E+11	2.37E+06	5.15E+15	3.21E+08
86	2.07E+12	5.50E+12	1.71E+09	5.E+09	4.17E+11	4.89E+06	7.03E+16	7.86E+08
87	7.16E+11	2.38E+13	2.49E+09	7.E+09	6.44E+11	7.55E+06	4.04E+17	1.36E+09
88	Infinite	1.50E+12	1.30E+10	4.E+10	4.49E+12	1.39E+07	1.32E+22	9.72E+08
89	Infinite	2.51E+21	1.73E+10	6.E+10	6.24E+12	3.15E+08	1.50E+23	2.37E+09
90	Infinite	6.65E+21	2.04E+10	7.E+10	7.59E+12	3.39E+08	7.45E+23	4.08E+09

TABLE F-3 Significance of Factors on Model Results

Factors	*p* -values					
	Australian	**Coal Ash Association**	**Kohn**	**NCHRP**	**South African**	**Uzan**
AC Thickness	<0.0001	<0.0001	<0.0001	<0.0001	<0.0001	<0.0001
CTB Thickness	<0.0001	<0.0001	<0.0001	<0.0001	<0.0001	<0.0001
CTB Modulus	<0.0001	<0.0001	<0.0001	<0.0001	<0.0001	<0.0001
Subgrade Modulus	<0.0001	<0.0001	<0.0001	<0.0001	<0.0001	<0.0001
AC Thickness*CTB Modulus	-	<0.0001	<0.0001	<0.0001	<0.0001	<0.0001
AC Thickness*CTB Thickness	0.0118	0.0043	0.0045	0.0071	<0.0001	<0.0001
AC Thickness*Subgrade Modulus	-	-	-	-	-	-
CTB Thickness*CTB Modulus	0.0002	<0.0001	<0.0001	<0.0001	<0.0001	<0.0001
CTB Thickness*Subgrade Modulus	-	-	-	-	-	-
CTB Modulus*Subgrade Modulus	-	0.0379	0.0403	0.0355	-	0.0024
AC Thickness*CTB Thickness*CTB Modulus	0.0008	<0.0001	<0.0001	<0.0001	<0.0001	<0.0001
AC Thickness*CTB Modulus*Subgrade Modulus	-	-	-	-	-	0.0145
CTB Thickness*CTB Modulus*Subgrade Modulus	-	0.0649	0.0614	-	-	0.0246

TABLE F-4 Sensitivity of Models to Factors

(a) AC Thickness

Observation	CTB thickness	CTB Modulus	Difference					
			Australian	Coal Ash Association	Kohn	NCHRP	South African	Uzan
1	12	1000	9.38E+02	2.82E+00	3.11E+00	3.80E+00	7.85E+00	2.04E+03
2	12	1250	2.11E+08	1.62E+00	1.76E+00	2.09E+00	3.09E+01	1.40E+03
3	12	1500	4.94E+02	1.11E+00	1.20E+00	1.40E+00	3.46E+00	9.98E+02
4	12	500	2.07E+03	1.62E+03	2.43E+03	6.75E+03	8.59E+01	4.74E+03
5	12	750	1.36E+03	8.20E+00	9.38E+00	1.25E+01	1.53E+01	3.08E+03
6	12	1000	2.41E+04	8.62E+01	1.10E+02	1.86E+02	1.45E+03	8.42E+04
7	6	1250	1.70E+04	2.80E+01	3.39E+01	5.06E+01	4.65E+02	6.83E+04
8	6	1500	1.55E+04	1.44E+01	1.69E+01	2.36E+01	2.38E+02	5.51E+04
9	6	500	3.51E+04	3.44E-01	3.20E-01	1.31E+00	5.84E+01	4.27E+00
10	6	750	2.91E+04	1.04E+03	1.52E+03	3.42E+03	2.89E+03	9.54E+04
11	9	1000	3.27E+03	8.79E+00	1.01E+01	1.35E+01	4.11E+01	8.28E+03
12	9	1250	2.37E+03	4.33E+00	4.83E+00	6.09E+00	2.13E+01	5.97E+03
13	9	1500	1.81E+03	2.76E+00	3.04E+00	3.71E+00	1.32E+01	4.36E+03
14	9	500	6.33E+03	2.82E+02	3.55E+02	4.38E+03	1.03E+03	2.28E+03
15	9	750	4.50E+03	3.95E+01	4.86E+01	7.55E+01	1.07E+02	1.18E+04
	Average		1.40E+07	2.09E+02	3.03E+02	9.95E+02	4.30E+02	2.32E+04
	Rank		1	6	5	3	4	2

(b) CTB Thickness

Observation	Asphalt Concrete Thickness	CTB Modulus	Difference					
			Australian	Coal Ash Association	Kohn	NCHRP	South African	Uzan
1	2	1000	1.22E+07	4.84E+02	6.79E+02	1.40E+03	2.50E+04	8.07E+07
2	2	1250	1.50E+07	1.20E+02	1.56E+02	2.73E+02	6.82E+03	1.22E+08
3	2	1500	2.34E+07	5.32E+01	6.65E+01	1.07E+02	3.14E+03	1.74E+08
4	2	500	4.59E+06	3.84E+01	4.31E+01	3.99E+02	3.12E+03	5.26E+02
5	2	750	7.99E+06	1.15E+04	1.92E+04	5.73E+04	6.35E+04	4.60E+07
6	6	1000	4.76E+05	2.02E+01	2.41E+01	3.49E+01	1.52E+02	1.96E+06
7	6	1250	1.86E+11	9.89E+00	1.14E+01	1.54E+01	4.66E+02	2.50E+06
8	6	1500	7.50E+05	6.45E+00	7.32E+00	9.52E+00	5.75E+01	3.15E+06
9	6	500	2.70E+05	4.75E+04	8.12E+04	1.17E+06	4.57E+03	4.74E+05
10	6	750	3.74E+05	1.01E+02	1.31E+02	2.25E+02	3.56E+02	1.48E+06
	Average		1.86E+10	5.99E+03	1.02E+04	1.23E+05	1.07E+04	4.32E+07
	Rank		1	6	5	3	4	2

TABLE F-4 Sensitivity of Models to Factors, Continued

(c) CTB Modulus

Observation	Asphalt Concrete Thickness	CTB Thickness	Difference					
			Australian	Coal Ash Association	Kohn	NCHRP	South African	Uzan
1	2	12	4.66E+02	2.98E+08	8.69E+08	9.92E+09	2.39E+03	1.16E+19
2	6	12	4.24E+06	3.89E+05	7.86E+05	3.53E+06	4.19E+02	2.46E+18
3	2	6	9.05E+01	2.17E+08	5.68E+08	3.69E+10	2.38E+03	3.53E+13
4	6	6	3.93E+01	2.48E+09	7.68E+09	3.94E+11	9.60E+03	3.70E+17
5	2	9	2.51E+02	3.05E+09	9.29E+09	7.69E+11	4.83E+04	7.75E+17
6	6	9	7.10E+01	4.04E+07	1.05E+08	8.28E+08	6.68E+02	1.48E+18
	Average		7.07E+05	1.01E+09	3.09E+09	2.02E+11	1.06E+04	2.79E+18
	Rank		5	4	3	2	6	1

(d) Subgrade Modulus

Observation	Difference					
	Australian	Coal Ash Association	Kohn	NCHRP	South African	Uzan
1	88.16	3.57	3.95	5.33	6.69	69.64
Rank	1	6	5	4	3	2